


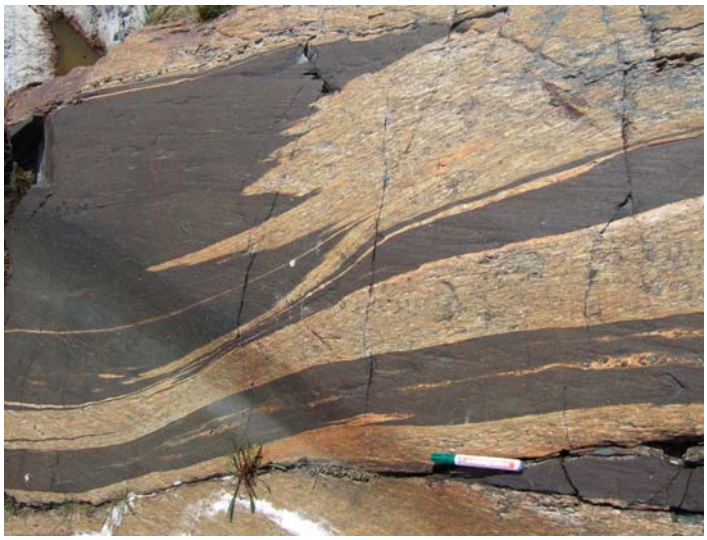


Der „Kleine Geländehelfer“

Ausgabe 2009
Arbeitsgruppe Västervik

Axel Vollbrecht

Vorwort

Die vorliegende „Kleine Geländehelfer“ enthält eine Sammlung von Arbeitsunterlagen für die strukturgeologische Geländeaufnahme und Interpretation der Daten. Die Auswahl erfolgte speziell im Hinblick auf die geologischen Gegebenheiten in der Västervik-Region (SE-Schweden), die durch komplexe strukturelle Beziehungen zwischen mehrphasig intrudierten Magmatiten, damit verbundenen Migmatiten sowie Metasedimenten mit gut erhaltenen Primärgefügen charakterisiert ist. Mehrphasige Deformationen werden durch komplexe Faltenstrukturen und verschiedene Generationen von Myloniten und Kataklasiten abgebildet. Hinzu kommen zahlreiche Gangscharen, die über einen langen Zeitraum in unterschiedlichen Spannungsfeldern angelegt wurden. Als weitere Phänomene werden Mischungen zwischen basischen und felsischen Magmen und metasomatische Überprägungen in unterschiedlichen Dimensionen beobachtet.

Es ist geplant, die Sammlung jährlich zu überarbeiten. Hierzu wären Verbesserungs- bzw. Ergänzungsvorschläge von Seiten der Anwender sehr willkommen.

Die Sammlung enthält neben einigen selbst gestalteten Unterlagen vor allem Kopien aus Lehrbüchern und speziellen Publikationen (siehe Literatur/Quellen) und sollte deshalb aus urheberrechtlichen Gründen nur dem persönlichen Gebrauch dienen. Für wenige Unterlagen konnte die Quelle nicht mehr ermittelt werden. Auch hierzu wären Hinweise willkommen.

Axel Vollbrecht

Feldbuch und orientierte Probennahme (aus Passchier et al. 1990)

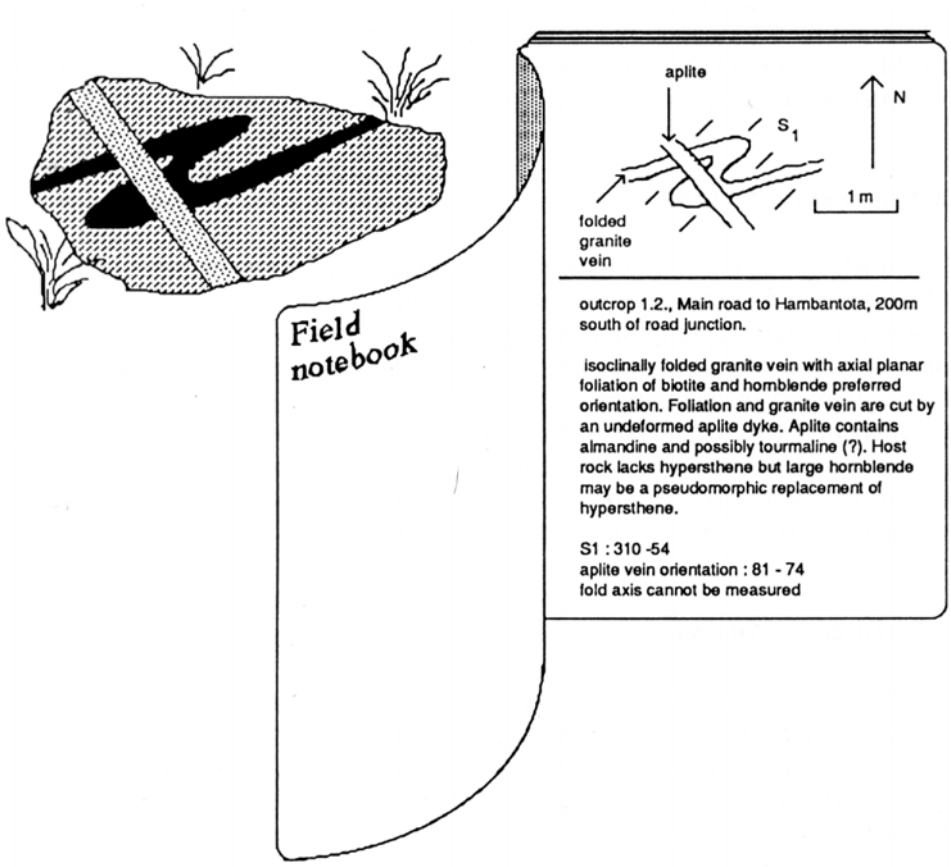

Fig. 2.1. Fabric elements visible in outcrop must be recorded by short descriptions and by sketches.

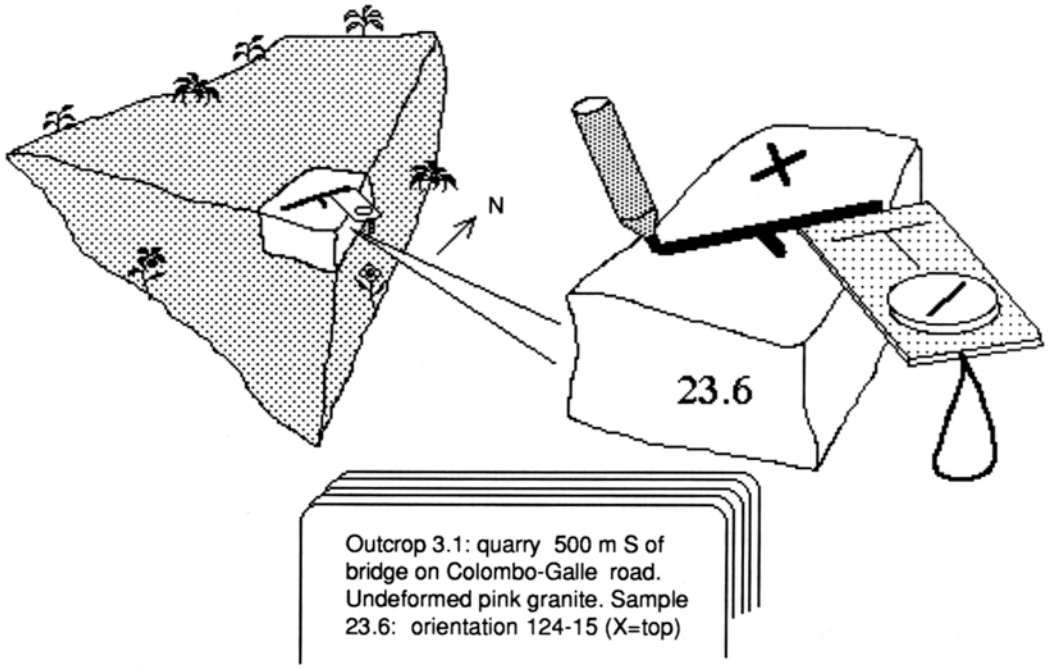

Fig. 2.5. Illustration of how to orient a sample; after detaching the sample, it is fitted back into its original position, and a (relatively) planar surface is selected for measurement. The orientation of this surface is marked with a dip and strike symbol. An extra mark (e.g. X for the top) is needed to indicate whether the measured surface is the top or bottom of the sample. The sample is then numbered, and the orientation of the marked surface is entered into the notebook. In this case dip direction (124) and dip (15) have been measured. A sketch of the setting where the sample is taken may be useful if the local structure is complex.

Beispiele für Geländenotizen (Quelle unbekannt)

Datum:	Aufschluß-Nr.:	Thema: 1
14.6.1976	3	Ösk. Kreid-Exk.

Lokalität:

topog. Karte:	H/R-Werte:	Höhe ü. NN
Blatt 21 Horn der ÖK 50	R 14500 H 483200	105m

Wegbeschreibung:

Talstraße von Mödring nach Pernegg, links und rechts am Kilometerstein 62

Aufschluß:

Art: Zwei kleiner Straßenaufschluß; Straßenanschnitt; z.T. schon überwachsen

Geom./Abm.:

Der angeschnittene Bereich erstreckt sich beiderseits über ca. 15m (ca. 3-4m hoch); ca. 100m weiter nach Pernegg treten noch kleine Anschnitte desselben Gesteins auf

Fotos: Nr. 16 und 17 Übersicht

Gesteinsbeschreibung: 2

hellbraunes, dunkelbraun anwitterndes Gestein mit rötlichen Einsprenglingen; ebener Bruch (splittrig)

Minerale: idiomorphe Staurolith-Einsprenglinge (bis 1cm); kleine (~0,5cm) Granate; feinkristalline Grundmasse; Biotit und Quarz erkennbar; feine Parallelextur

Gestein: Staurolith führender Granatglimmerschiefer

Die rötlichen Granate sind lagenweise angereichert (primäre Schichtung?); sind Granate selten, so werden sie dafür größer (> 1cm)

Staurolithsäulchen (braun) sind parallel ausgerichtet

Proben: A 13.1 (mit großem Granat + Staurolith)
A. 13.2 (mit kleinem Granat, ohne Staurolith)

Fotos: 18+19 Detailaufnahme (Profil)

Tektonik: 3

Das Gestein ist mit einer flachen Schieferung durchzogen.

Die parallel ausgerichteten Staurolithsäulchen streichen ~270°

Der Aufschluß 100m weiter zeigt folgende Werte:

sf		ss?	
	135/25		175/40
	130/25		170/30
	130/25		180/30
	130/20		180/30

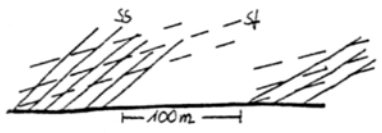

ss Lagen
180/50
180/55
185/55
190/60

sf
130/20
135/20
140/30
125/15
125/20

Fotos: /

Zeichnungen: 4

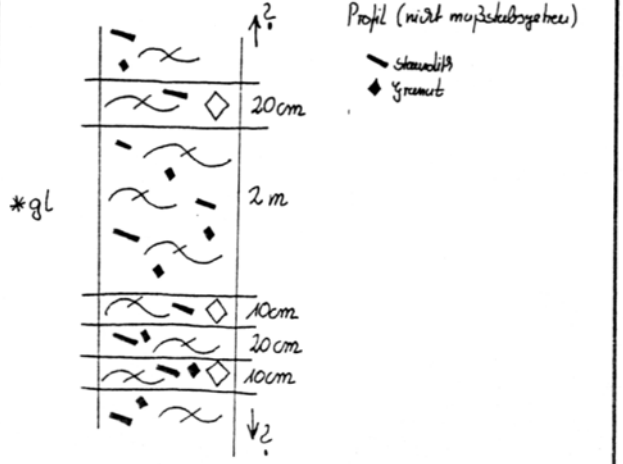

Bemerkungen: /

Datum:	Aufschluß – Nr.:	Thema: 1
13.6.1876	11	Österreich-Exk.

Lokalität:

topog. Karte:	H/R-Werte:	Höhe ü. NN
Blatt 13 westl. der ÖK 50	R 15310 H 484550	690m

Wegbeschreibung:

Straße nach Landshaag; nach Ortseinfahrt links zum Kraftwerk Aschach (Schild); nach Donaubrücke den Berg hinauf fahren zum ersten Parkplatz auf der rechten Seite (ca. 2 km); Zugang zum Steinbruch (Warnschild)

Aufschluß:

Art: künstlicher Aufschluß; alter Steinbruch, z.T. schon zugewachsen; wird leider als Müllkippe benutzt

Geom./Abm.:

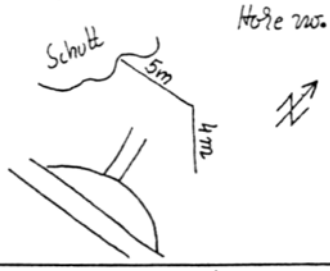

Fotos: 3+4 Steinbruchübersicht

Gesteinsbeschreibung: 2

S. Profil

① hell; grau mit rosa Stich; splittriger Bruch; mittelkörnig; Minerale: große, rötliche, idiomorphe Orthoklase (bis 1cm); Plagioklas, Quarz und wenig Biotit und Hornblende
Gestein: Plutonit; Granodiorit

② hell, aber etwas dunkler als ①
Minerale: wie ①; jedoch weniger Orthoklas (weiß)
Gestein: Plutonit; Granit

③ wie ①+②; Orthoklas und Quarz treten aber weiter zurück, während der Plagioklas- und Hornblendeanteil zunimmt
Gestein: Plutonit; Diorit (bis Monzodiorit)

① Quarz (20-60%); Orthoklas zu Plagioklas (~1:3)
Mafitanteil (< 10%)

② Quarz (20-60%); Orthoklas zu Plagioklas (~1:1)
Mafitanteil (< 10%)

③ Quarz (< 20%); Orthoklas zu Plagioklas (1:5 ?)

Proben: ① A 26.1 ② A 26.2 ③ A 26.3

Fotos: /

Tektonik: 3

Die Gesteine werden von parallelen Brüchen (Klüften) durchsetzt; sie sind offen

Kf	350/80	355/80	365/75
	350/80	360/85	355/80

ss: /

sf: /

Fotos: s. Foto 3+4

Zeichnungen: 4

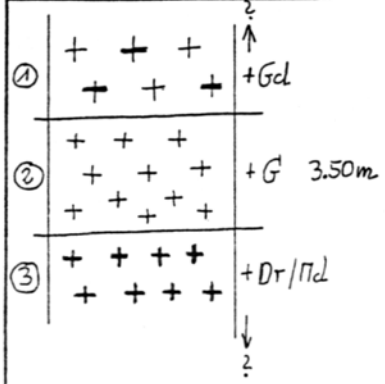

Bemerkungen: /

Strukturgeologische Symbole (aus: Hatcher 1995)

Mesoscopic Structures

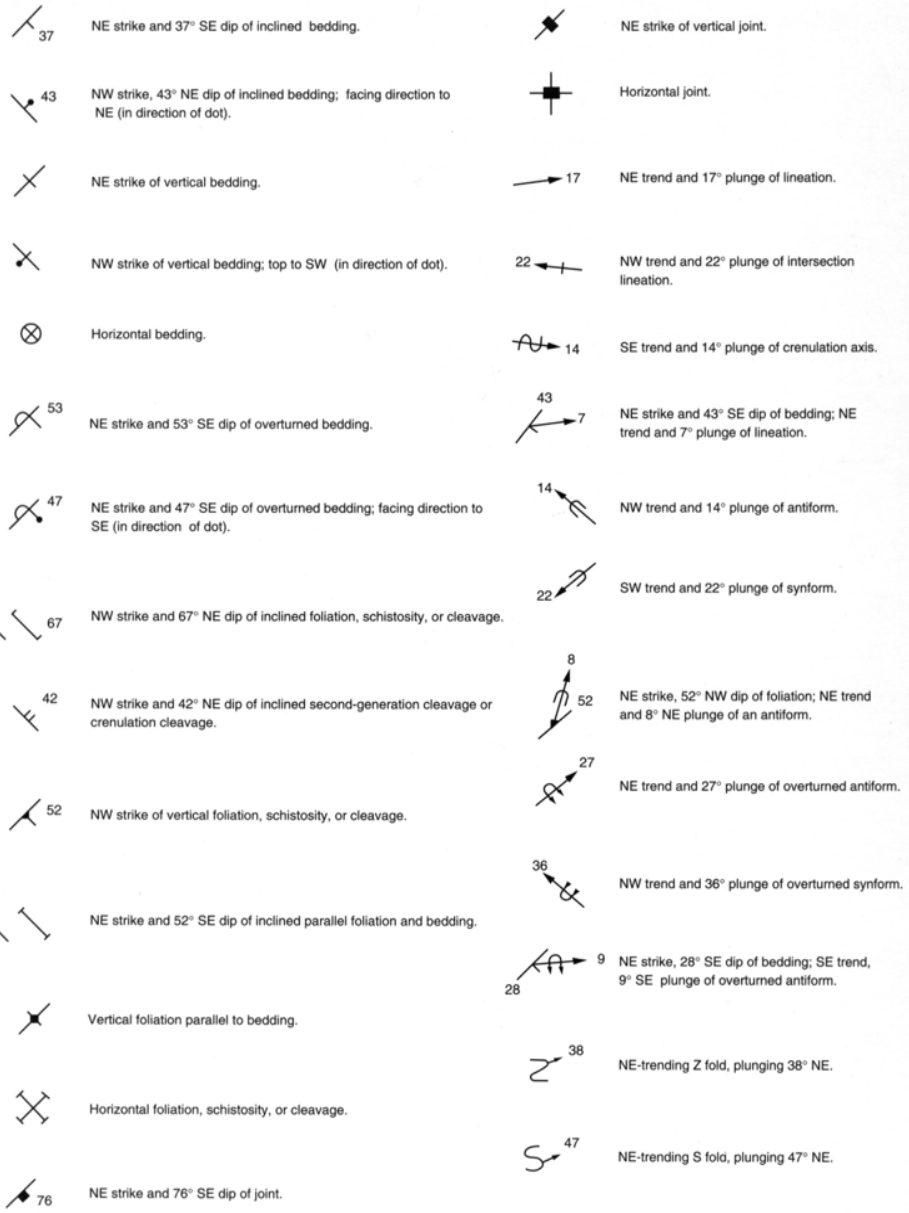

Map-Scale Structures

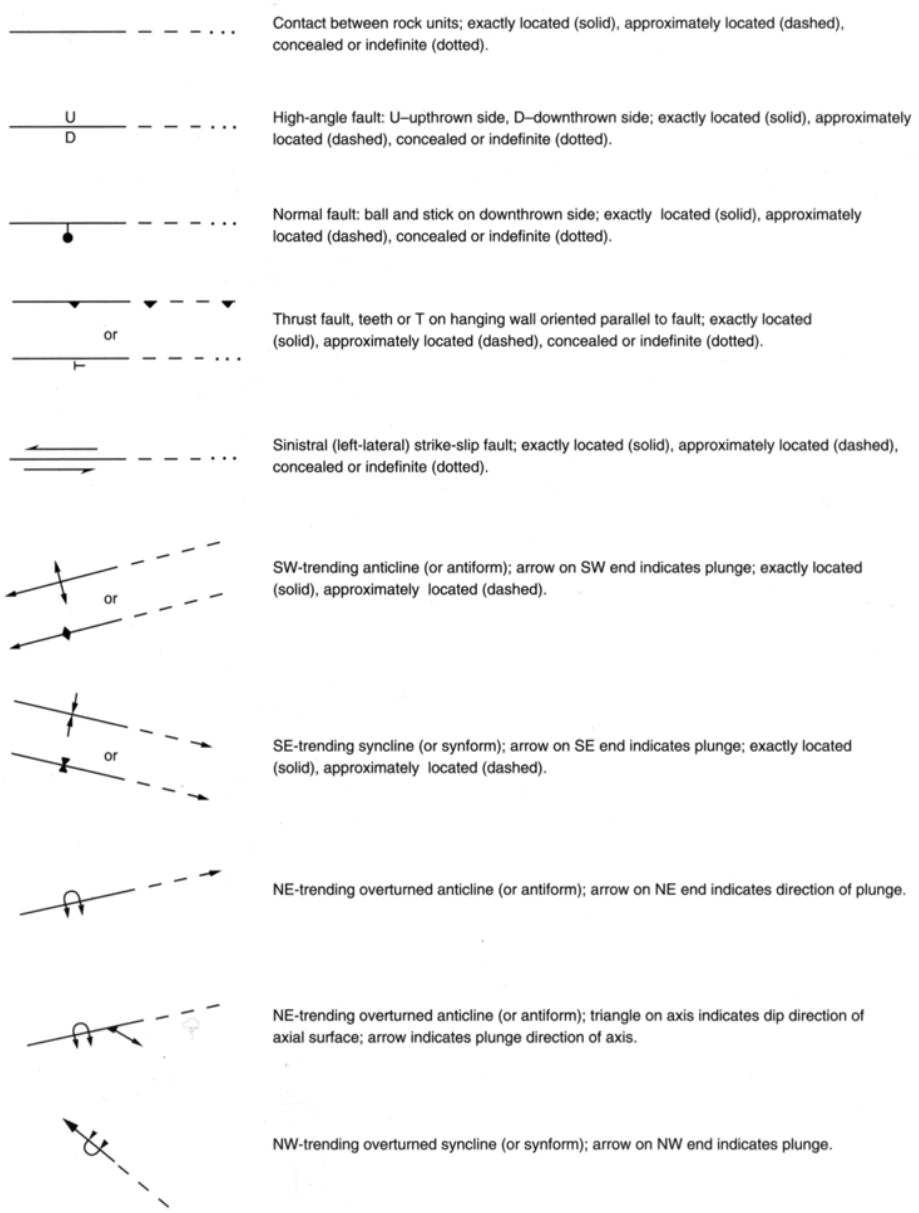

Platznahme von Granitoiden

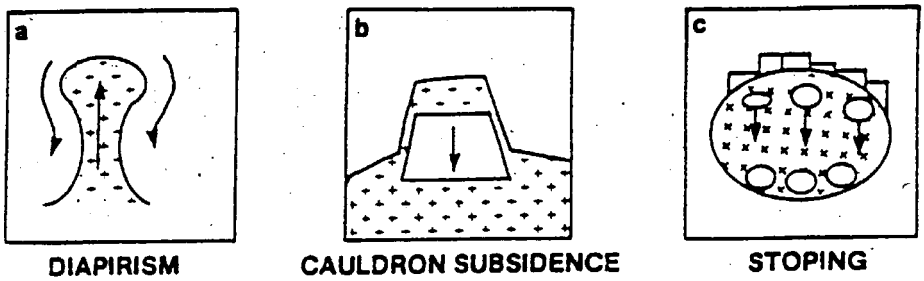

COUNTRY ROCKS MOVE DOWN
(vertical cross-sections)

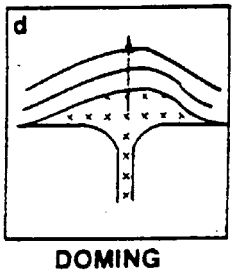

COUNTRY ROCKS MOVE UP
(vertical cross-sections)

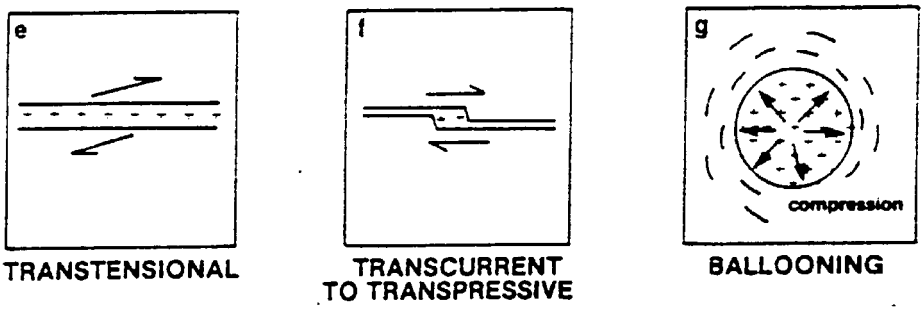

COUNTRY ROCKS MOVE LATERALLY
(pian views)

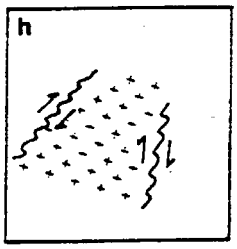

COUNTRY ROCKS MOVEMENT POST-MAGMATIC
(plan or section)

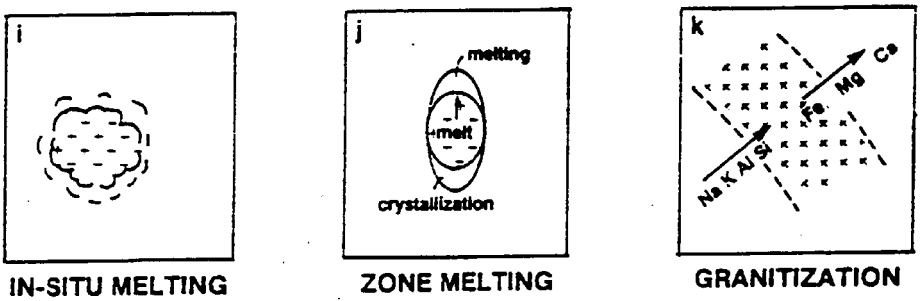

COUNTRY ROCKS DO NOT MOVE

Table 2.2 Field characteristics relevant to the level of emplacement of granitoid intrusions. Plutons intruded at intermediate levels show transitional characteristics

Feature	*Shallow intrusions*	*Deep-seated intrusions*
Contact relations with country rocks	predominantly sharp and discordant	predominantly diffuse and concordant
Pluton shapes	discrete isotropic to mildly anisotropic plutons	domes, conformable sheets
Contact facies of the granitoid	may be finer-grained	no chilled margins
Internal structures	internally controlled; structures unrelated to those in country rocks	externally imposed; structures similar to those in country rock
Textures	massive, may be porphyritic, granophyric	foliated, aphyric to augen gneisses
Regional metamorphic grade of country rocks	greenschist, lower amphibolite	upper amphibolite, granulite
Thermal aureole	prominent in rocks of suitable composition, e.g. pelites	obscure in most cases
Migmatites	local; restricted to contacts	regional (see Fig. 15-12 in Compton, 1985)
Other possible diagnostic (?) characteristics	miarolitic cavities; pegmatite dykes; hydrothermal alteration; granophyric textures; roof pendants; breccia dykes; cogenetic volcanic rocks nearby; abundant country rock xenoliths	

Table 2.3 Characteristics of some styles of ascent and emplacement

Emplacement style	*Type**	*Exocontact*	*Contact***	*Endocontact*
Diapirism (Marsh 1982, 1984; Bateman 1984, 1985) (Fig. 2.12a)	F	contact-parallel foliation; aureole porphyroblasts syn-kinematic with diapiric foliation; compressional features, deflected structures, (e.g. rim synclines)	shearing along contact possible	pluton circular in plan; marginal foliation parallel to contact
Cauldron subsidence, stoping (Daly 1933; Marsh 1982) (Fig. 2.12b,c)	P	country rocks structurally undisturbed; thermal aureole	sharp to diffuse	abundant country rock xenoliths, chilled margin
Fracture exploitation (Shaw 1980; Castro 1987) (Fig. 2.12b–f)	F	dilation, offsets, shearing	straight, curved; fault-gouge, breccia; mylonite	?
Fluidization (Reedman *et al.*, 1987)	F	possible diffusion and infiltration metasomatic effects	sharp	*heterogeneous mixture of* rounded blocks and finer matrix
Ballooning (Pitcher and Read, 1963; Bateman, 1985; Ramsey, 1989) (Fig. 2.12g)	F	aureole deformation continuous with that in pluton; intensity of deformation decreases away from contact; contact minerals synkinematic	deformation parallel to contact	*flattening*
Post-magmatic tectonic (Guineberteau *et al.*, 1987; Jamieson *et al.*, 1987; Marre, 1986) (Fig. 2.12h)	F	brittle and/or ductile deformation; shearing, cataclasis, mylonitization, drag folds, tension gashes, thermal aureole absent	sharp to diffuse; straight to arcuate; fault gouge, slickensides	brittle and/or ductile deformation; shearing, cataclasis, mylonitization
In-situ melting (Joplin, 1962; Currie and Pajari, 1981) (Fig. 2.12i)	P	regional migmatite	diffuse transition from country rock to 'pluton'	
Zone melting (Harris 1957; Marsh 1982) (Fig. 2.12j)	P	country rocks structurally undisturbed; thermal aureole	diffuse	no evidence(?)
Granitization (Kresten, 1988) (Fig. 2.12k)	P	basic front?	diffuse	

F = forceful
P = passive

aus: Pitcher 1993

Intrusionsstrukturen 1 (aus: Price & Cosgrove 1990)

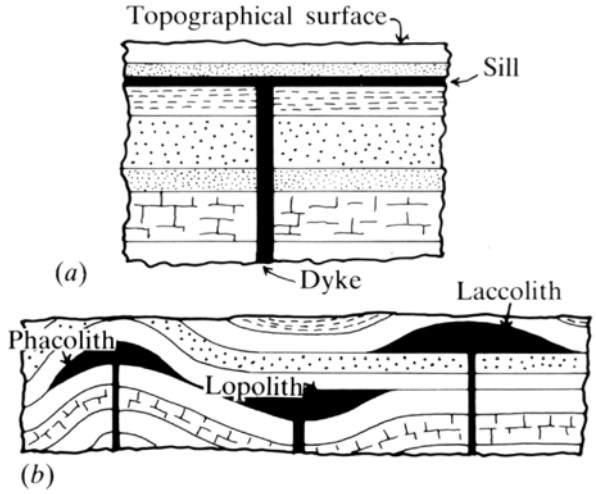

Fig. 3.1. (*a*) Near-planar concordant and discordant intrusions, (sill and dyke) in flat-lying sediments. (*b*) Types of non-planar concordant intrusions: a laccolith may have a flat base but an upward concave roof; a lopolith may have saucer-shaped or approximately flat roof and downward-curved (sagging) floor and a phacolith has a concavo-convex form. Phacoliths when they are ore bodies are termed saddle-reefs.

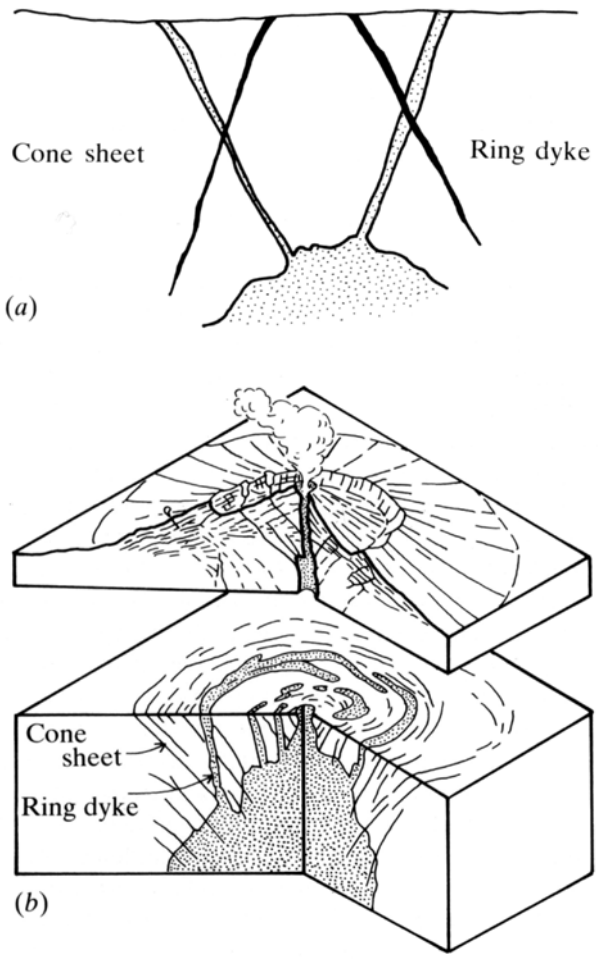

Fig. 4.43. (*a*) Idealised geometry of cone sheets and ring dykes. (*b*) Ring structures in relationship to a major intrusion. (After Cloos, 1936.)

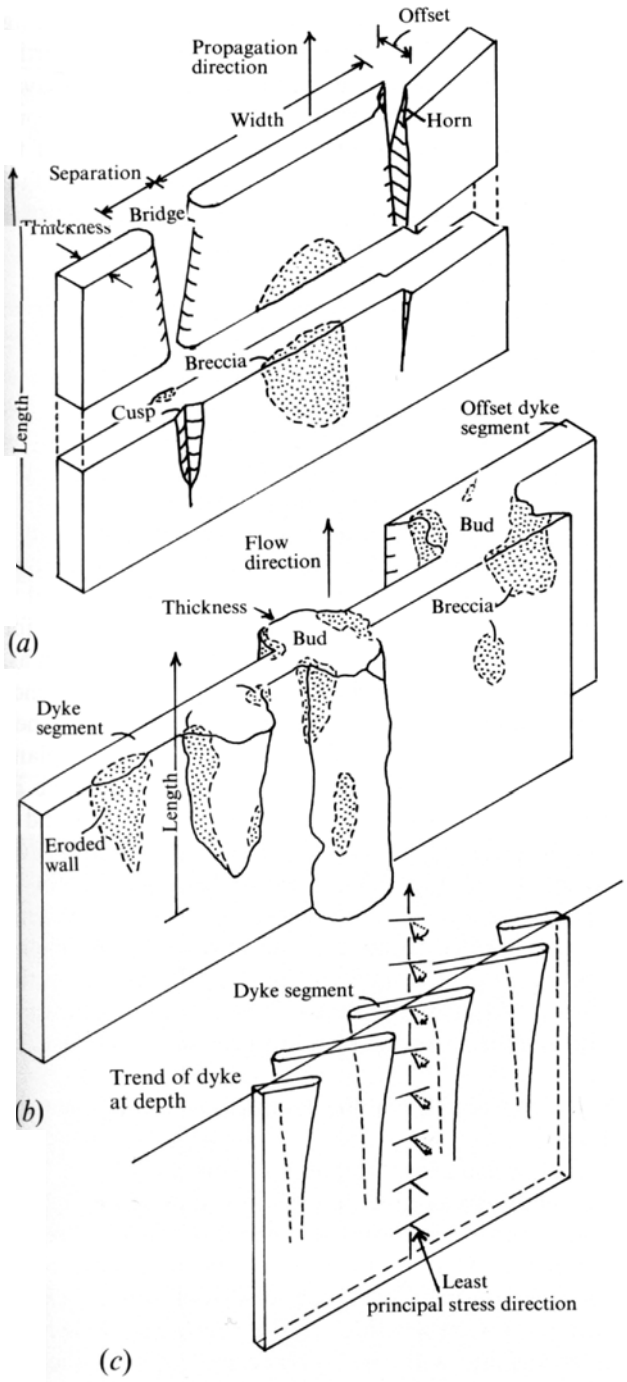

Fig. 3.30. (*a*) Terms used to describe discontinuous and off-set dykes. (*b*) Further morphological features of off-set dykes. (*c*) Postulated change of orientation of stresses with depth necessary to cause the development of en echelon dykes. (*a*), (*b*) and (*c*) after Delaney & Pollard, 1981.)

Intrusionsstrukturen 2 (aus: Price & Cosgrove 1990)

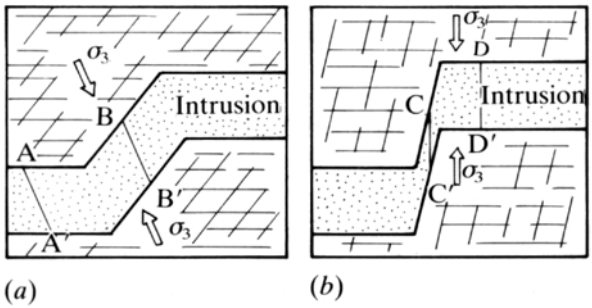

Fig. 3.35. Geometry of an intrusion along oblique planes of weakness in relation to the orientation of the axis of least principal stress.

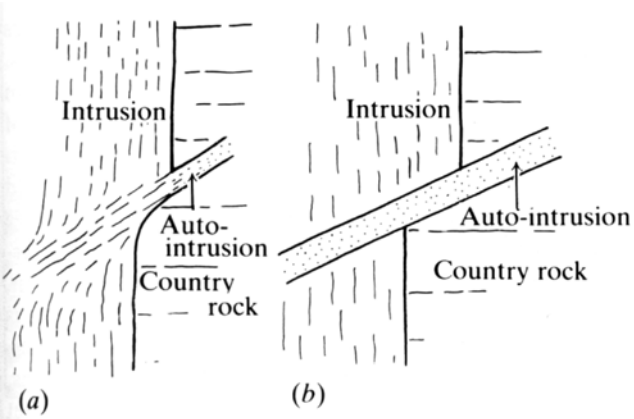

Fig. 4.29. (*a*) Ductile and (*b*) 'brittle' auto-intrusions.

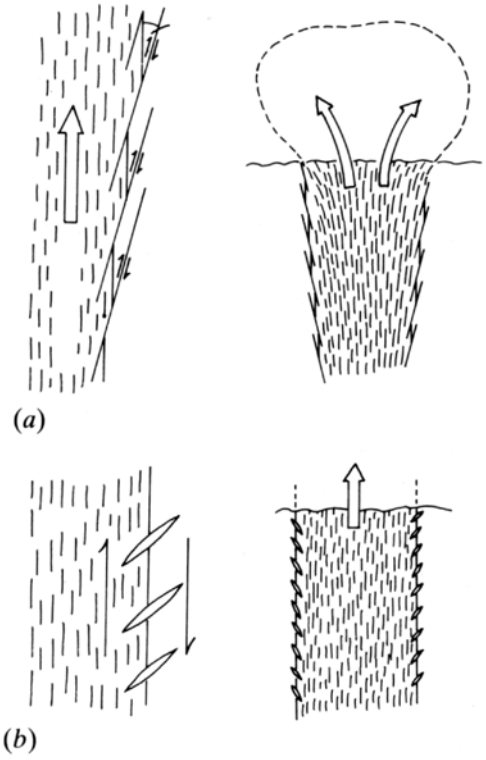

Fig. 4.30. Examples of how the geometry of an intrusion may be inferred from (*a*) thrusts and (*b*) extension fractures which develop near the interface between intrusion and country rock.

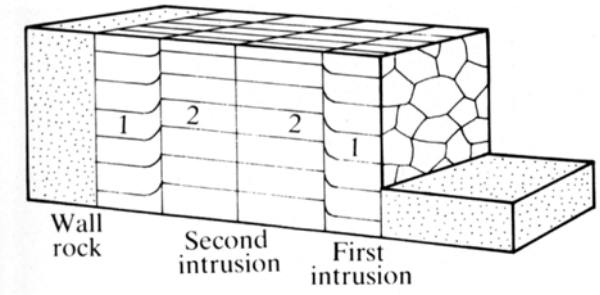

Fig. 3.43. Schematic morphology of horizontal, polygonal columns in a dyke which has experienced two phases of emplacement and exhibits a central suture. A later phase of intrusion may cause distortion of earlier polygons.

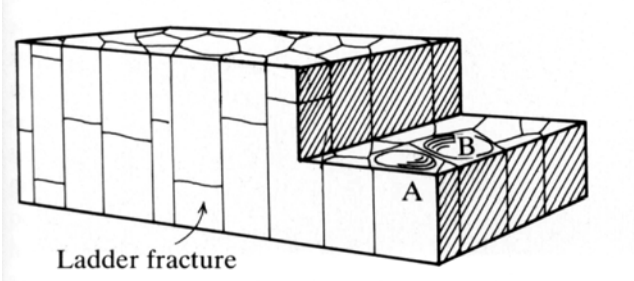

Fig. 3.45. Schematic representation of polygonal columns in a sill with ladder fractures. Dome and basin form of the ladder fractures are shown at A and B respectively.

Intrusionsstrukturen 3 (aus: Shelley 1993)

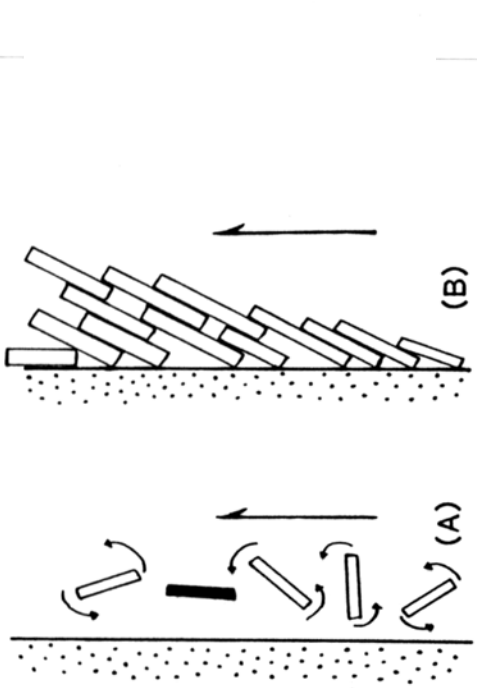

Fig. 8.4 (A): Tumbling of crystals due to laminar flow adjacent to a solid interface such as a dyke wall or chamber floor. The crystal (black) subparallel to the interface is in a metastable position. (B): Mutual interference of crystals causes tiling and prevents further tumbling.

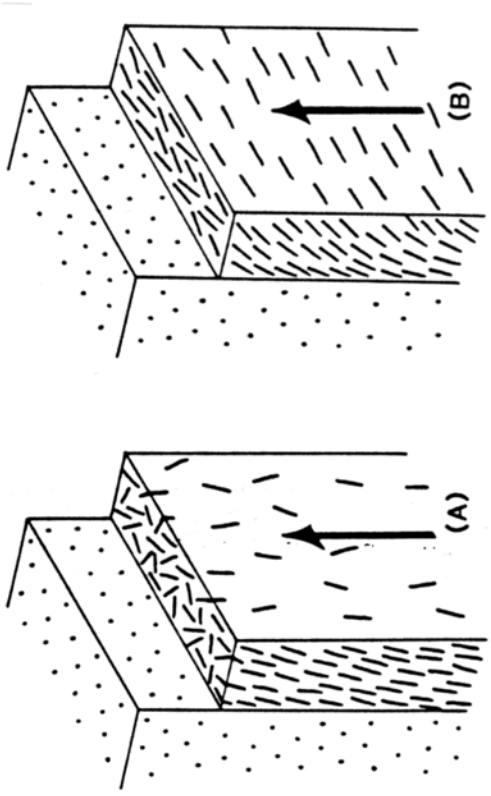

Fig. 8.5 Orientations of feldspar laths in dykes adjacent to the wall (stippled). (A): Tiling and well-developed girdle of poles to (010) around the flow direction. Lineation parallel to flow direction. (B): Poorly developed girdle combined with marked tiling pattern and intersection lineation perpendicular to the flow direction.

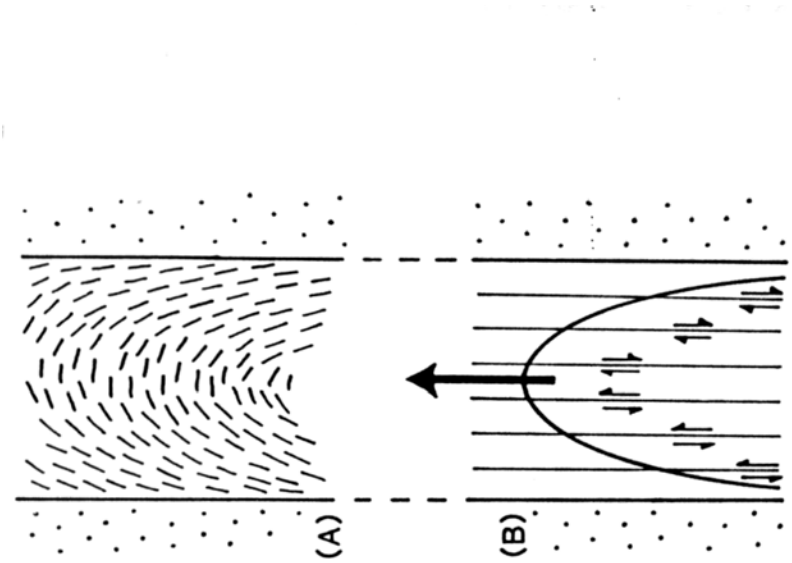

Fig. 8.3 Cross-sectional view of dyke, parallel to the flow direction, showing the typica curved pattern of feldspar or other platy minerals (A), and its relation to the velocity profil and laminar flow (B).

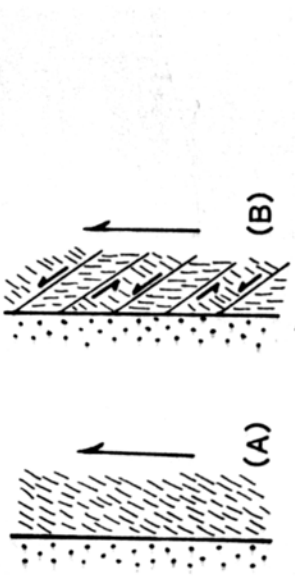

Fig. 8.8 (A): Tile-pattern due to laminar flow adjacent to a solid interface such as a dyke wal or chamber floor. (B): Continued laminar flow crenulates the foliation along secondary shears.

Strukturformen im Kontaktbereich von granitischen Intrusionen (Quelle unbekannt)

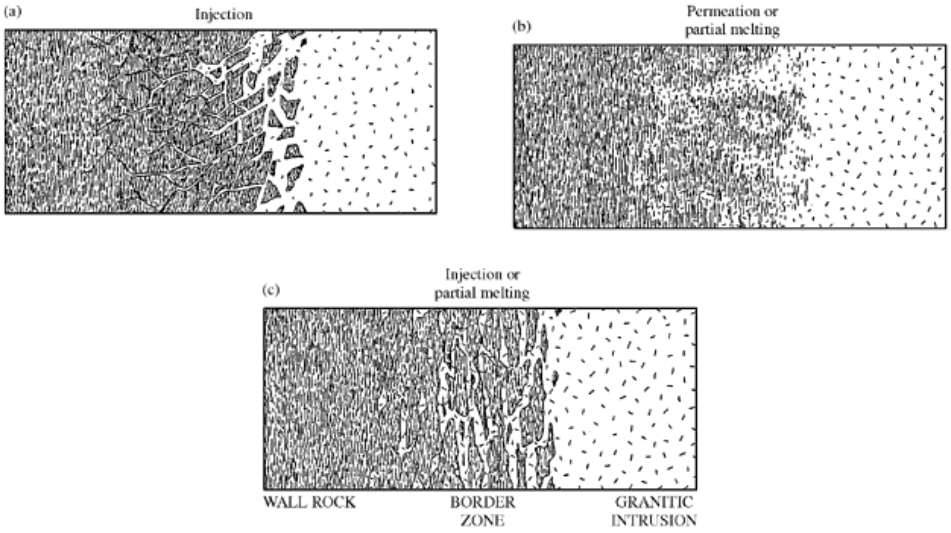

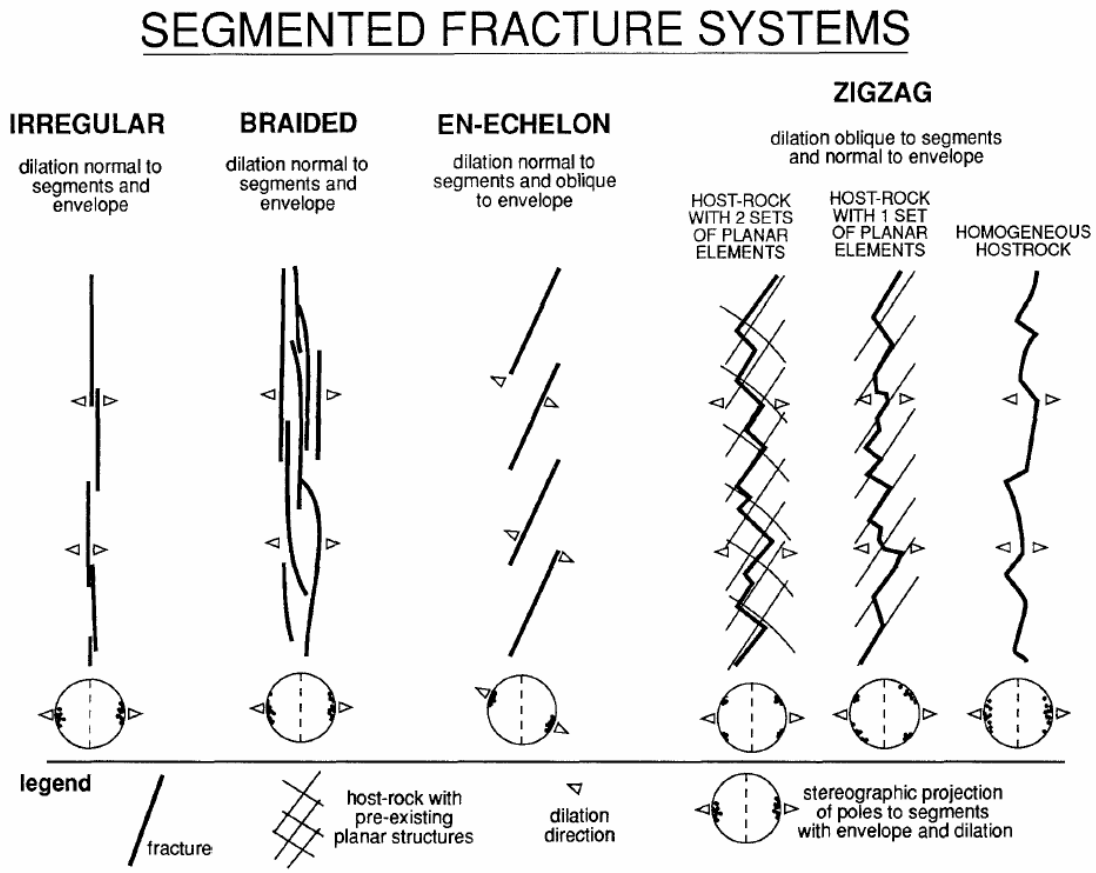

Fig. 6. Classification of dyke-fracture geometry in cross section.

aus: Hoek 1991

Möglickeiten der Foliationsbildung in Granitoiden (Quelle unbekannt)

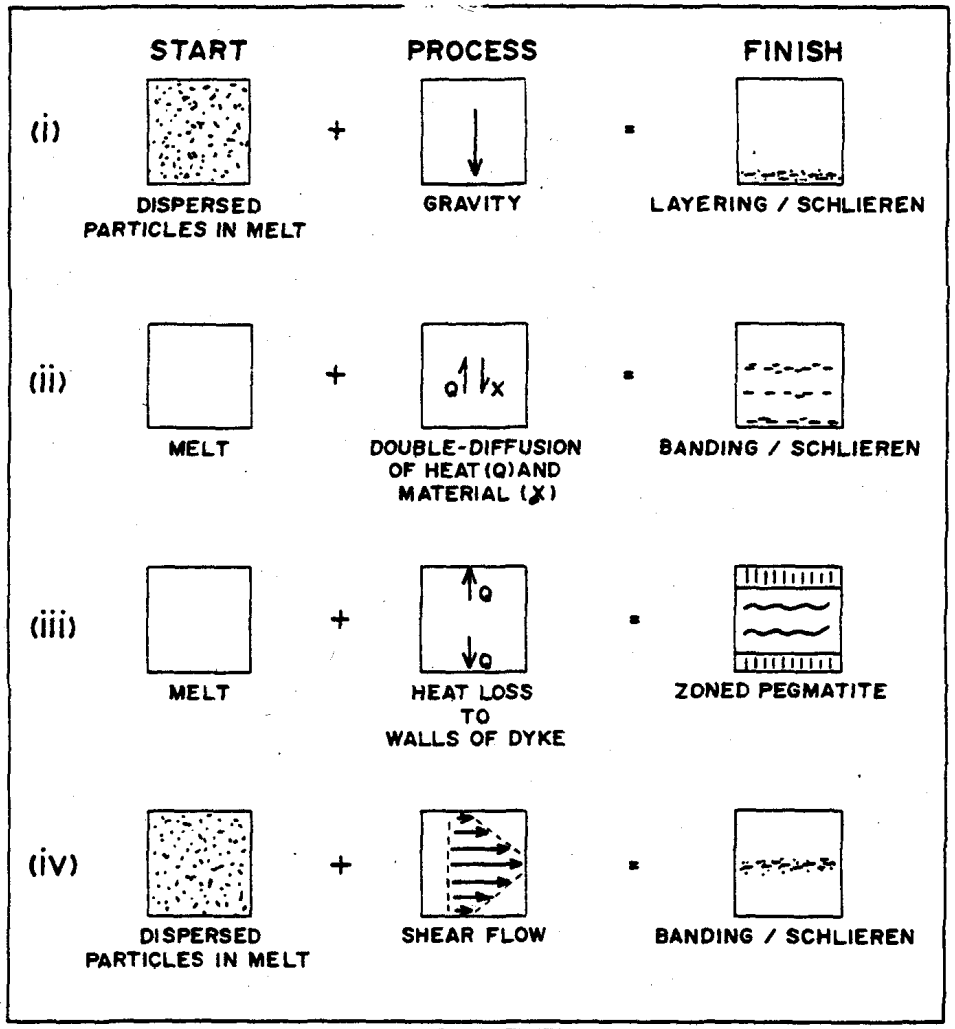

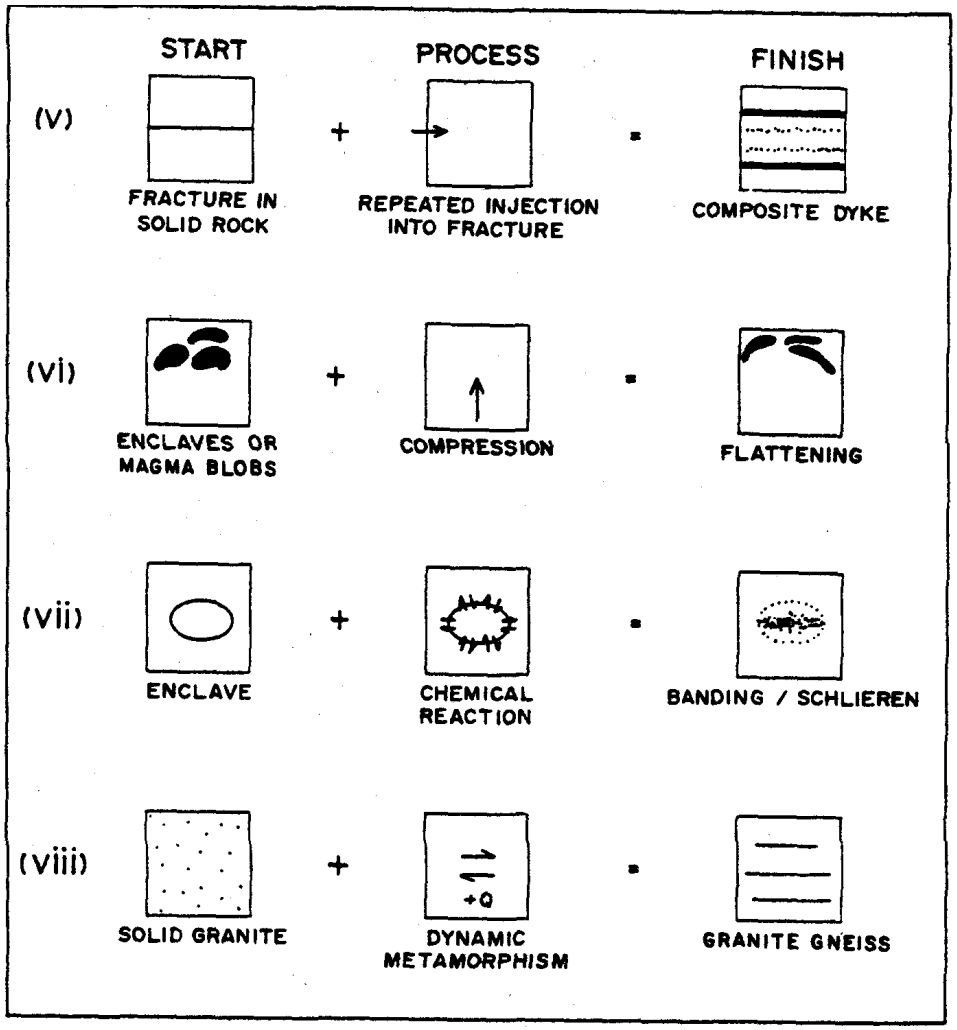

Fig. 2.8 Methods of formation of foliation and banding in granitic rocks

Stofflicher Lagenbau in Plutoniten (aus: Shelley 1993)

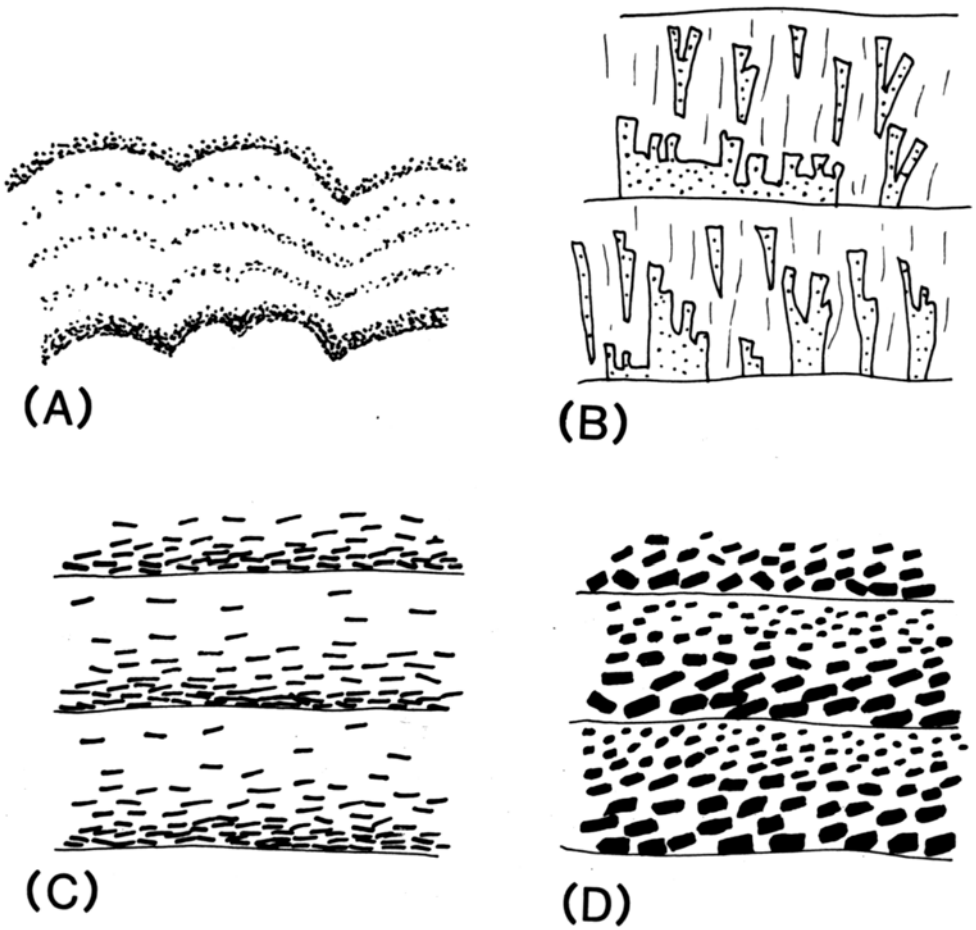

Fig. 4.33 Schematic views of features associated with layering in plutonic rocks. (A): Colloform layering with individual mounds of the order of 1 m across. (B): Crescumulate texture with crystals elongate at a high angle to layering. (C): Density grading, with heavier minerals typically concentrated at the base of layers. (D): Grain-size grading with coarser grains typically at the base of layers.

Interne Intrusionskontakte in Plutoniten (aus: Pitcher 1993)

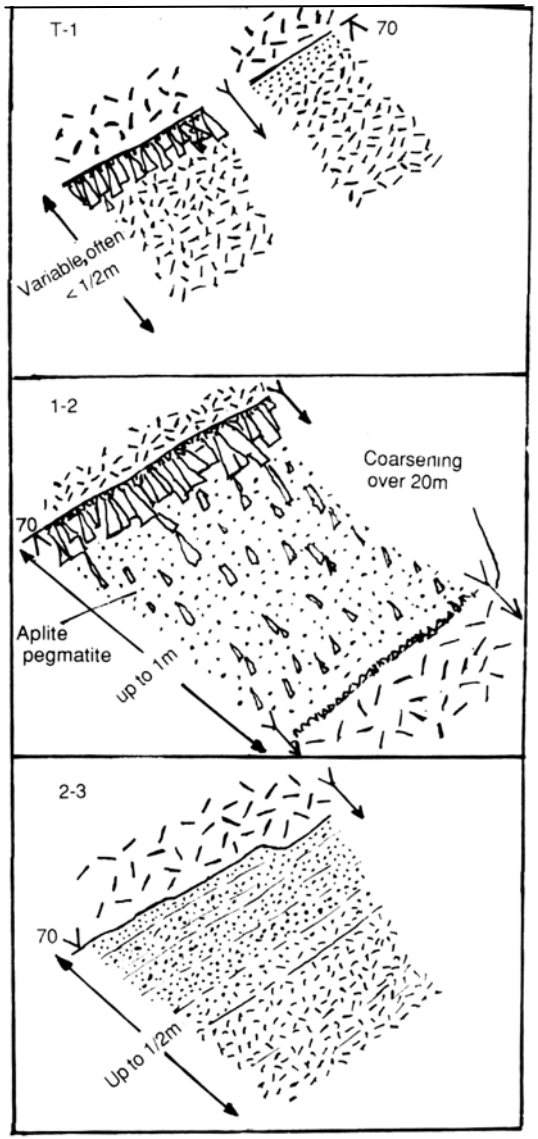

Figure 6.2 Types of internal contacts within the Rosses pluton, Donegal. T-1, outer contact; 1–2, contact between pulses 1 and 2; 2–3, contact between pulses 2 and 3. Stipple depicts changes of grain size. Triangle-like shapes depict potassium feldspar crystals; arrows indicate younging direction.

Klassifizierung der Magmatite nach Streckeisen

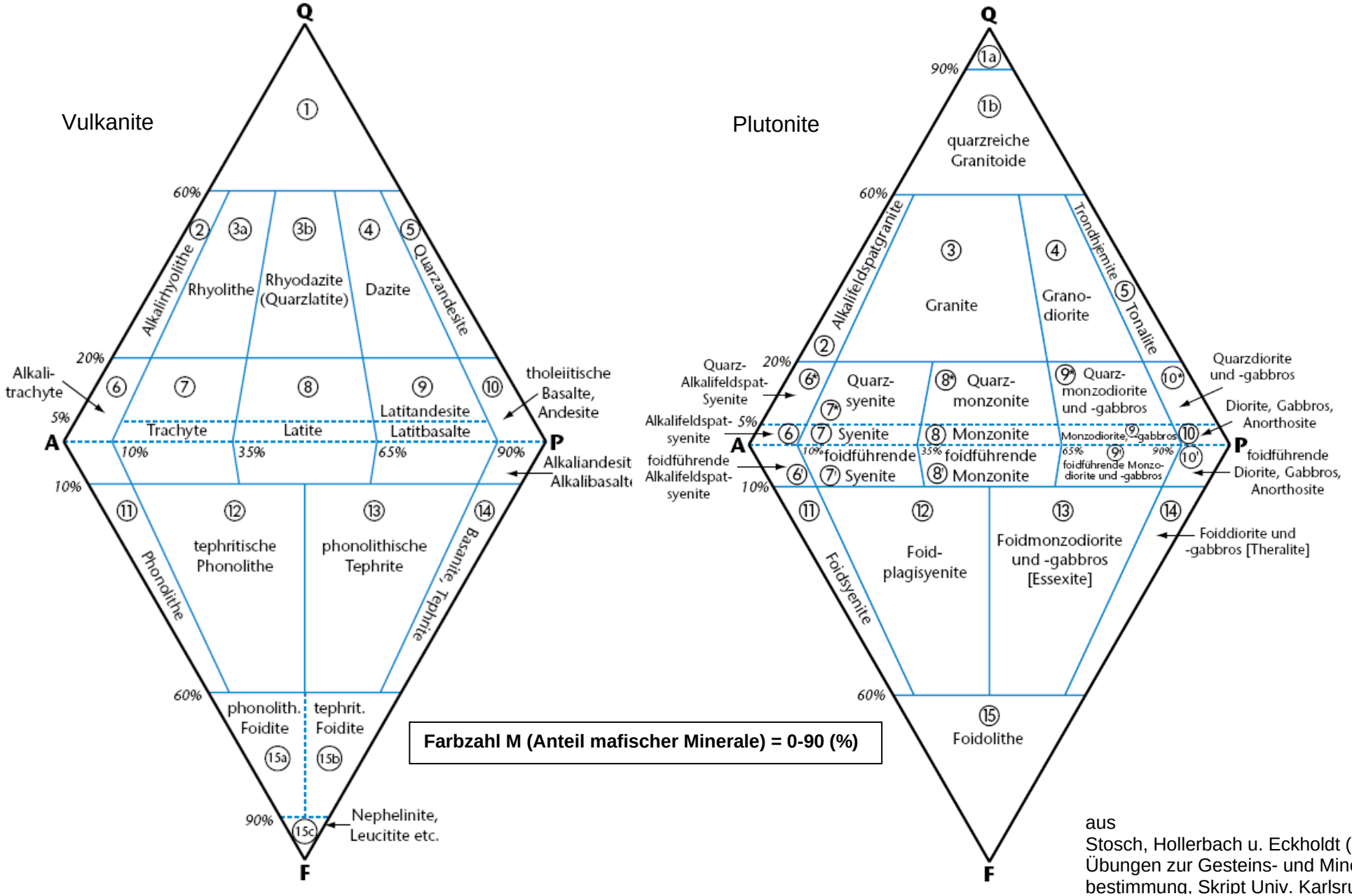

Farbzahl M (Anteil mafischer Minerale) = 0-90 (%)

aus
Stosch, Hollerbach u. Eckholdt (2001): Übungen zur Gesteins- und Mineralbestimmung, Skript Univ. Karlsruhe

Gabbroide Gesteine

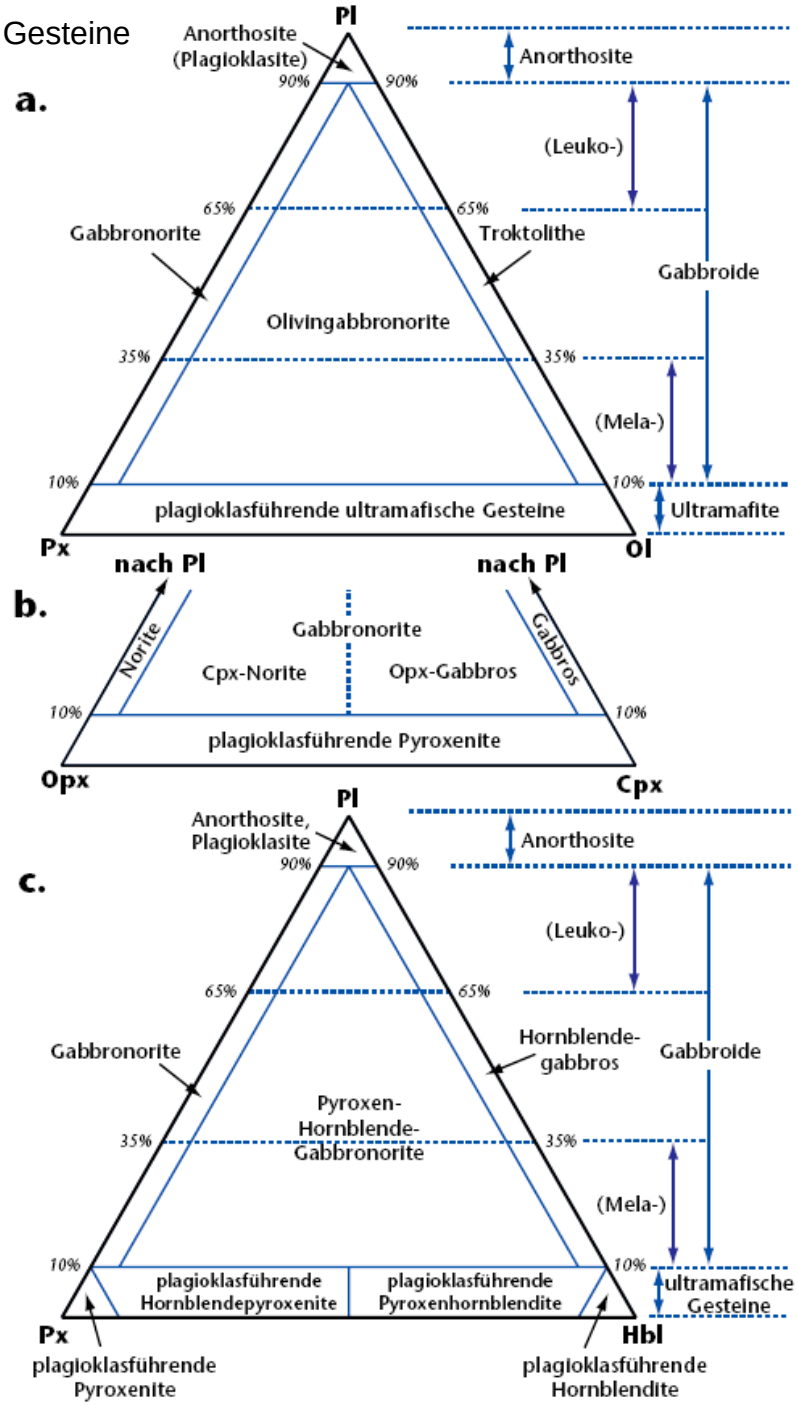

Ultramafite

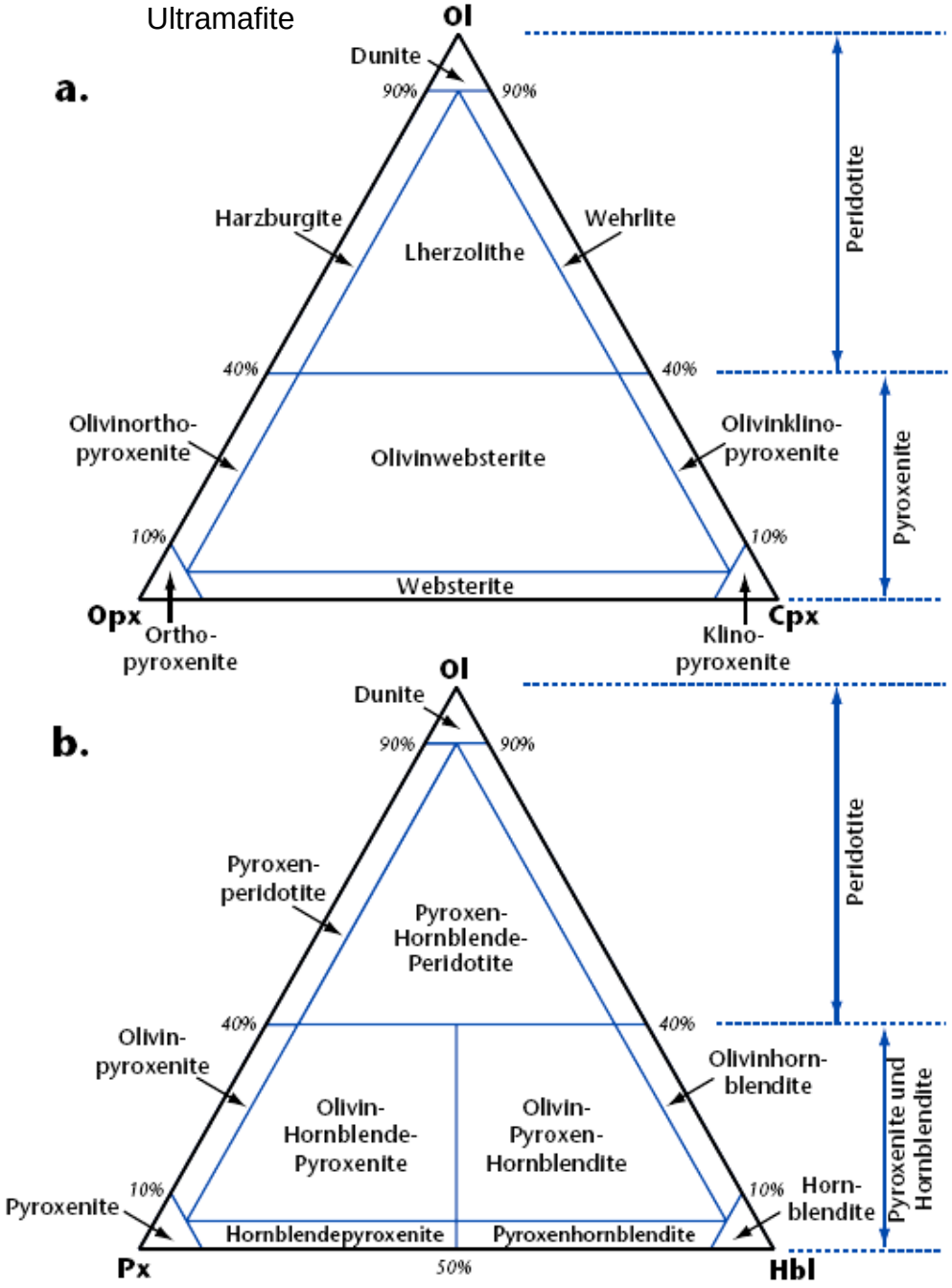

Zusammensetzung Magmatite

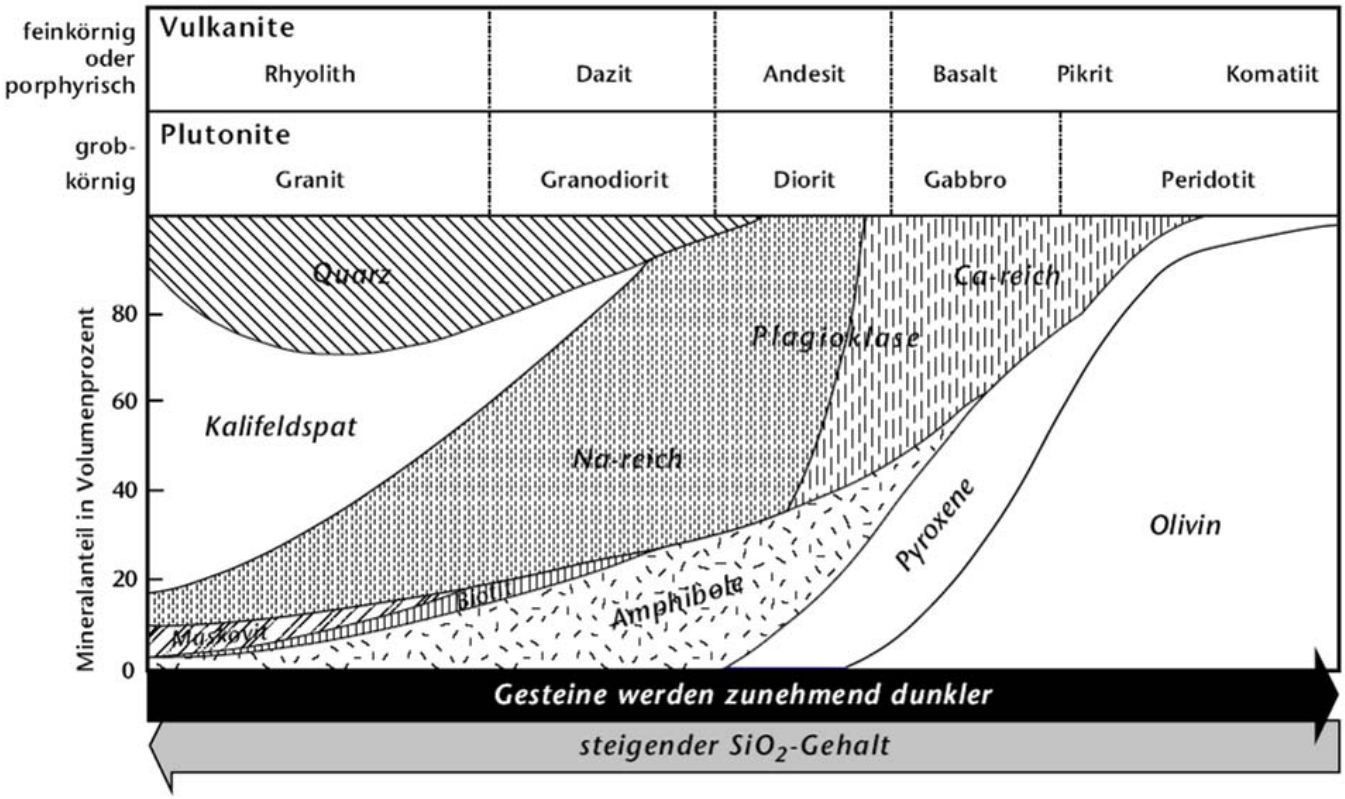

Quelle unbekannt

Table 8.1. Summary of the distinctive features of the S- and I-type granites of the Lachlan Fold Belt as originally proposed by Chappell and White (1974).

I-types	*S-types*
(i) Metaluminous mineralogy; hornblende common and more abundant than biotite in mafic samples; accessory sphene common	Peraluminous mineralogy: biotite and muscovite predominate; no hornblende; some cordierite and/or aluminosilicates; monazite may be accessory
(ii) Hornblende-rich igneous-appearing xenoliths	*Pelitic or quartzose metasedimentary* xenoliths
(iii) Relatively high Na_2O	Relatively low Na_2O
(iv) Molecular $Al_2O_3/(Na_2O + K_2O + CaO) < 1.1$	Molecular $Al_2O_3/(Na_2O + K_2O + CaO) > 1.1$
(v) Normative diopside or small amounts of normative corundum	Normative corundum >1%
(vi) Broad spectrum of compositions from mafic to felsic	Narrow range of more felsic rocks
(vii) Regular inter-element variations within plutons; linear or near linear variation diagrams	More irregular variation diagrams
(viii) Mafic hornblende-bearing enclaves	Metasedimentary enclaves
(ix) Initial $^{87}Sr/^{86}Sr$ 0.704–0.706	Initial $^{87}Sr/^{86}Sr$ >0.708
(x) Usually unfoliated; contacts strongly discordant; well developed contact aureoles	Often foliated; sometimes surrounded by high grade metamorphic rocks

aus Pitcher 1993

Magmenmischungen
(felsisch + basisch)

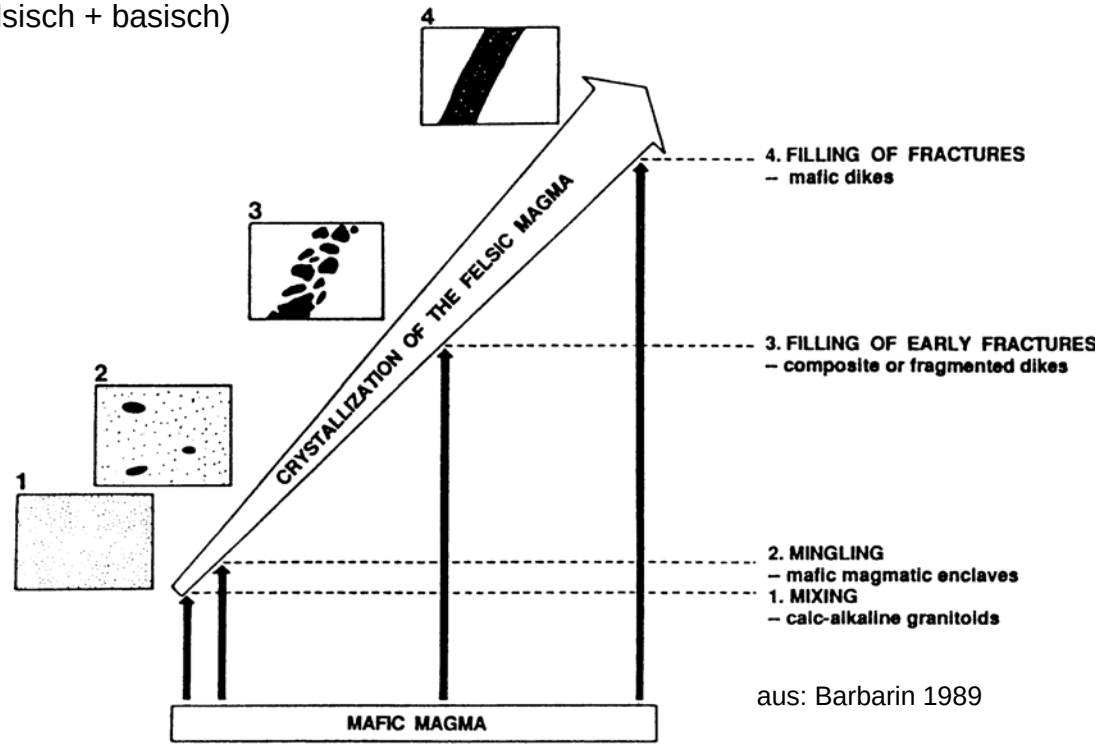

aus: Barbarin 1989

Im Experiment beobachtete Strukturen
(aus: Koopmann 2004)

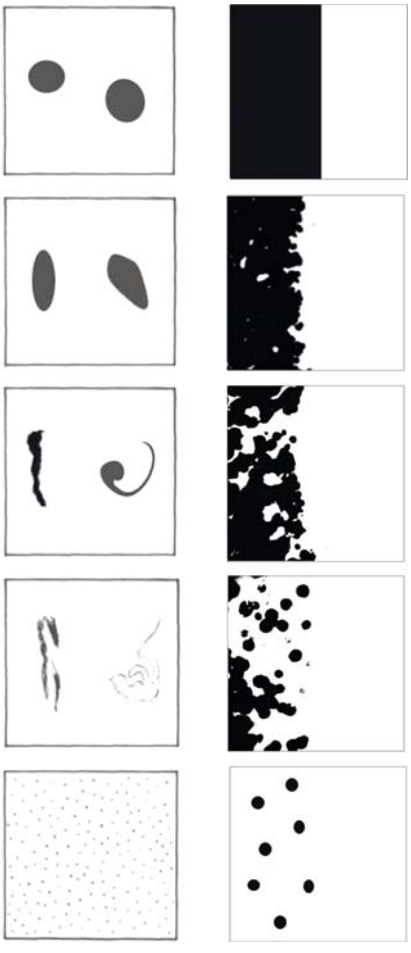

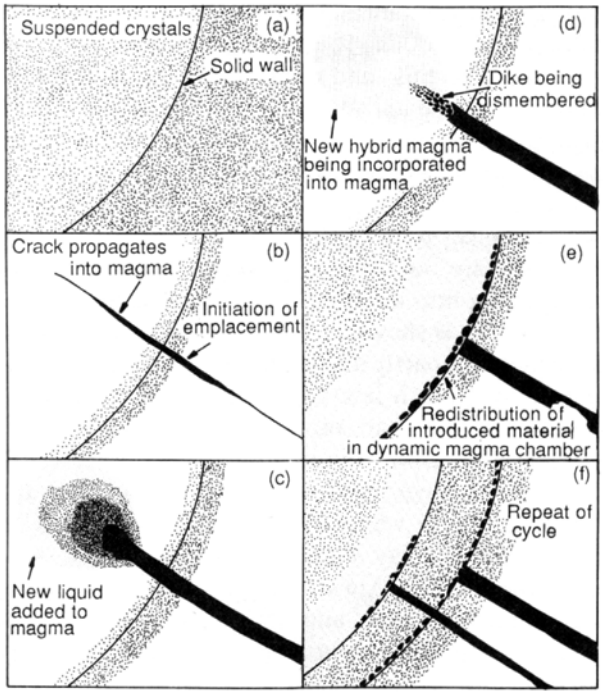

Figure 9.4 Diagram illustrating inferred relationship between mafic dykes and inclusion trains. (a) Wall of crystallizing magma chamber showing solidified material to right and magma containing suspended crystals to left. (b) Propagating crack intersects solid–magma interface. Mafic liquid is then emplaced along the crack. Magma adjacent to the pluton wall behaves in a brittle manner at the time-scale of crack propagation and dyke emplacement. (c) Flow of liquid through conduit, with inferred addition of liquid to the volume of liquid already resident in the chamber. (d) Mixing of new liquid with old liquid, probably accompanied by considerable precipitation of plagioclase and hornblende because of the temperature difference between the dyke liquid and the ambient temperature within the magma chamber. Partly solidified dyke is veined by tonalitic liquids from the magma chamber; pillows of mafic liquid may form, depending on viscosity contrast between the resident and added liquids. (e) Re-establishment of convective system within the magma chamber. Hybrid liquids, suspended crystals, and disaggregated dyke rock are redistributed parallel to the pluton walls. (f) Repeat of cycle. Reproduced from Hill (1988) in dedication to the author and with the permission of the *Journal of Geophysical Research*

aus: Pitcher 1993

Enklaven

	Term	Nature	Contact	Shape	Features
ENCLAVE	Xenolith	Piece of country rocks (hornfels)	Sharp	Angular	Contact-metam. texture & minerals
	Xenocryst	Isolated foreign crystal	Sharp	Globular	Corrosion Reactional aureole
	Surmicaceous enclave	Residue of melting (restite)	Sharp with biotitic crust	Lenticular	Metamorphic texture Micas & Al-rich minerals
	Schlieren	Disrupted enclave	Gradual	Oblate	Planar orientation
	Felsic microgranular enclave	Disrupted fine-grained margin	Sharp or gradual	Ovoid	Fine-grained Igneous texture
	Mafic microgranular enclave	Blob of coeval magma	Mostly sharp	Ovoid	Fine-grained Igneous texture
	Cumulate enclave (Autolith)	Disrupted cumulate	Mostly gradual	Ovoid	Large-grained Cumulate texture

Beziehung zwischen Enklaven und Wirtsgesteinen

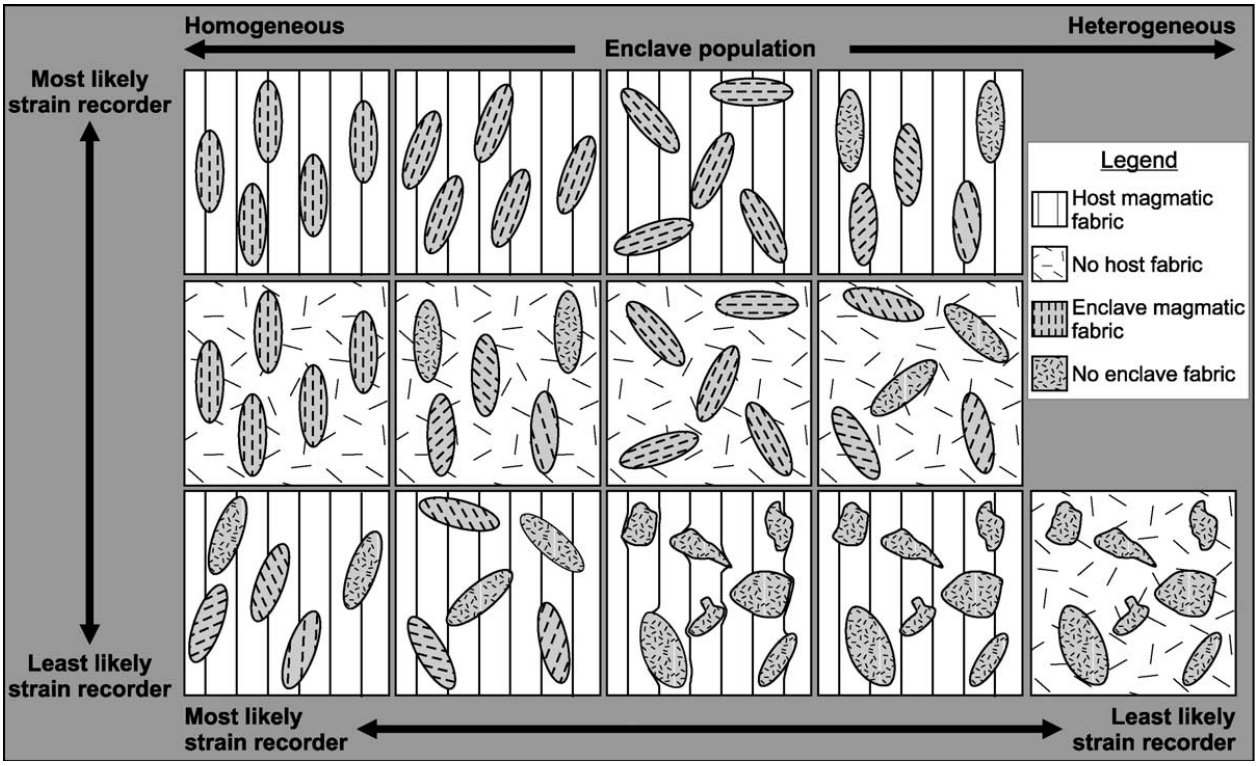

Cartoon showing the range of possible relationships between enclave shapes, internal magmatic mineral fabrics in enclaves, and magmatic mineral fabrics in the host granite. Although it is impossible to do so completely, the examples have been arranged to emphasize relationships most likely to result from simultaneous strain of enclaves and matrix (top left) to those indicating that enclaves were rigid objects during final matrix strain. Note, however, that even the most likely could have formed by high temperature strain of enclaves (to form enclave shape and internal mineral alignment) and subsequent rigid rotationparallel to the matrix foliation.

aus Paterson et al. (2004)

Magmatische Grenzflächen (auch Hangend- Liegendkriterien)

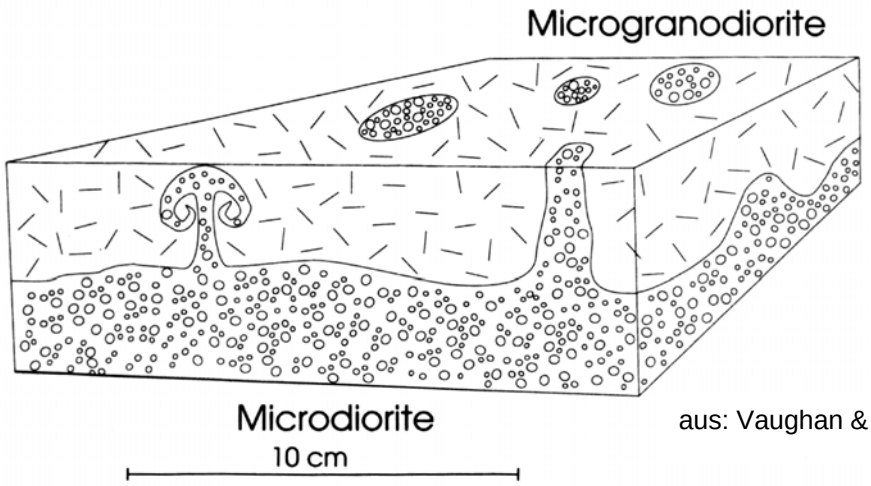

aus: Vaughan & Thistlewood 1995

Fig. 4. Block diagram summarizing the relationship between the structures of Fig. 2 and Fig. 3.

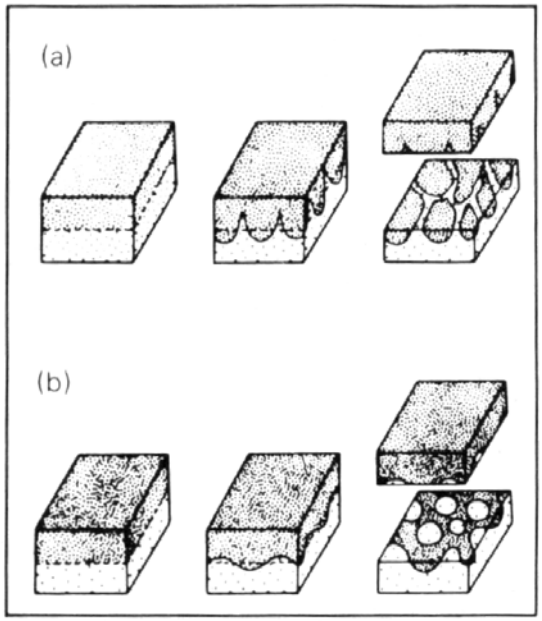

Fig. 3.15 Schematic illustration of the development of (a) flame structures and (b) load casts in laminated igneous rocks subject to plastic deformation caused by reversed density gradients prior to final consolidation (i.e. dark stippled material is heavier than light stippled material). In (a) the light material has lower viscosity than in (b), hence the relatively narrow flame structures and broader load casts, respectively. In both (a) and (b) the sequence from left to right shows the evolution of the structures with time.

aus Thorpe & Brown 1985

Klassifizierung pyroklastischer Gesteine

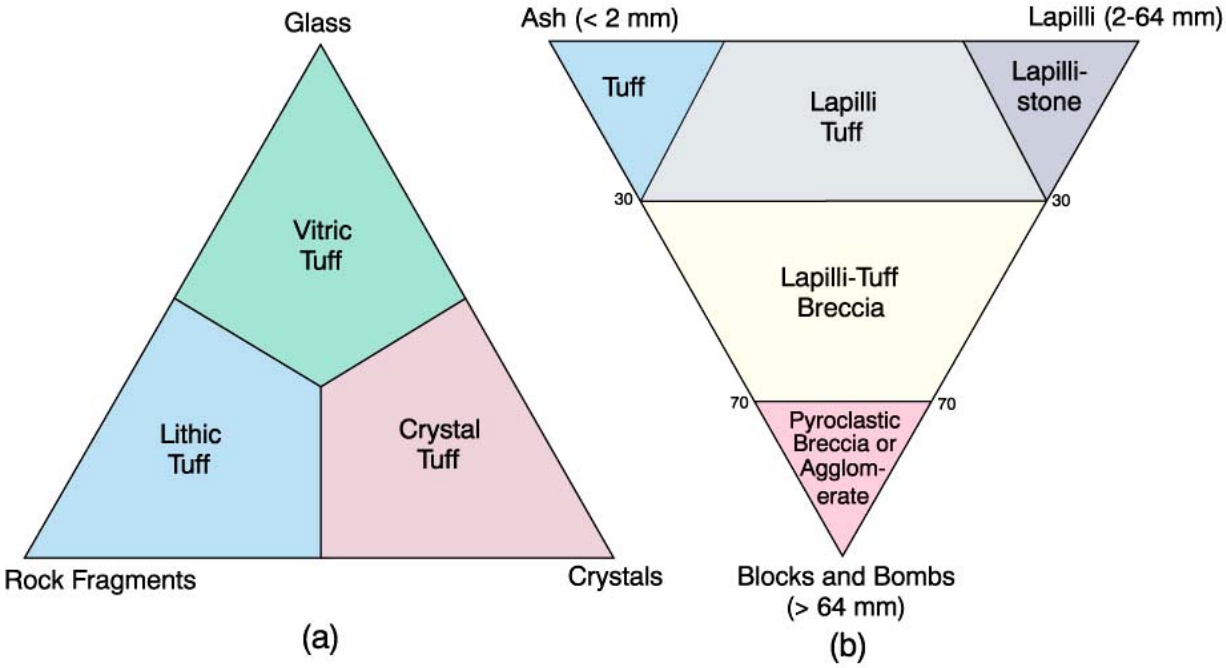

www.whitman.edu/geology/winter/

Klassifizierung siliziklastischer Gesteine

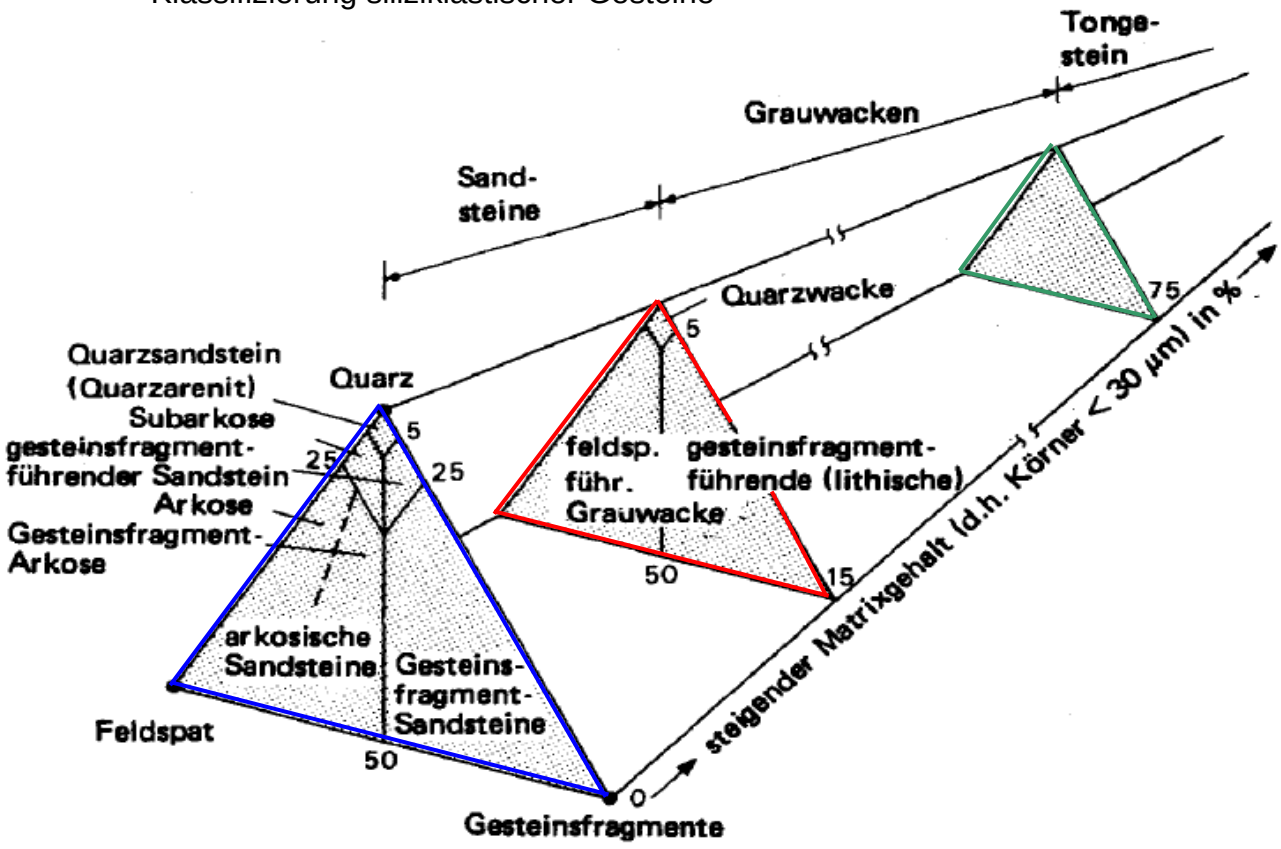

(aus Tucker 1985, nach Pettijohn et al. (1973)

Klassifizierung von Metamorphiten

Klassifikation der metamorphen Gesteine (aus MURAWSKI 1992)

Kontakt-metamorphose					Hornfels, Adinol				Kalksilikatfelse	Marmor	And Cor Sil Bt
					Garben-, Fleck-, Fruchschiefer, Spilosit, Desmosit						
		Konglomerat	Quarzsandstein	Granit	toniger Sandstein	Grauwacke, sandiger Ton	Diorit	Mergelton	Gabbro	Mergel, Mergelkalk	Kalk	Neubildungen
Regionalmetamorphose	Epizone	konglom. Quarzit, Quarzphyllit	Quarzit	geschieferter + mylonitisierter Granit	Quarzphyllit	Phyllit	Hornblendeschiefer	Kalk-Chlorit-schiefer	Grünschiefer	Kalkphyllite	Marmor	Sz Ch Ab Epi
	Mesozone	konglom Quarzit, Quarzglimmerschiefer			Quarzglimmerschiefer	Glimmerschiefer		Hornblendeschiefer, Para-Amphibolit	Ortho-AmphibolitEklogit	Kalkglimmerschiefer		Bt Mu Hbl St Dis Gra
	Katazone	Geröllgneis		Orthogneis, Granulit, Hälleflinta, Leptite	Leptite, Granulite	Paragneis	Hornblendegneis	Hornblendegneis, Eklogit	Eklogit	Kalksilikatgneise, -felse		Fsp Bt Gra Sil

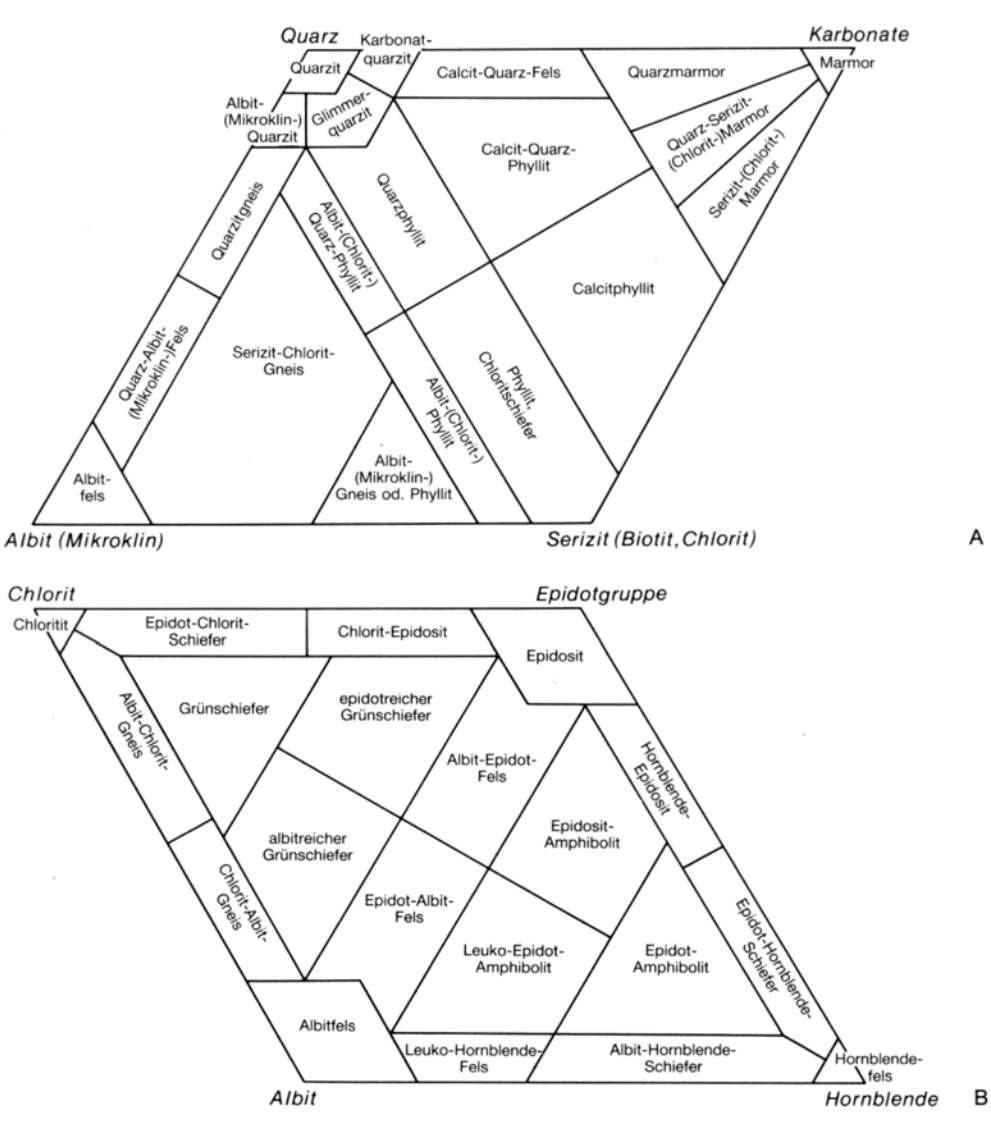

A) Klassifikation der niedrig metamorphen Metamorphite mit Quarz, Alkalifeldspäten, Serizit und Karbonaten als Hauptgemengteilen. Nach FRITSCH, MEIXNER & WIESENEDER 1967.

B) Klassifikation der niedrig metamorphen Metabasite und Albitgesteine (Quelle wie A).

aus: Wimmenauer 1985

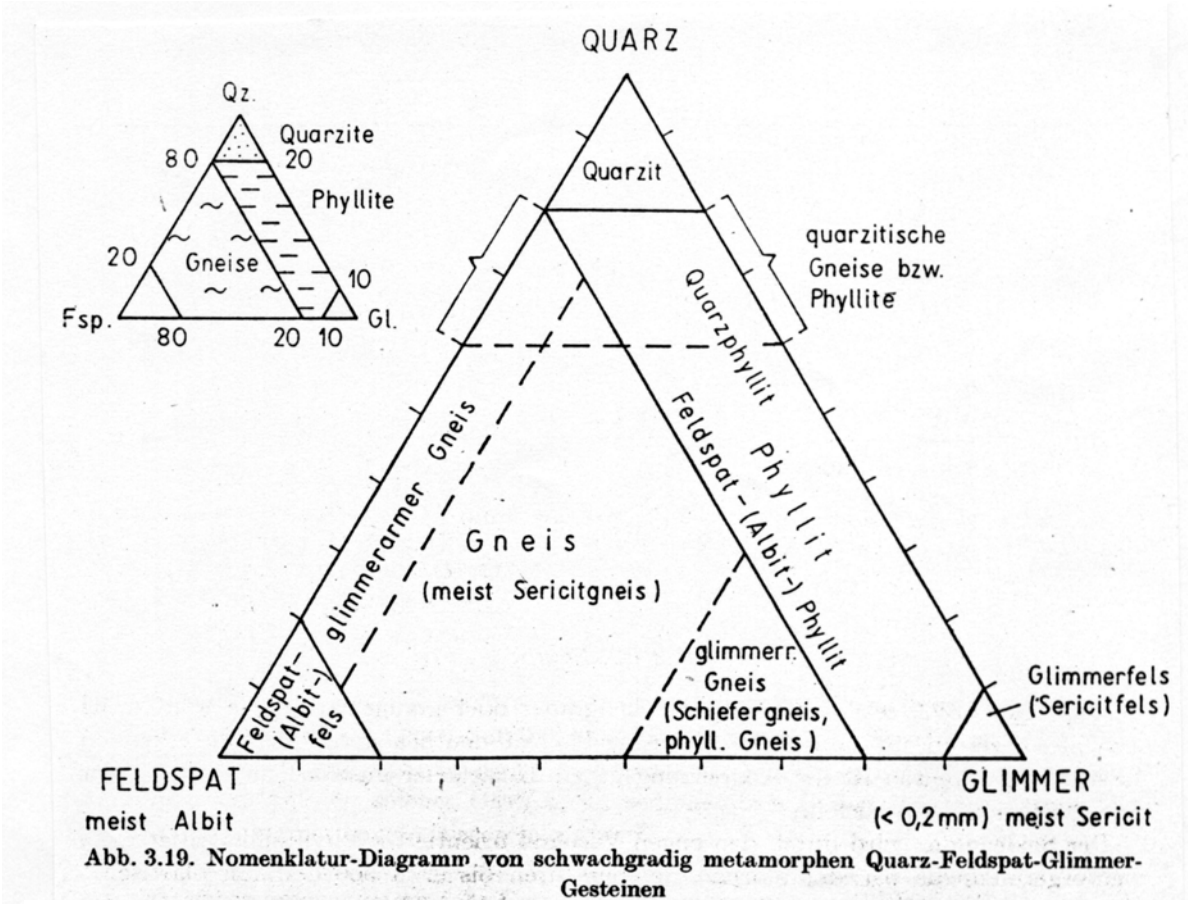

Abb. 3.19. Nomenklatur-Diagramm von schwachgradig metamorphen Quarz-Feldspat-Glimmer-Gesteinen

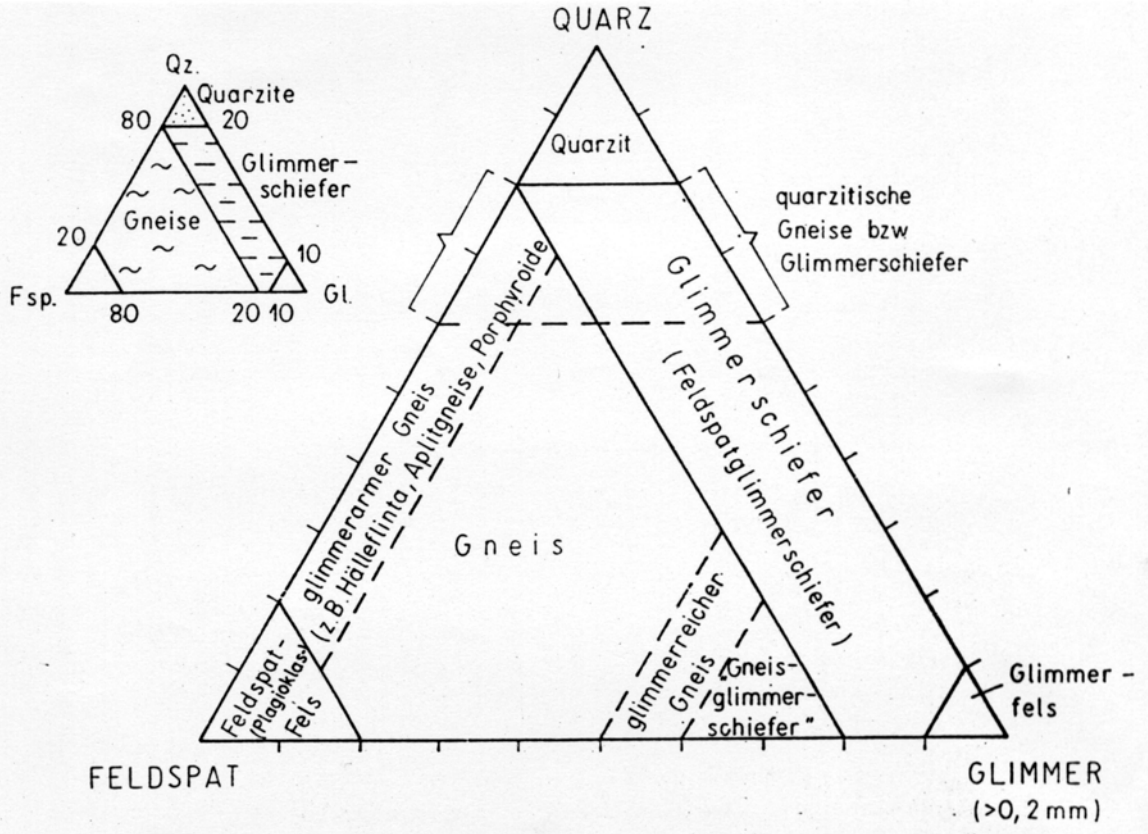

Abb. 3.20. Nomenklatur-Diagramm von mittelgradig metamorphen Quarz-Feldspat-Glimmer-Gesteinen

Appendix III: Petrogenetic grid for pelites (and psammites)

Key to reaction curves shown on P–T grid of this appendix (Figure A.III). Mineral abbreviations are after Kretz (1983), and are summarised in Appendix I.

(1) '(Stp + Ms)-out' ⇌ '(Bt + Ms)-in' (after Nitsch, 1970).
(2) Arg ⇌ Cal transformation (after Johannes and Puhan, 1971; Crawford and Hoersch, 1972).
(3) Cld ⇌ St (based on data from Hoschek, 1969; Ganguly and Newton, 1969).
(4) Chl + Ms + Qtz ⇌ Crd + Bt + Al_2SiO_5 + H_2O (after Hirschberg and Winkler, 1968).
(5) Prl ⇌ Al_2SiO_5 + Qtz + H_2O (based on data of Hemley, 1967; Kerrick, 1968, extended to higher P–T using calculations of phase equilibria from Wall and Essene, 1972).
(6) Kln + Qtz ⇌ Prl + H_2O (based on data of Thompson, 1970).
(7) Ms + Qtz ⇌ Kfs + Al_2SiO_5 + H_2O (Althaus et al., 1970).
(8) Ab + Ms + Qtz + H_2O ⇌ melt + Al_2SiO_5 (Storre and Karotke, 1971).
(9) Ab + Or + Qtz + H_2O ⇌ melt (Tuttle and Bowen, 1958; Merrill et al., 1970).
(10) pure Sps-in
(11) pure Alm-in } (Hsu, 1968).
(12) Alm_{87}-Sps_{13}-in
(13) Type Ib ⇌ Type IIb chlorite (based on Hayes, 1970).
(14) approximate position marking mixed-layer clays-OUT (after Hoffman and Hower, 1979).
(15) 2M-Mica-IN (approximate) (after Hoffman and Hower, 1979).

V = vitrinite reflectance values (R_m) in relation to temperature (after Teichmuller, 1987).
ILLITE-field is based on Hoffman and Hower (1979).
Calculated JADEITE curves are from Brown and Ghent (1983) based on studies by Newton and Smith (1967), Ganguly (1973) and Wood et al. (1980).
Al_2SiO_5 stability fields based on experimental work of Salje (1986).

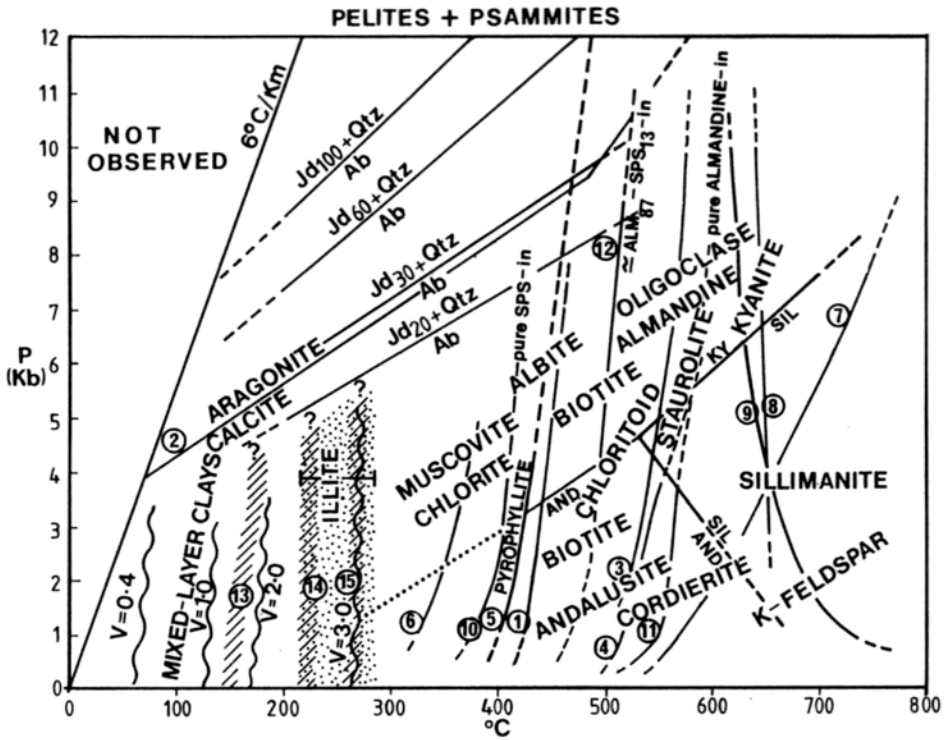

Figure A.III Petrogenetic grid for pelites (and psammites).

aus: Barker 1990

Appendix IV: Petrogenetic grid for metabasites

Key to reaction curves shown on the P–T grids of Figures A.IVa and A.IVb. Mineral abbreviations are after Kretz (1983), and are summarised in Appendix I.

(1) Arg ⇌ Cal transformation (after Johannes and Puhan, 1971; Crawford and Hoersch, 1972).
(2) maximum stability field for natural GLAUCOPHANES (after Maresch, 1977).
(3) '(Stp + Ms)-out' ⇌ '(Bt + Ms)-in' (after Nitsch, 1970).
(4a) Prh + Chl ⇌ Pmp + Act + Qtz) (after Winkler, 1979).
(4b) Prh + Chl ⇌ Pmp + Act + Czo).
(4c) Prh ⇌ Zo + Grs + Qtz + H_2O (data from Liou, 1971a) (upper stability limit of prehnite in CaO–SiO_2–Al_2O_3–H_2O system).
(5a–f) from Liou et al., 1985.
(5a) Hul ⇌ Lmt + Qtz + H_2O.
(5b) Lmt + Pmp ⇌ Czo + Qtz + H_2O.
(5c) Prh + Chl + Qtz ⇌ Czo + Tr + H_2O.
(5d) Prh + Chl + Qtz ⇌ Pmp + Tr + H_2O.
(5e) Pmp + Chl + Qtz ⇌ Czo + Tr + H_2O.
(5f) Gln + Czo + Qtz + H_2O ⇌ Tr + Chl + Ab.
(6a) 'Olg-in' (from Maruyama et al., 1983).
(6b) zone (stippled) of 2-plagioclases (from Maruyama et al., 1983).
(7) Actinolite ⇌ Hornblende (generalised zone of transition based on petrographic observation, geothermometry and geobarometry).
(8) Lws ⇌ Zo + Mrg + Qtz + H_2O (Nitsch, 1974).
(9) Mg-pmp ⇌ Czo + Chl + Grs + Qtz + H_2O (Schiffman and Liou, 1980).
(10) 'Pyx(Hy)-in' (often corresponds to 'Hbl-out') (generalised position based on petrographic observation, geothermometry and geobarometry).
(11) Spl-Lherzolite ⇌ Grt-Lherzolite (O'Neill, 1981).
(12a) Spl-Pyroxenite ⇌ Grt-Pyroxenite (Herzberg, 1978).
(12b) Ol + Pl ⇌ Opx + Cpx + Spl.
(13) Anl + Qtz ⇌ Ab + H_2O (Campbell and Fyfe, 1965).
(14) Wr ⇌ Qtz + An + H_2O (Liou, 1970, 1971b).
(15) Lmt ⇌ Wr + H_2O.
(16a) Lmt ⇌ Lws + Qtz + H_2O (Liou, 1971b).
(16b) Lws + Qtz ⇌ Wr.
(17a) 'Pl-out' [Ol-Tholeite]
(17b) 'Pl-out' [Peridotite]
(17c) 'Pl-out' [Qtz-Tholeite]
(18a) 'Grt-in' [Ol-Tholeite]
(18b) 'Grt-in' [Peridotite]
(18c) 'Grt-in' [Qtz-Tholeite]
(17a–18c) (Saxena and Eriksson, 1985).
(19a) Ol + Opx + Cpx + Pl ⇌ Pl + Opx + Cpx + Spl (for peridotite).
(19b) Ol + Opx + Cpx + Spl ⇌ Ol + Opx + Cpx + Grt (for peridotite) (Wyllie, 1971, 1979).

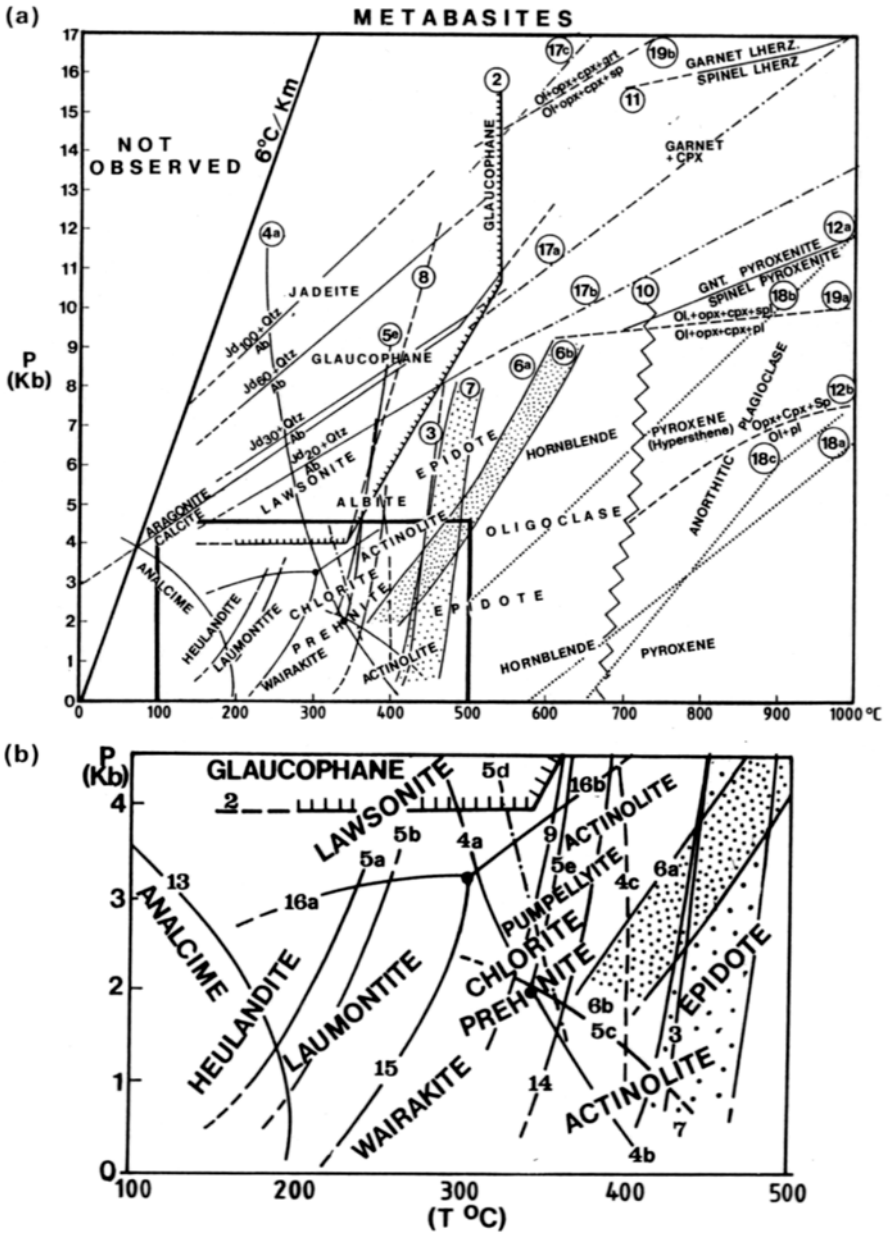

Figure A.IV (a) Complete petrogenetic grid (P = 0–17 kbar; T = 0–1000°C). (b) Detail of low grade portion of petrogenetic grid (P = 0–4.5 kbar; T = 100–500°C).

aus: Barker 1990

Mögliche Edukte metamorpher Gesteine

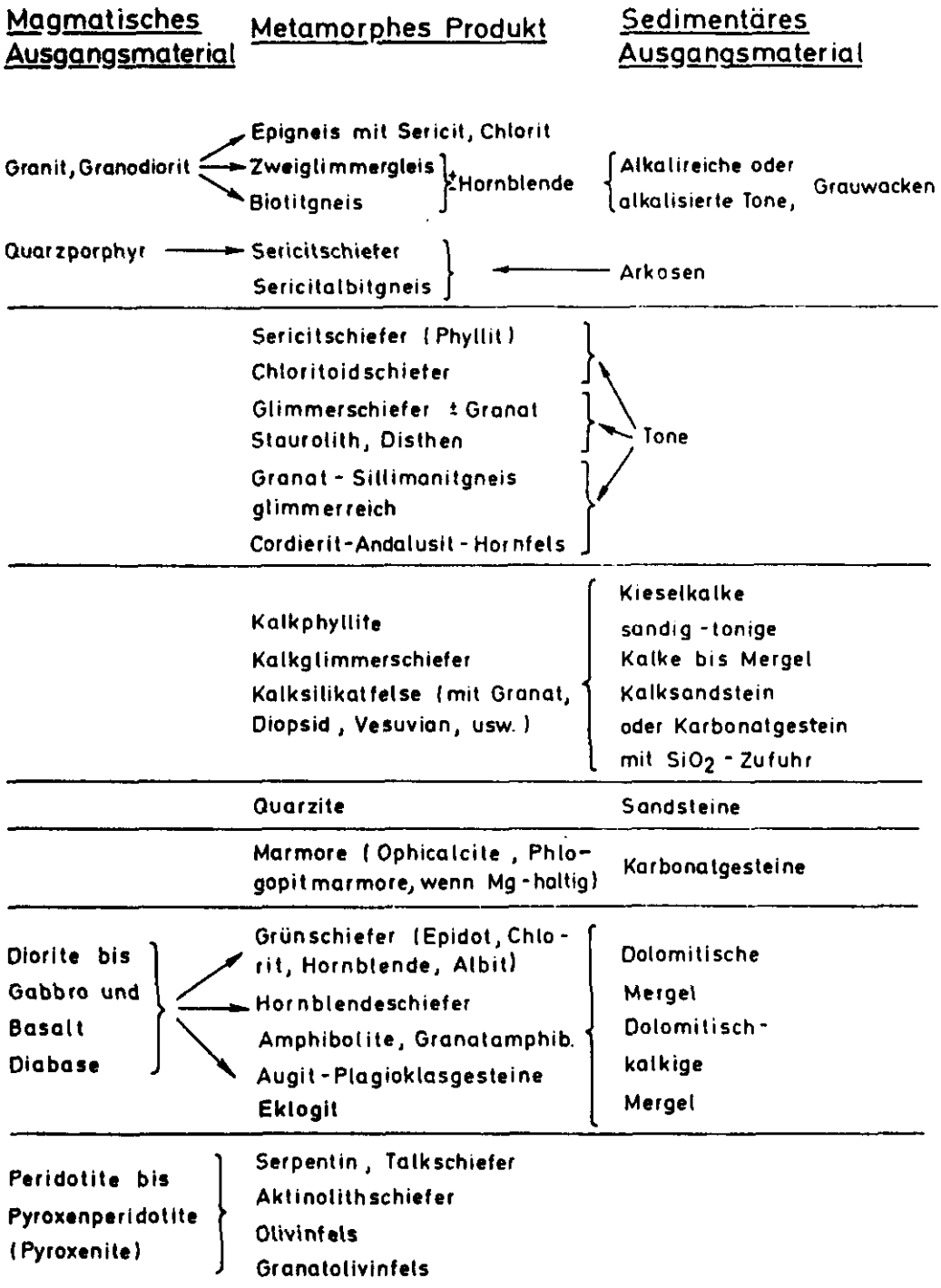

Kontaktmetamorphose

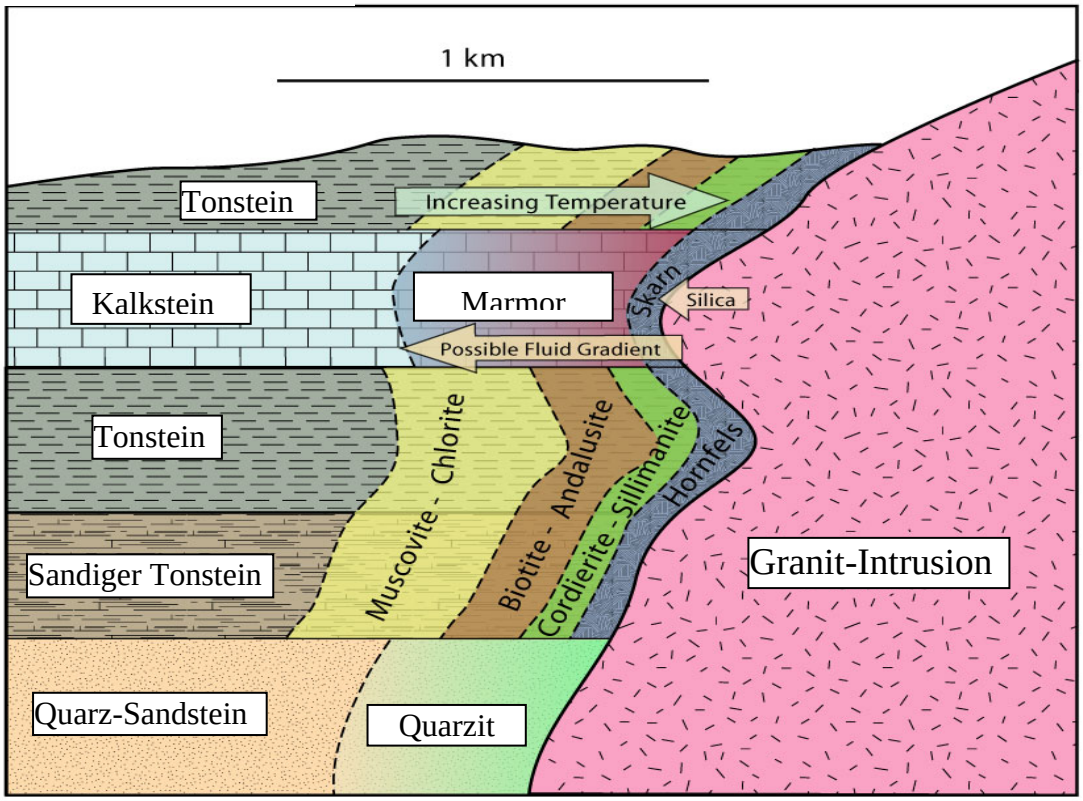

www.whitman.edu/geology/winter/

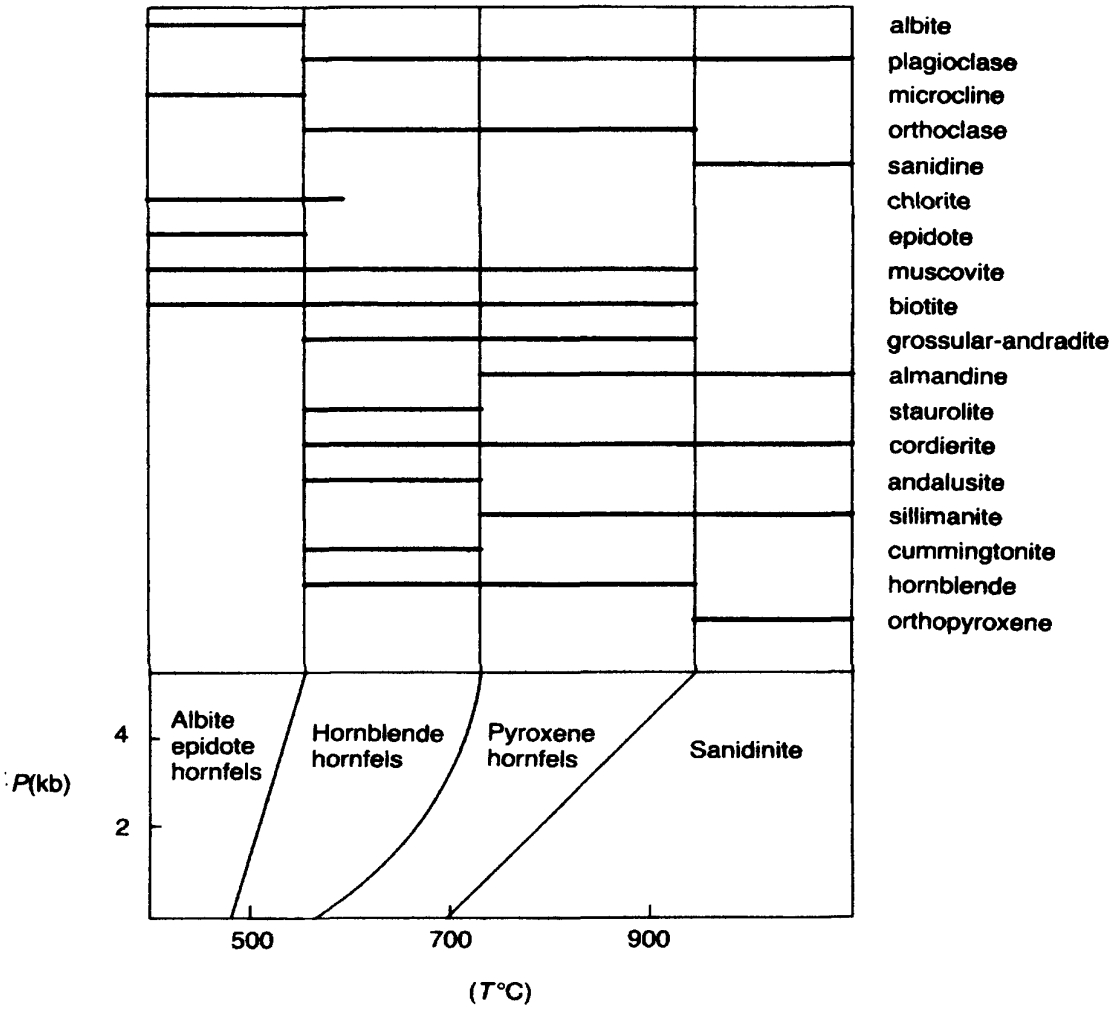

Migmatite 1

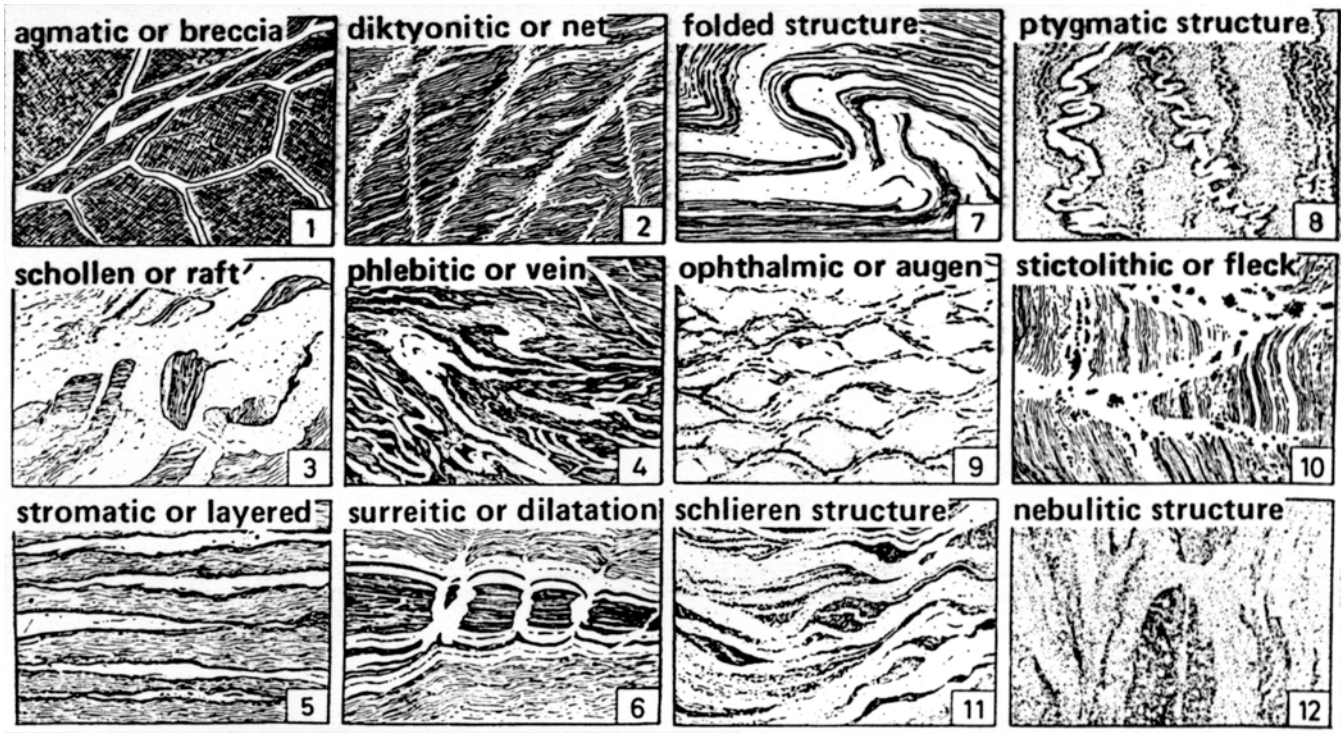

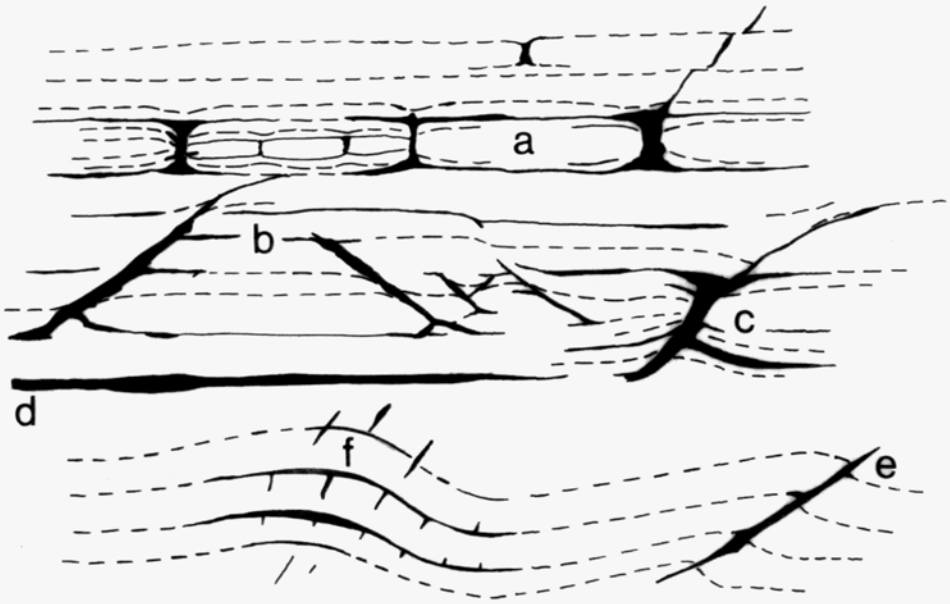

Fig. 2. Schematic representation of some of the structural sites in which the leucosome in dilational metatexite migmatites can be expected to occur. Solid areas and lines represent leucosome, whereas the dashed black lines are the traces of bedding or foliation. (a) Leucosome in interboudin partitions that develop in the competent layers of migmatites; these layers may be paleosome resisters, or even melanosome. Some boudins contain smaller internal boudins. (b) Leucosome located in extensional shear bands; both synthetic and antithetic examples are shown. (c) Leucosome located in an asymmetrical foliation boudin. (d) Stromatic leucosome oriented parallel to the principal plane of anisotropy, which may be either bedding or foliation. (e) Leucosome located in a reverse shear, cutting the short limb of an asymmetrical fold. (f) Leucosome associated with parallel folds; leucosome in the fold hinges is located in the space between dilated bedding planes; shorter domains of leucosome are located in extensional fractures developed on the outside of the folded competent layers and are not axial-planar, but tend to be radially disposed. Leucosome that is located parallel to a fold's axial plane occurs in the less competent layers.

aus: Sawyer 2008

Definitionen und Fakten zum Thema **MIGMATITE** aus dem Matthes:

"mixed rocks" Mischung aus magmatischen und metamorphen Gefügen, entstanden durch großregionale Aufschmelzungsprozesse (Anatexis).
Nach Mehnert (1968):

Paläosom unverändertes, hochmetamorphes Ausgangsgestein (teilweise auch Mesosom genannt, besser nicht benutzen).

Neosom durch selektive Aufschmelzungsprozesse migmatisch verändertes Gesteinsprodukt, teilt sich in Leuko- un Melanosom:

Leukosom magmatisches Kristallisationsprodukt partieller Aufschmelzung, hell, grantische Zusammensetzung (Qz, Plag, Kfspat).

Melanosom dunkle, mafische Minerale (und Überschuß-Plag und –Qz) im metamorphen lagigen Gefüge.

Restit Das veränderte metamorphe Gestein, aus dem das Leukosom ausgetreten ist (Biotit, Hornblende, Cordierit, Sillimanite, Granat etc.) = Melanosom.

Metatexite Anfangsstadium, helle Leukosome (magmatisch), dunkle Melanosome (Restite, metamorph)

Diatexite fortgeschrittene Aufschmelzung, kein klares Erkennen von Leuko- und Melanosom. Schlierig, nebulitisch, Gestein wird wieder homgener.

Anatexit (= anatektischer Granit) Gestein, das an Ort und Stelle (in-situ) aus einer Aufschmelzung (Anatexis) entstanden ist.

Die partielle Schmelzbildung verbraucht Qz, Kfspat, Plag und H_2O im kotektischen Verhältnis. Überschuss-Qz und –Plag bleibt in der Regel im Restit.

Anatexis beginnt bei 700°C wenn P_{H2O}=2.000 bar, 650°C wenn P_{H2O}=4.000 bar, bei hoeheren Wasserdruck auch tiefere Temperaturen möglich.
Die Anatexis des gleichen Gneises kann bei verschiedenen, erreichten Temperaturen verschiedene Schmelzen erbringen. Mit steigender Temperatur bilden sich erst granitische, dann granodioritische, dann quarzdioritische Schmelzen.
Max. Temperatur, die durch regionale Anatexis erreicht werden kann, ist 800°C.
Partien innerhalb von Migmatitgebieten, die aufgrund ihrer mineralogischen Zusammensetzung nicht angeschmolzen sind (Quarzite, Amphibolite, Kalksilikatfelse) heißen **Resisters**.
Metatekte (Leukosome in Metatexiten) konnen **Ektekte** oder **Entekte** sein.
Ektexis schmilzt das Leukosom vor Ort aus, es gilt die Stoffbilanz: Leukosom + Melanosom = Paläosom.
Bei Entekten ist das Leukosom in das Paläosom eingedrungen (Injektion), das Melanosom fehlt (keine Restitsäume an den Grenzen des Leukosomes).

Matthes, S. (1996): Mineralogie. – 5. Auflage, 499 S., Springer.
Mehnert, K. R. (1968): Migmatites and the origin of granitic rocks. 391 S., Amsterdam.

Alle Definitionen nach Mehnert (1968) werden empfohlen von der IUGS Subcommission on the Systematic of Metamorphic Rocks (www.bgs.ac.uk/scmr/).
Dies gilt nicht für: "Ektekte" und "Entekte". Diese Begriffe werden von der Kommission nicht diskutiert, es werden allerdings auch keine Alternativen vorgeschlagen, also ruhig benutzen.

Hangend-Liegend-Kriterien in Migmatiten (aus: Burg 1991)

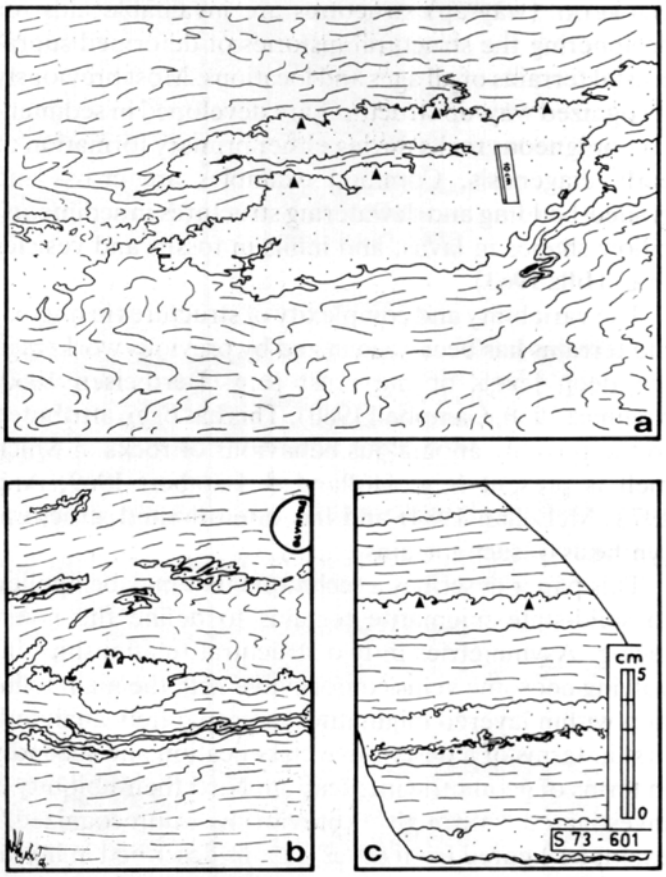

Fig. 2. Examples of cauliflower structures at different scales sketched from photographs. Quartz, plagioclase (and K-feldspar ?) veins = leucosomes (dotted) in gneisses (dashed). Triangles point toward the inferred hanging-wall. (a) "Migmatitic phenomenon" photographed by Mehnert in Granholmen, Sweden, drawn after fig. 1.1 of Ashworth (1985). (b) "Discontinuous segregations that are conspicuously coarser-grained than the moderately well-foliated, dark-coloured hornblende–biotite feldspar schist" drawn from part of fig. 11-9 of Best (1982), unspecified location. Note that the inferred top-side is consistent with growing grass in the lower left corner. (c) "Migmatite hand specimen" from Arvika, Sweden, drawn after fig. 14 of Johannes (1983). While this article was being refereed, a convincing plate with a top-side interpretation has been published by Culshaw & van Breemen (1990, fig. 7c).

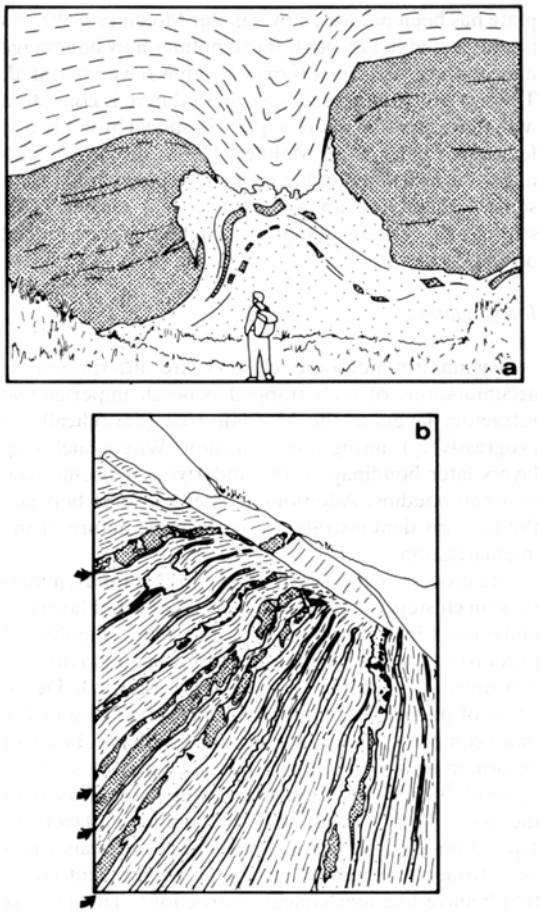

Fig. 4. Examples of asymmetric vein clusters sketched from field photographs. Leucosomes and pegmatitic veins (dotted) in gneiss (dashed) with boudinaged amphibolites (stippled dark). (a) "Spectacular boudinage of a Kangâmiut dyke in the north-east part of Sondre Stromfjord" drawn after fig. 77 of Escher & Watt (1976). Note that the pegmatoid vein lies below the dyke only. Ascent of the pegmatitic vein occurred between boudins (incipient destruction of the vein cluster structure) and developed cauliflower structures eradicating the rock foliation on the top-side. Both cauliflower and asymmetric vein cluster structures consistently indicate the top-side. (b) "Thin boudinaged layers of amphibolite in differentiated gneiss" at Sondre Stromfjord Airport, drawn after fig. 4(a) of van der Molen (1985b). Asymmetric vein clusters (arrowed) were partly destroyed by progressive deformation. This intensely deformed stage includes leucosome segregation in zones between boudins and veining along the upper boundary. The resulting product of progressive deformation leads to the widespread occurrence of fragments floating within remarkably planar pegmatitic layers as described in many field areas. Possible 'cauliflower structures' (triangles) are consistent with the top-side as defined by the sloping sky-line.

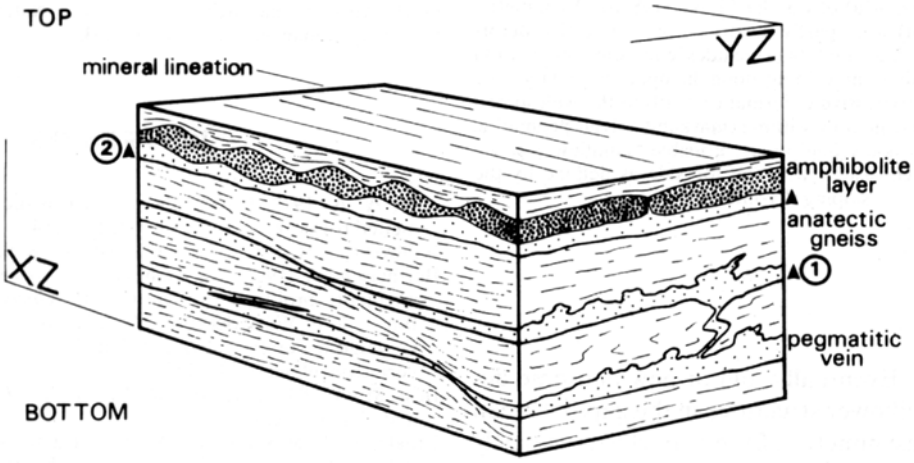

Fig. 3. Schematic block diagram illustrating cauliflower (1) and asymmetric vein cluster (2) structures in an idealized normal sequence of flat-lying anatectic gneisses. Arrows point towards the top of the sequence. Observations in the *YZ* plane of finite strain are essential. Shear deformation as indicated by shear bands in *XZ* sections is top-to-the-right.

Foliationen und Lineationen als Bezugssystem

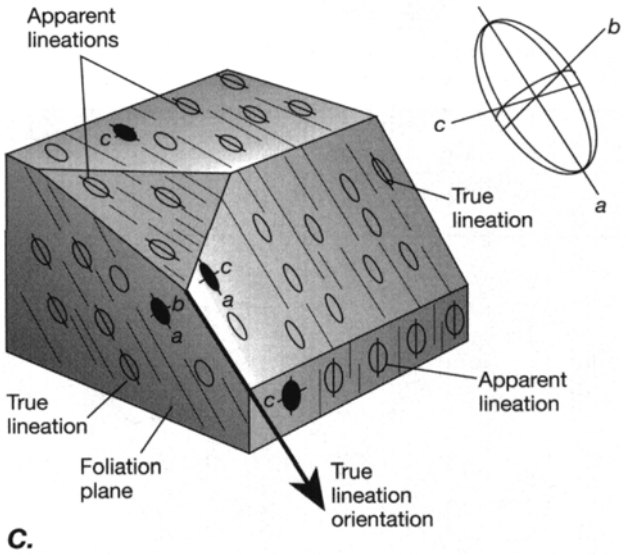

Figure 13.19 Discrete lineations. *A*. A stretched pebble conglomerate showing quartzite pebbles flattened parallel to the foliation and elongated to define a lineation. *B*. Alteration spots in a slate. The foliation is perpendicular to the plane of the photo, and the maximum and minimum axes of the ellipsoids are exposed (*a* and *c*; see also part C). *C*. True and apparent lineations associated with ellipsoidal structures. The true lineation orientation is shown on any plane containing the *a* axis (longest axis) of the ellipsoid. Planes of other orientations show elliptical sections through the ellipsoidal structures that do not define the true orientation of the lineation.

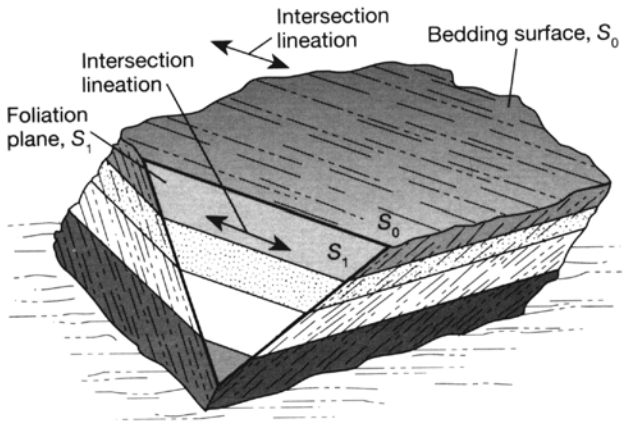

Figure 13.20 Intersection lineations. *A*. The intersection of a foliation and a bedding surface. The trace of the secondary foliation S_1 on the bedding S_0 and the trace of S_0 on S_1 are essentially the same lineation. *B*. Pencil cleavage in argillite, an intersection lineation defined by the intersection of two foliations, one of which may be bedding. Cleavage of the rock along both foliations produces elongate prisms, or pencils, of

aus: Twiss & Moores 1992

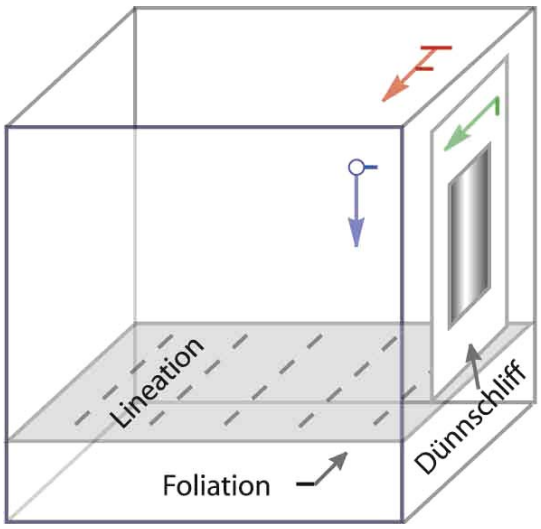

Referenzsystem für die Orientierung von Dünnschliffen

Grüner Pfeil: Orientierungsmarker auf Dünnschliffträger mit definierter Ausrichtung zu Lineation und Foliation.

aus: Eimer 2008

Lineations in tectonites (surficial or penetrative)	Structural	Discrete	Pebbles Ooids Fossils Alteration spots
		Constructed	Hinge lines Intersections Boudin lines Mullions Structural slickenlines
	Mineral	Polycrystalline	Rods Mineral clusters Mineral slickenlines Nonfibrous overgrowths
		Mineral grain	Acicular habit grains Elongated grains Mineral fibers Fibrous vein filling Slickenfibers Fibrous overgrowths

Figure 13.18 Morphological classification scheme for lineations.

Quelle unbekannt

Foliationen und Lineationen

sedimentär, diagenetisch, deformativ, magmatisch

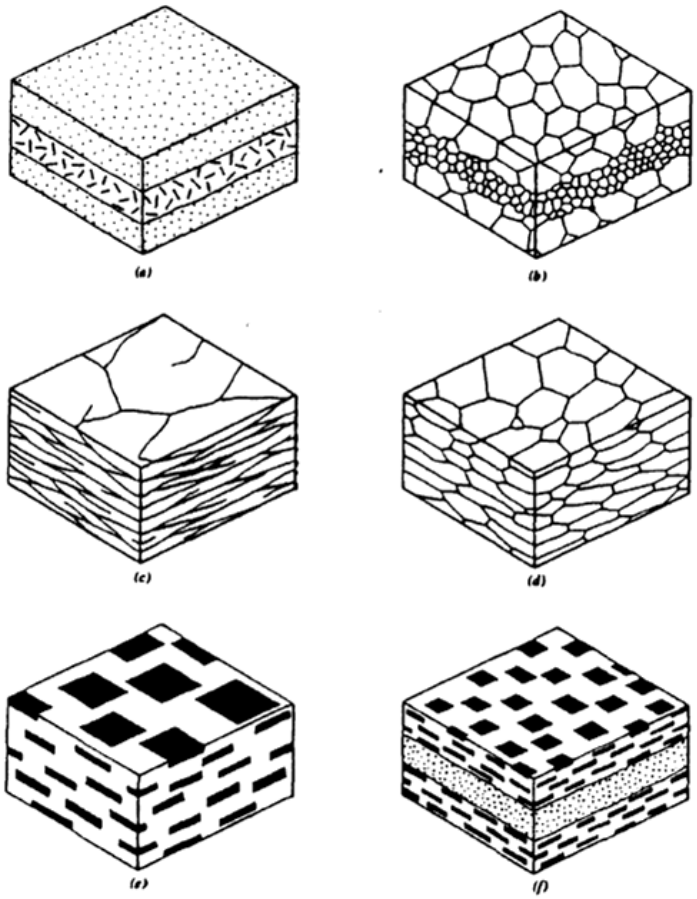

FIGURE 5.1 Diagrammatic representation of various types of foliation. The foliations are defined by: (*a*) compositional layering; (*b*) grain-size variation; (*c*) closely spaced, approximately parallel discontinuities such as microfaults or fractures; (*d*) preferred orientation of grain boundaries; and (*e*) preferred orientation of platy minerals or lenticular mineral aggregates. These various microstructures can be combined and (*f*) shows a combination (*a* + *c*) that is very common in both sedimentary and metamorphic rocks.

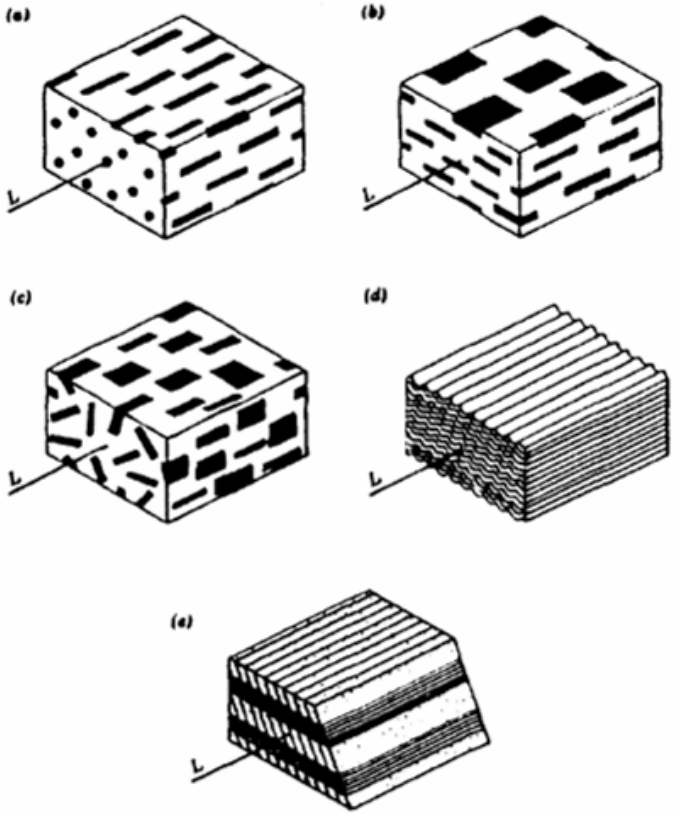

FIGURE 6.1 Diagrammatic representation of lineation (*L*). The elements represented by the idealized black shapes in (*a*), (*b*), and (*c*) may be individual grains, metamorphic mineral aggregates, or any other bodies such as fossils, pebbles, and so on. (*a*) Simple linear fabric defined by preferred orientation of linear bodies. (*b*) Combined lineation and foliation defined by preferred orientation of elongate tabular bodies. (*c*) Linear fabric defined by common axis of intersection of variably oriented, tabular bodies. (*d*) Linear fabric defined by penetrative folding. (*e*) Lineation defined by intersection of two foliations.

magmatisch

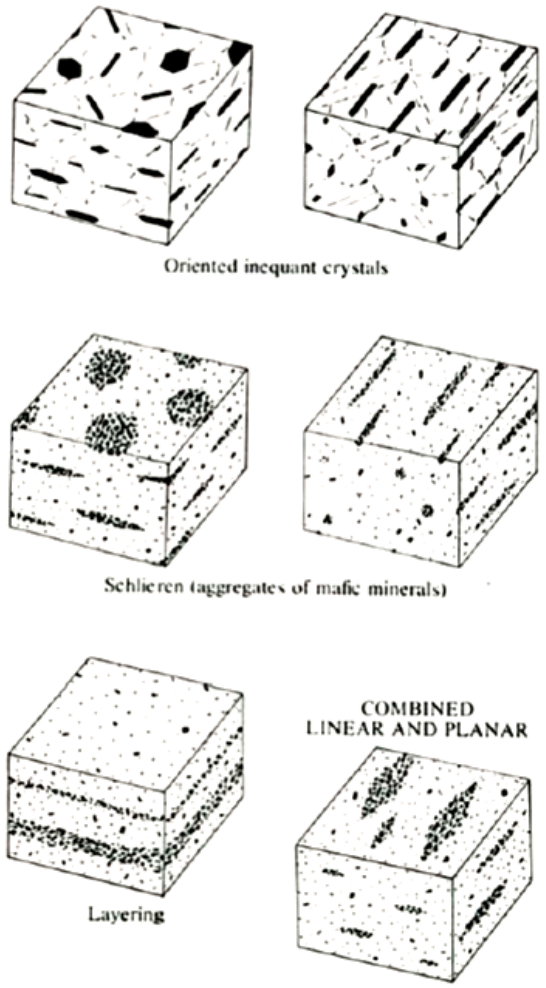

Figure 4-6 Anisotropic fabrics in granitic, dioritic, and some other types of plutonic magmatic rocks.

Foliation durch Deformation (Vergneisung); aus: Passchier et al. 1990

einfach

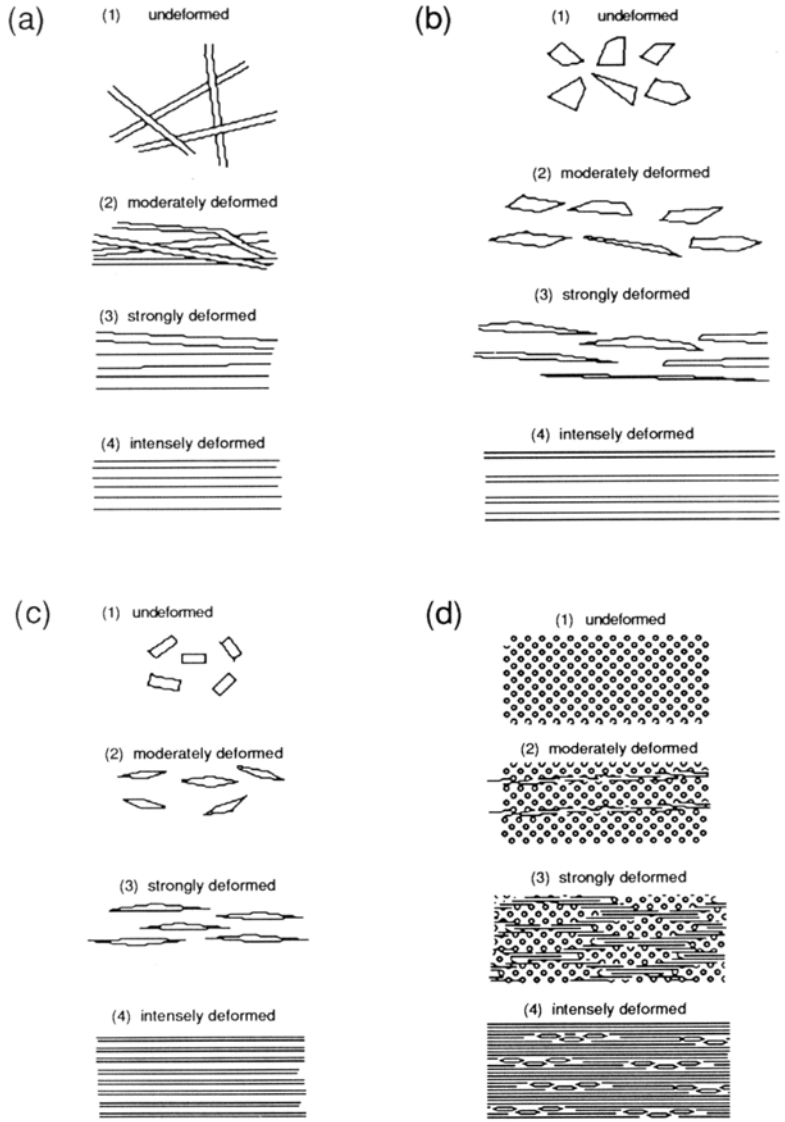

Fig. 3.8. Four examples of outcrop-scale progressive deformation typical of high-grade gneiss terrains, all leading to a uniform, parallel-layered gneiss; (a) homogeneous deformation of vein networks; (b) homogeneous deformation of rock fragments; (c) homogeneous deformation of a homogeneous igneous rock with heterogeneous grain size, e.g. porphyritic granite; (d) inhomogeneous deformation of a homogeneous igneous rock, e.g. gabbro.

komplex, mehrphasig

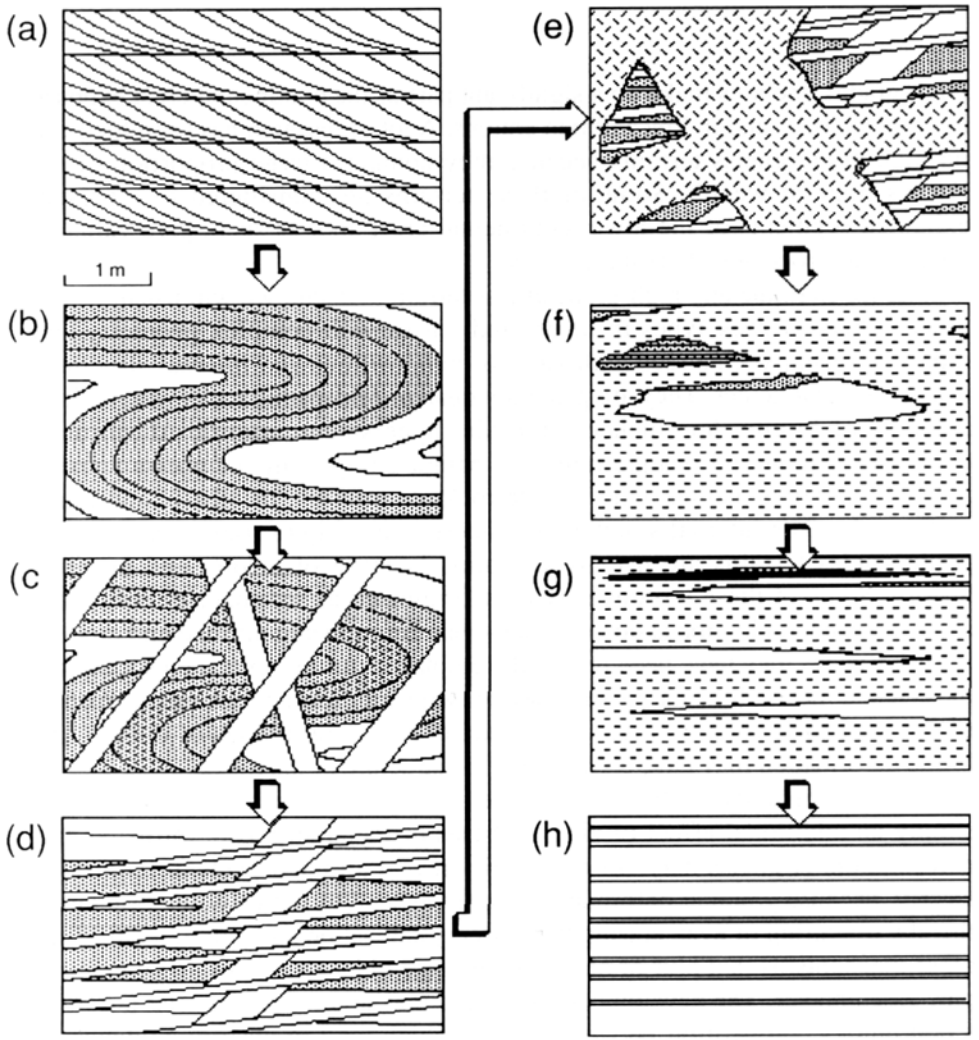

Fig. 1.1. A homogeneous, apparently undeformed layered gneiss (h) may have been derived by the sequence of events a-h: starting as a sediment (a), followed by phases of deformation (a-b, c-d, e-h) and intrusion (b-c, d-e). The intensity of deformation and the amount of igneous material involved is much greater than would be expected from the final result. The original volume of sedimentary rocks (in grey) forms only a small percentage of the final gneiss.

Temperaturabhängige Verformungsprozesse in Granitoiden im Subsolidus-/Solidusbereich

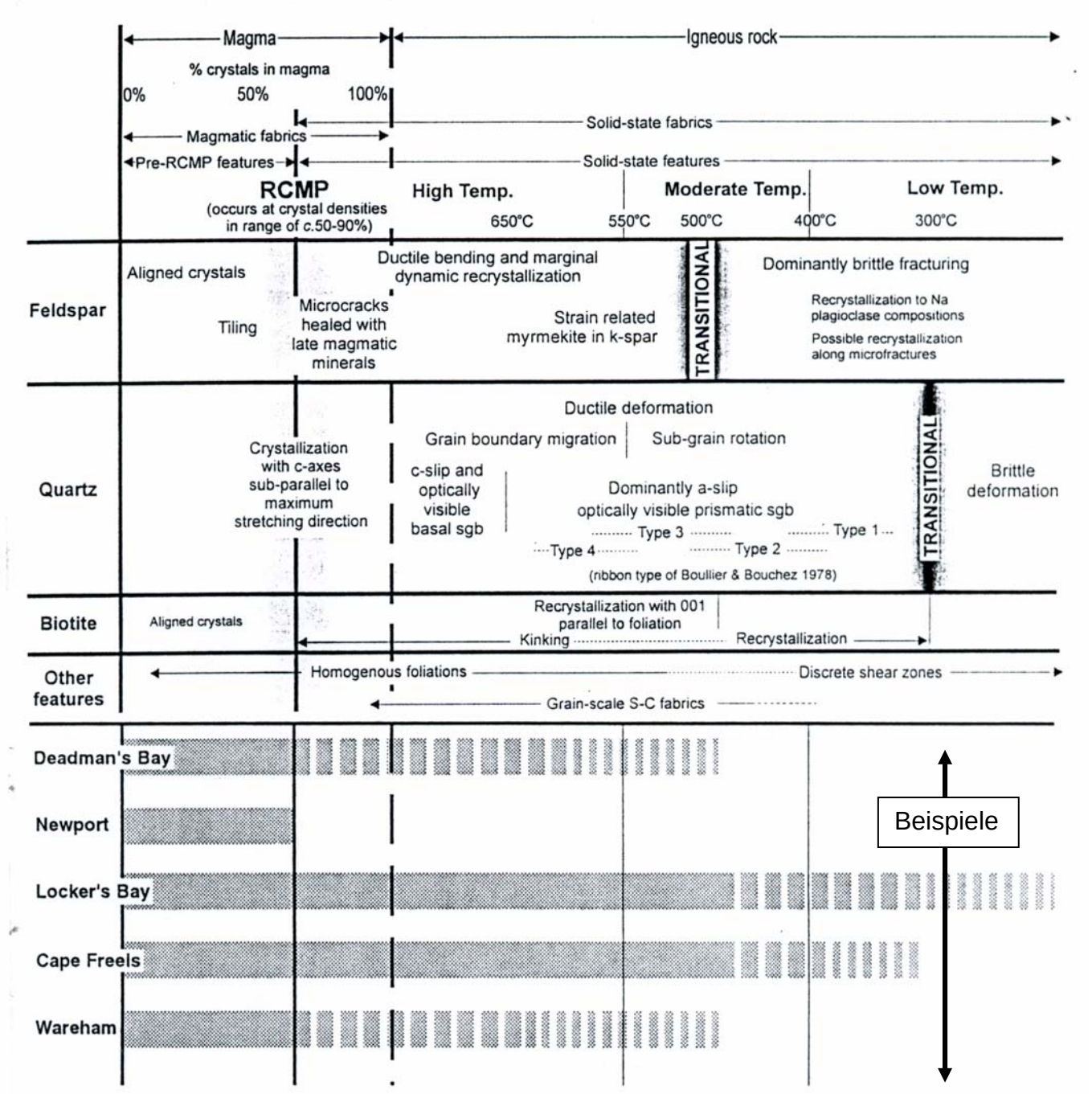

Fig. 7. Summary table showing the relationship between mineral microstructures, temperature and degree of crystallinity in a cooling syn-tectonic granite (after Tribe and D'Lemos, 1996 and references therein), also summarizing the micro-structural styles preserved by the individual plutons as a result of their contrasting cooling.

RCMP = **R**heological **C**ritical **M**elt **P**ercentage (bei etwa 70 % Kristallvolumen im Magma

aus: Schofield & D´Lemos 1998

Klassifizierung von Falten 1

Table 3.1 Terms used to describe the tightness of folds

	Interlimb angles	*Fold tightness*
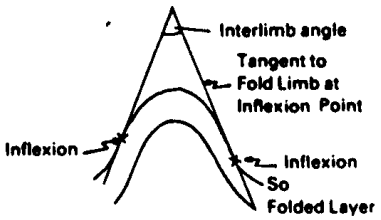	180°–120°	Gentle
	120°–70°	Open
	70°–30°	Close
	30°–0°	Tight
	0°	Isoclinal
	less than 0°	Elasticas
	-ve angle	or Ptygmatic

Table 3.2 Terms describing the attitude of folds

Dip of the fold axial surface or plunge of the fold axis	*Dip of hinge surface (i.e. attitude of axial plane)*	*Plunge of hinge line (i.e. attitude of fold axis)*
0°	Recumbent fold	Horizontal fold
1°–10°	Recumbent fold	Sub-horizontal fold
10°–30°	Gently inclined fold	Gently plunging fold
30°–60°	Moderately inclined fold	Moderately plunging fold
60°–80°	Steeply inclined fold	Steeply plunging fold
80°–89°	Upright fold	Sub-vertical fold
90°	Upright fold	Vertical fold

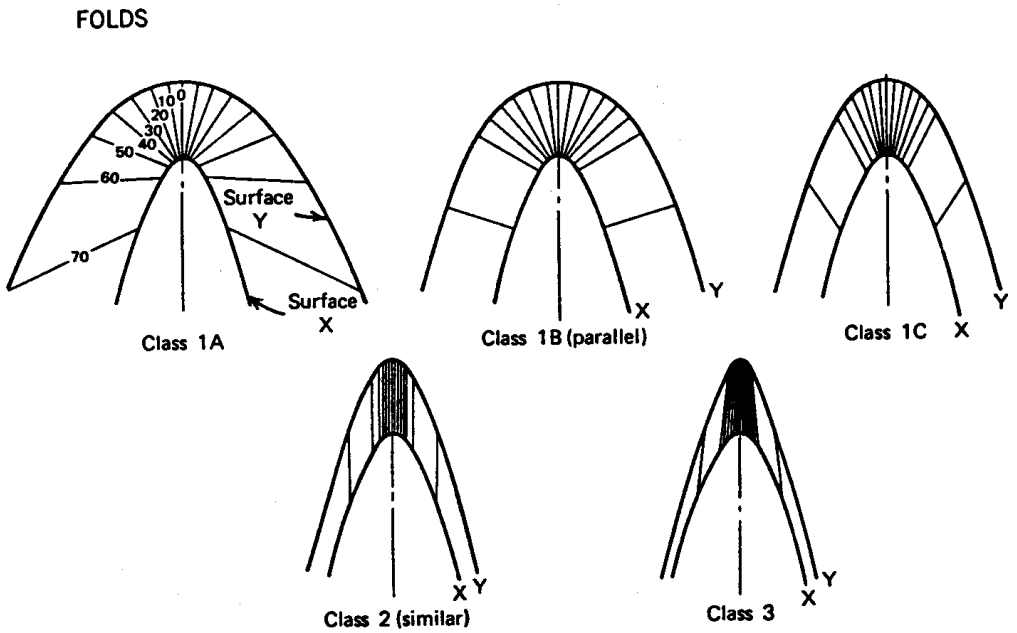

FIGURE 4.26 Classification of folds based on dip isogons; Dip isogons have been drawn at 10° intervals from the lower to upper surfaces X and Y. [From J. G. Ramsay (1967), *Folding and Fracturing of Rocks.* Copyright © 1967, McGraw-Hill Book Co. Used with permission of McGraw-Hill Book Co.]

Klassifizierung von Falten 2

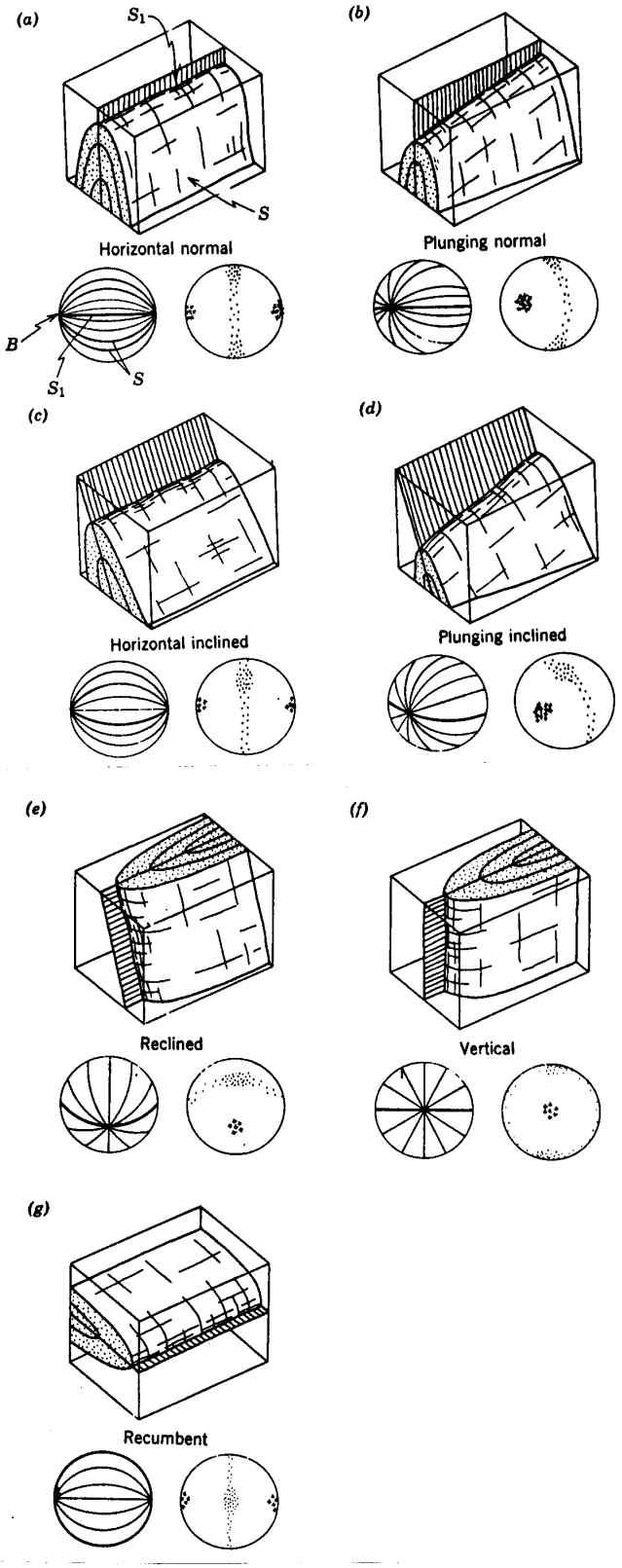

FIGURE 4.25 Classification of folds based on orientation of hinge line and axial surface (see Table 4.1); after Turner and Weiss (1963). Diagrammatic projections below each block diagram show orientation data; left-hand projections show cyclic representation of several S planes and the axial plane (heavy line) for ideally cylindrical folds. The right-hand diagrams are a more realistic representation of poles to S ($\perp S$) and of the orientation of the fold axes measured at different points on a fold that is statistically cylindrical.

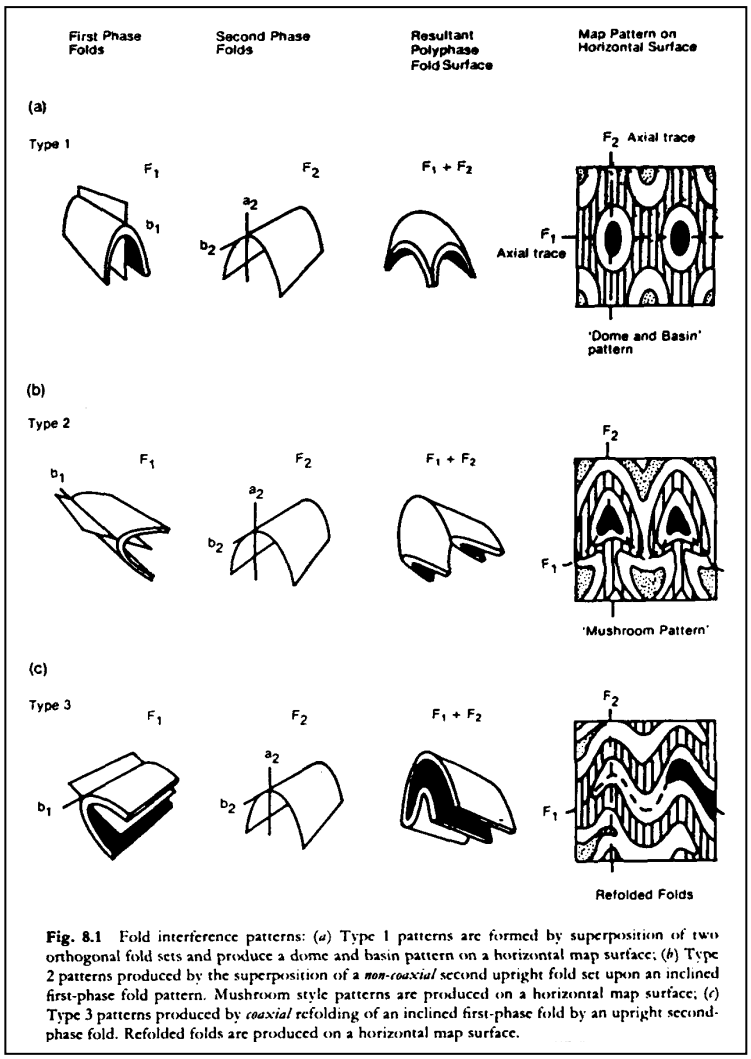

Fig. 8.1 Fold interference patterns: (*a*) Type 1 patterns are formed by superposition of two orthogonal fold sets and produce a dome and basin pattern on a horizontal map surface; (*b*) Type 2 patterns produced by the superposition of a *non-coaxial* second upright fold set upon an inclined first-phase fold pattern. Mushroom style patterns are produced on a horizontal map surface; (*c*) Type 3 patterns produced by *coaxial* refolding of an inclined first-phase fold by an upright second-phase fold. Refolded folds are produced on a horizontal map surface.

Klassifizierung von Falten 3

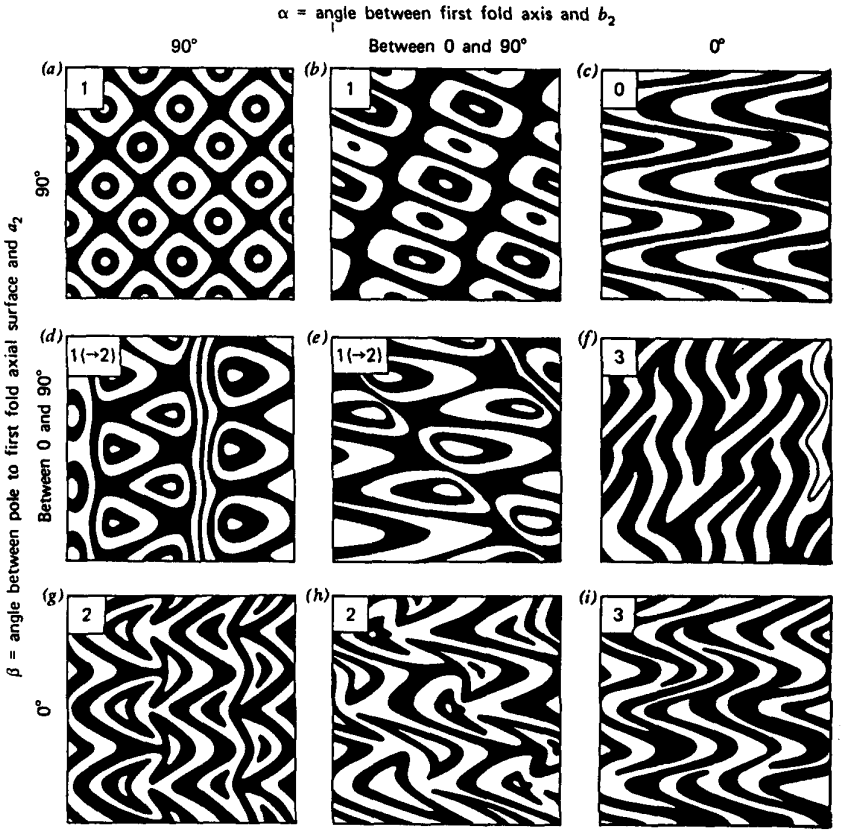

FIGURE 8.8 Two-dimensional interference patterns resulting from superposition of two generations of folds. The second-generation folds are assumed to be ideally similar so that the geometrical relationship between the two generations can be described, for B_2, in terms of kinematic axes a_2 and b_2 (see Section 4.7). The numbers in the top left-hand corner of each figure denote end members in the spectrum of interference patterns. Patterns 1, 2, and 3 result from overprinting relationships of the type depicted in Figures 8.9, 8.10, and 8.11, respectively. 1(−2) are transitional patterns resulting from overprinting relationships transitional between those depicted in Figure 8.9 and 8.10. O is a special case where B_1 and B_2 have parallel axes and axial surfaces and, therefore, do not produce any characteristic interference pattern. [From J. G. Ramsay (1967, *Folding and Fracturing of Rocks*. Copyright © 1967 by McGraw-Hill Book Co. Used with permission of McGraw-Hill Book Co.]

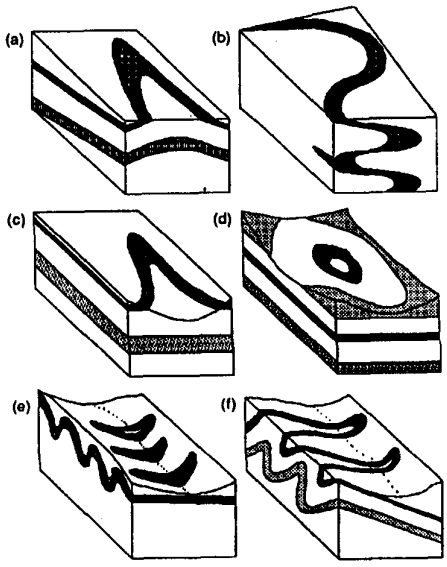

5a-f. Geometric patterns as a function of the orientation of planar and curved outcrop : (a) Apparent tight folding of gently folded layering. (b) Apparent open folding of folded layering. (c) Apparent tight folding of planar layering. (d) Apparent fold nce patterns of Type I in planar layering; apparent fold interference patterns of Type II Type III (f) in layering with one phase of folding.

Geopetale Gefüge (Hangend- Liegendkriterien): sedimentär

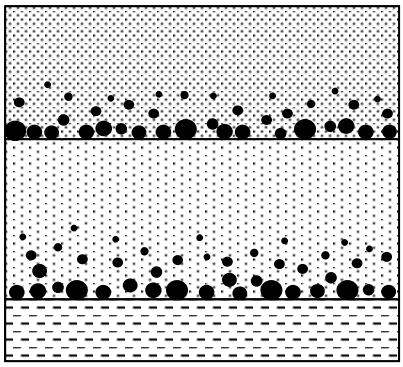

Gradierung

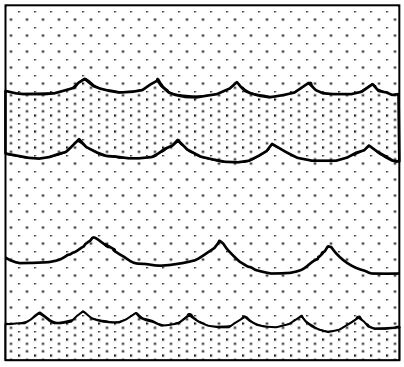

Oszillationsrippeln

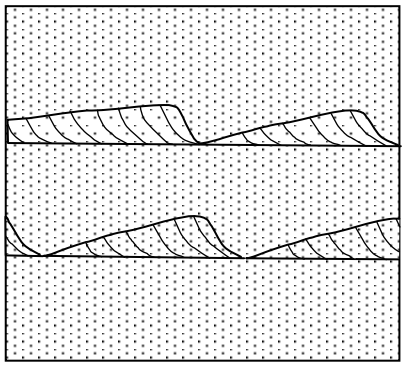

Strömungssrippeln

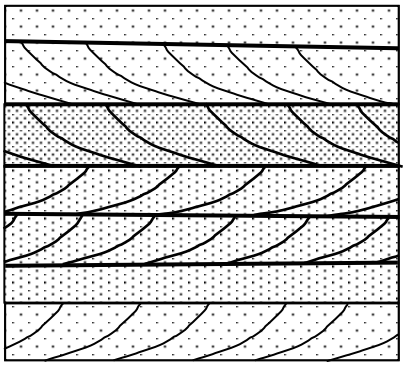

Schrägschichtung

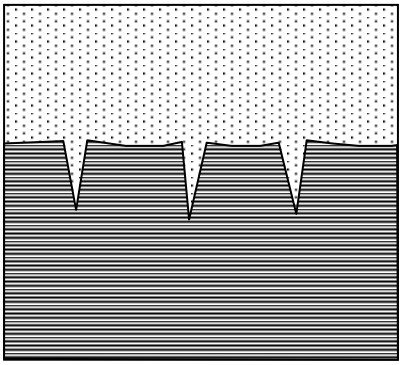

Trockenrisse

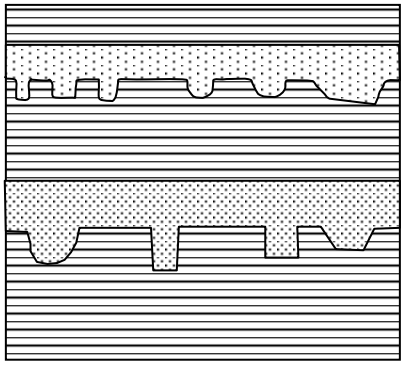

Sohlmarken (Abdrücke, Schleifspuren etc.)

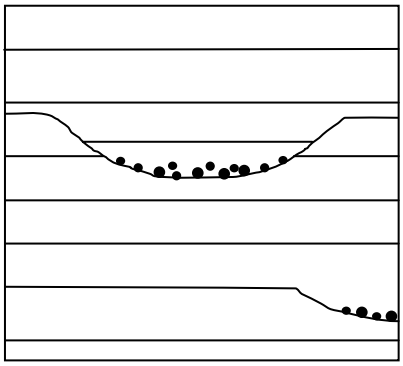

Rinnensedimente

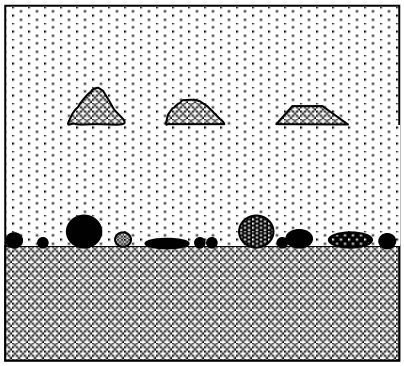

Auflagefläche / stabile Lage

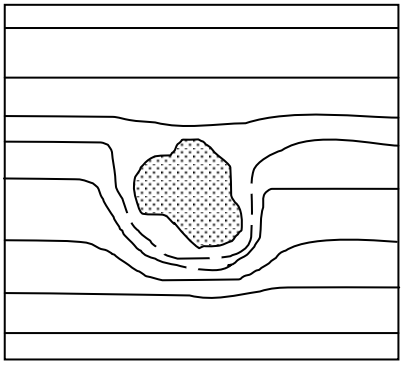

Dropstone

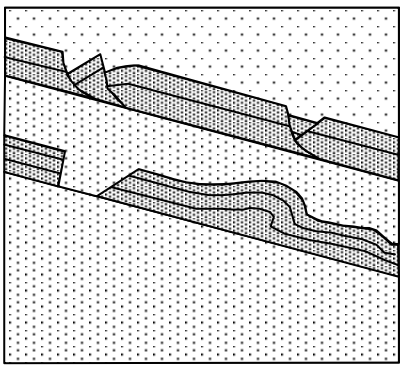

Rutschstrukturen

Geopetale Gefüge (Hangend- Liegendkriterien): diagenetisch

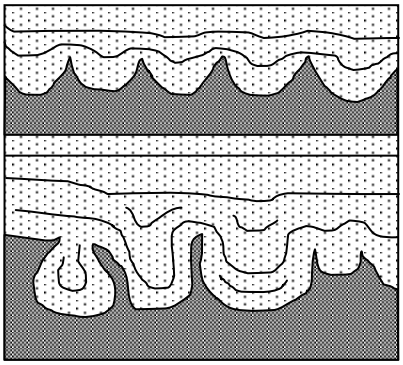

Belastungsmarken

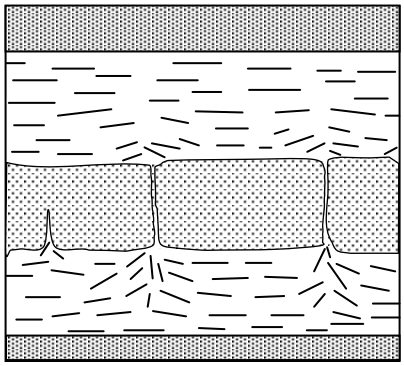

Entwässerungsstrukturen

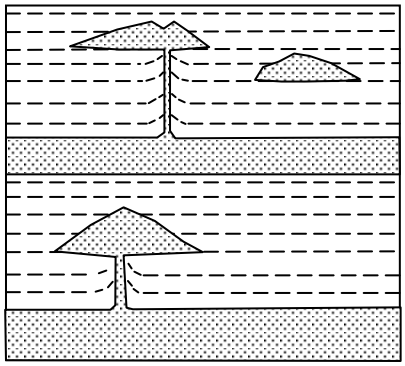

Sandvulkane

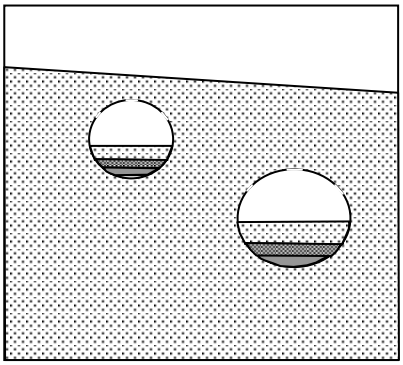

Hohlraumsedimente u. -kristallisate

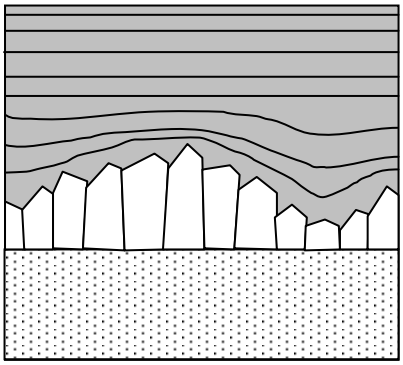

Kristallrasen, frühdiagenetisch

Geopetale Gefüge (Hangend- Liegendkriterien): biogen/sedimentär

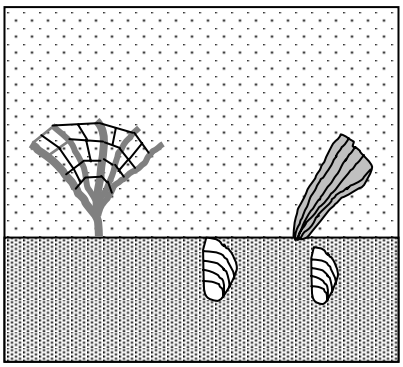

Fossilien in Lebendstellung

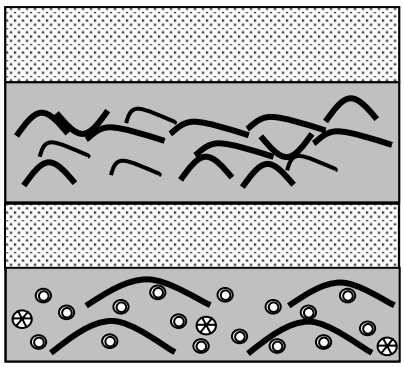

Schilllagen

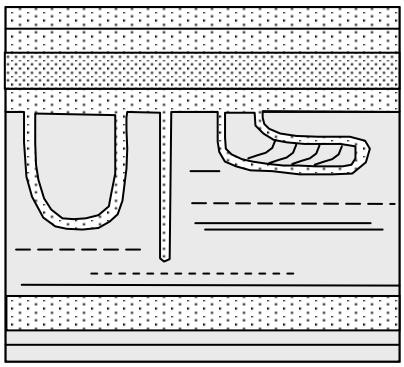

Grabbauten

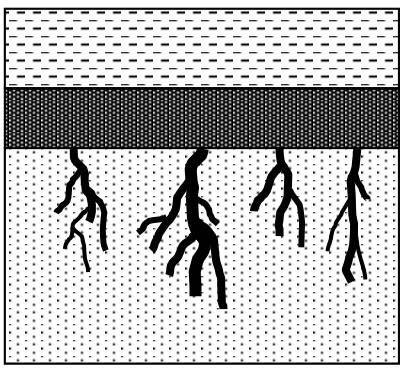

Wurzelböden

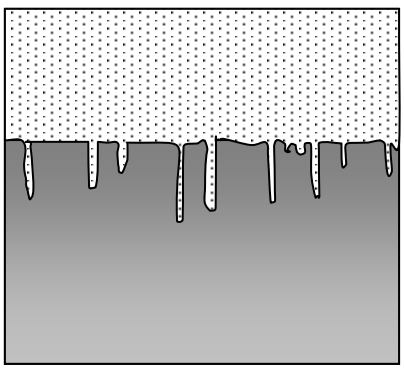

Bohrgänge in Hartgründen

Geopetale Gefüge (Hangend- Liegendkriterien): magmatisch

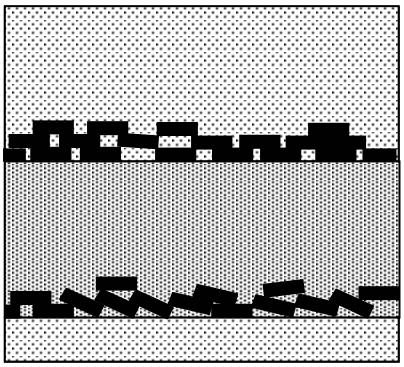

Kumulate (nach Dichte)

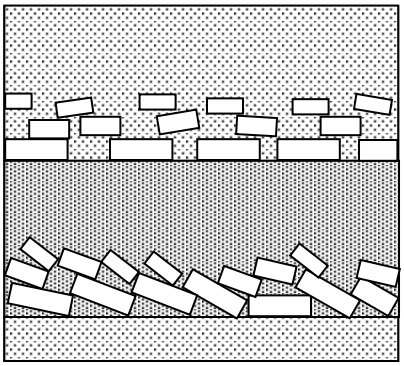

Kumulate (nach Korngröße)

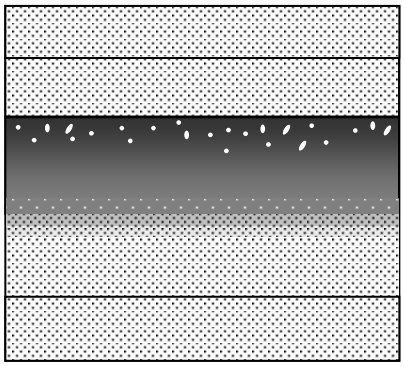

Flow , Basiskontaktzone u. Internzonierung

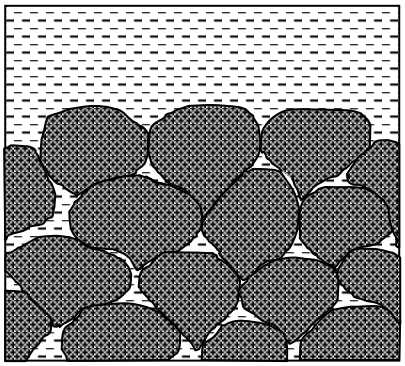

Basaltpillows

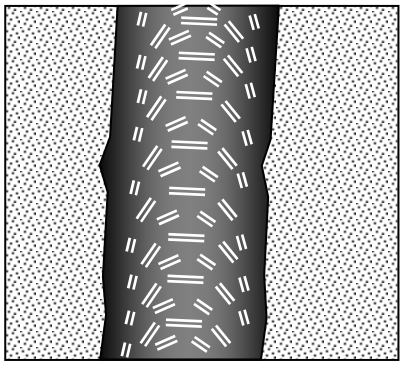

Einströmgefüge in magm. Gängen

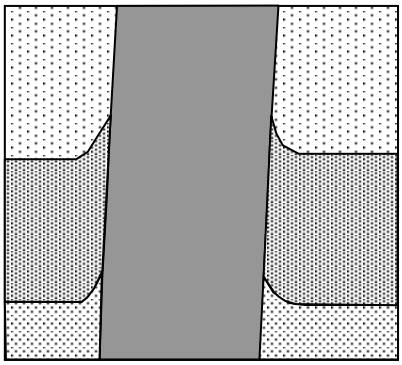

Schleppung an magmatischen Gängen

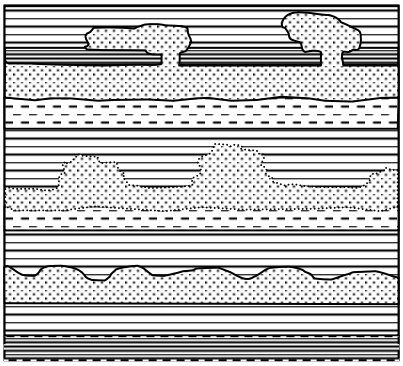

Leukosome in Migmatiten

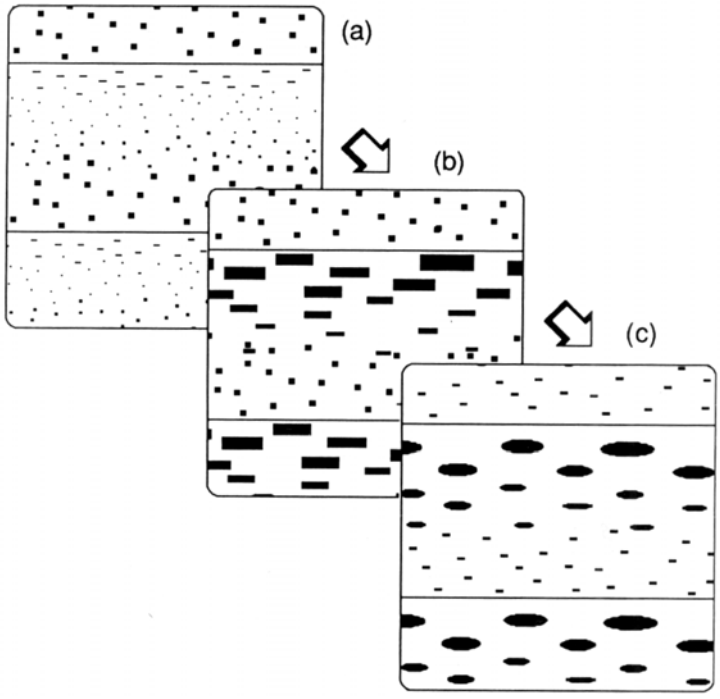

Fig 4.6. A possible sequence showing the reversal of sedimentary fining-upward graded bedding to coarsening-upward graded layering during metamorphism: the original structure (a) is overgrown by Al-rich porphyroblasts which grow to maximum size in the Al-rich pelitic top of the beds (b): subsequent deformation (c) may preserve this reversed sequence but obscure the porphyroblastic origin of the Al-silicates.

aus: Passchier et al. 1990

Klassifizierung Mylonite / Kataklasite

Cataclastic rocks					
Fabric	Texture	Name		Clasts	Matrix
Generally no preferred orientations	Cataclastic: sharp, angular fragments	Breccia series	Megabreccia	> 0.5 m	<30%
			Breccia	1–500 mm	<30%
			Microbreccia	<1 mm	<30%
		Gouge		<0.1 mm	<30%
		Cataclasite		Generally ≤ ~10 mm	>30%
		Pseudotachylite			Glass, or grain size ≤1 μm

Mylonitic rocks					
Fabric	Texture	Name		Matrix grain size	Matrix
Foliated and lineated	Metamorphic: Interlocking grain boundaries, sutured to polygonal	Mylonitic gneiss		>50 μm	
		Mylonite series	Protomylonite	<50 μm	<50%
			Mylonite	<50 μm	50%–90%
			Ultramylonite	<10 μm	>90%

[a] The terminology applied to fault rocks is by no means generally agreed upon. The definitions of the different categories, and the quantitative boundaries we have placed on them, should therefore be understood as guidelines to present usage, which can vary from one geologist to another. We believe, for example, that what we have defined as mylonite would fit anyone's definition, but other geologists use *mylonite* in a broader sense, even to include what we call mylonitic gneiss.

aus: Twiss & Moores 1992

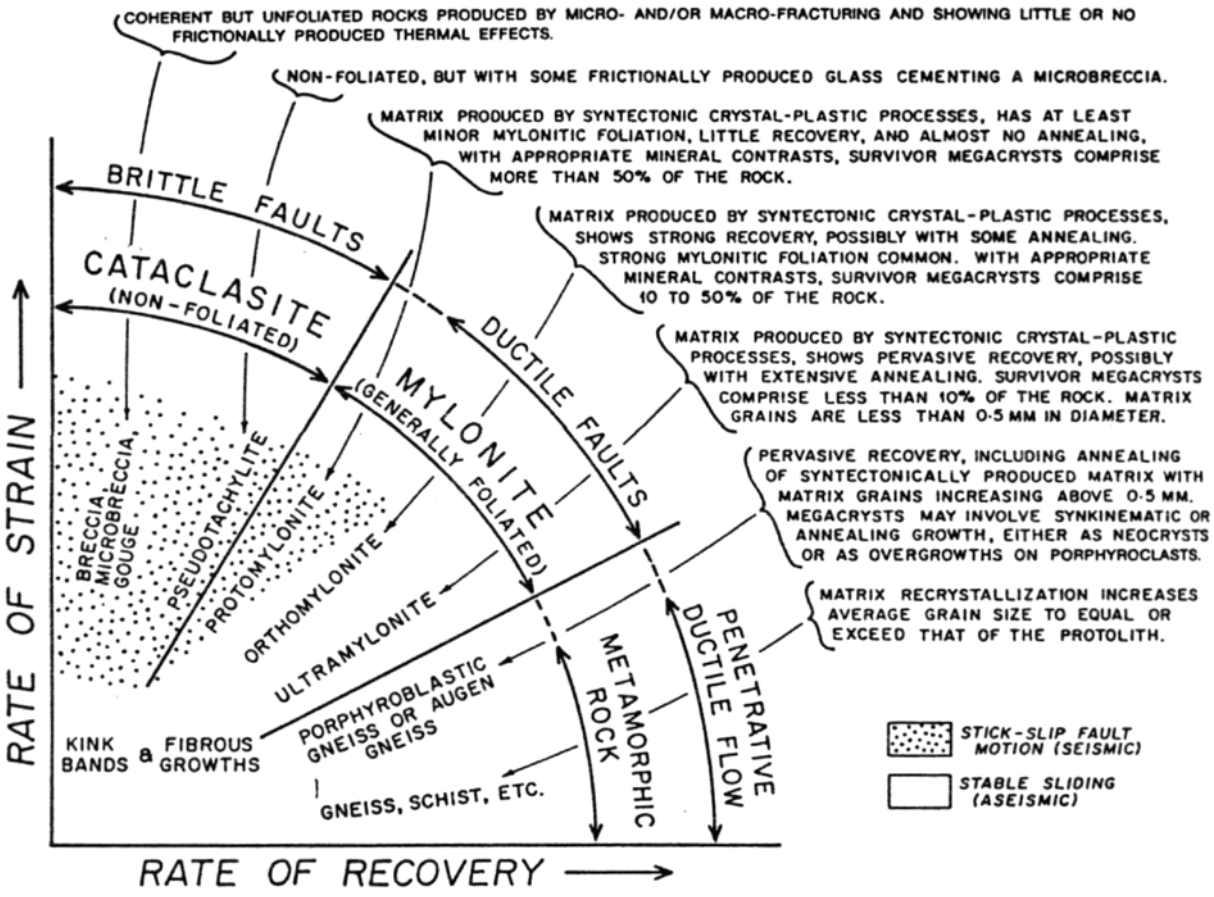

aus: Wise et al. 1984

Einfache Kriterien zur Unterscheidung von magmatischen und mylonitischen Fließgefügen (granitoide Ausgangsgesteine)

Dimension: Makro: Aufschluss u. größer; Meso: Aufschluss/Handstück; Mikro: Optische Mikroskopie u. kleiner. *Qualität:* Aussagekraft u. Häufigkeit

Kriterium	magmatisch	mylonitisch	Dimension Qualität
Foliation	meistens homogen, abgebildet durch Formregelung der Feldspäte und Glimmer, stofflicher Lagenbau undeutlich bzw. fehlend	bei fortgeschrittener Mylonitisierung stark ausgeprägt (gute Spaltbarkeit); Formregelung der Hauptkomponenten, zusätzlich oft stofflicher Lagenbau; z.T. mit unregelmäßigen Abständen,	Mikro/Meso ++
Grenze zum nicht foliierten Rahmengestein	oft diffus	oft deutlich bis abrupt	Meso +
Korngröße verglichen mit nicht-foliiertem Rahmengestein	keine oder nur geringfügige Unterschiede	meistens deutlich kleiner	Mikro/Meso ++
Gradierung	möglich nach Dichte und/oder Korngröße falls primär Kumulatgefüge vorliegen (evtl. rhythmische Wh.)	nach Größe durch dynamische Kornzerkleinerungen, symmetr. zur Scherzone (feinkörnige Kernbereiche)	Meso +
Quarzteilgefüge	oft als Netzwerk zwischen formgeregelten Feldspäten und Glimmern	meistens deutlich gestreckte (linsige) Aggregate oder dünnplattige Lagen	Mikro/Meso ++
Quarzrekristallisation	fehlend oder nur statische Korngrenzenmigration bzw. Equilibrierung	alle Formen dynamischer Rekristallisation möglich (Migrations-Rotations- und Bulging-Rekristallisation)	Mikro ++
Texturen in Quarzpolykristallen	fehlend oder nur sehr schwach entwickelt	i.d.R. sehr deutlich	Mikro +++
Feldspatteilgefüge	z.T. in Form von dachziegelartiger Anordnung (Tiling), Einzelkörner, keine Rekristallisat-Bänder	tendenziell Langachsen in der Foliation ggf. parallel zum Streckungslinear; ggf. Rekristallisat-Bänder	Meso ++
Grobkörnige Feldspäte	(porphyrartig), keine Rekristallisatsäume	(porphyroklastische), Rekristallisatsäume möglich	Mikro/Meso ++
		(HT-Mylonite, relativ geringer Quarzgehalt)	
retrograde Mineralumwandlungen	keine im Vergleich zum nicht foliierten Rahmengestein	häufig im Vergleich zum Rahmengestein (evtl. nur mikroskopisch erkennbar)	Mikro/Meso ++
Verknüpfung mit anderen Verformungsstrukturen	tendenziell geringer	tendenziell höher (z.B. mechanische Zwillinge in Plagioklas)	Mikro/Meso ++
Position und Raumlage	tendenziell durch Magmenkörper diktiert	durch regionales Spannungsfeld diktiert; deshalb auch entsprechende Ausrichtung der Foliationen in anderen Lithologien o. benachbarten Granitkörpern möglich.	Meso/Makro +

Komplexe Entwicklung nicht auszuschließen: magmatische Fließgefüge werden mylonitisch überprägt.

Scherverformungsgefüge / Schersinn-Indikatoren 1

a: simoidale Schleppung (Glimmerfisch)
b: Fragmentzüge

c: Sigma-Klast
d: Delta-Klast
(Rekristallisate oder Neomineralisate in Druckschatten-Zonen („Strain shadows“)

e: Mikroscherbrüche (hier antithetisch), „Dominostruktur“
f: Schneeballstruktur durch synkinematische Blastese

g: S-C-C`-Gefüge (sekundäre Scherbänder u. assozierte Formregelungsgefüge)

h: Mikro-Pull-apart-Strukturen mit Mineralfaser-Wachstum (Risssiegel)
i: vergente Mikrofalten und „Überschiebungen“

aus/nach: Eisbacher 1991

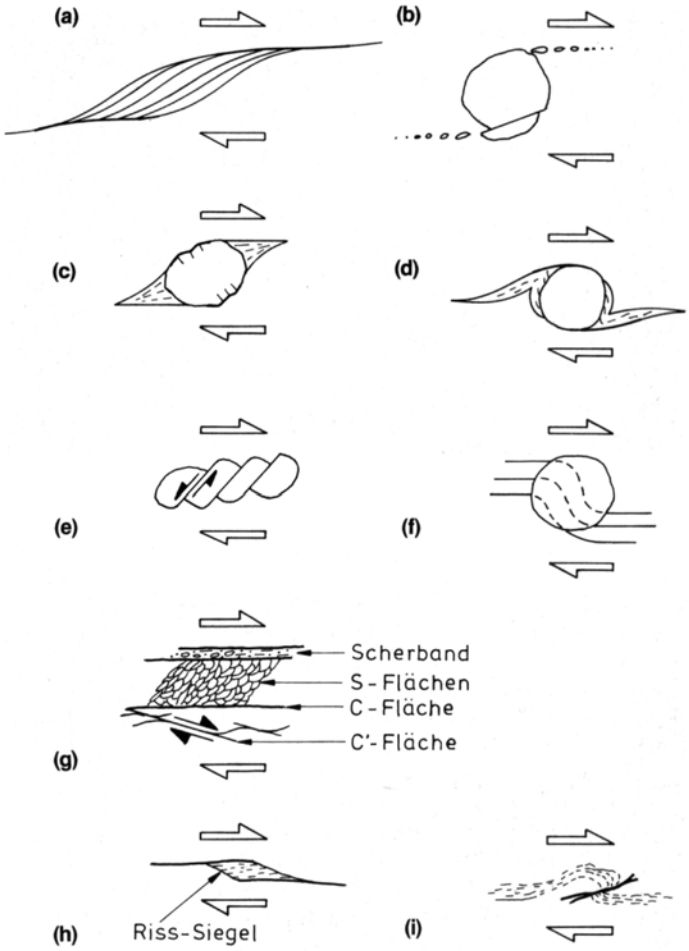

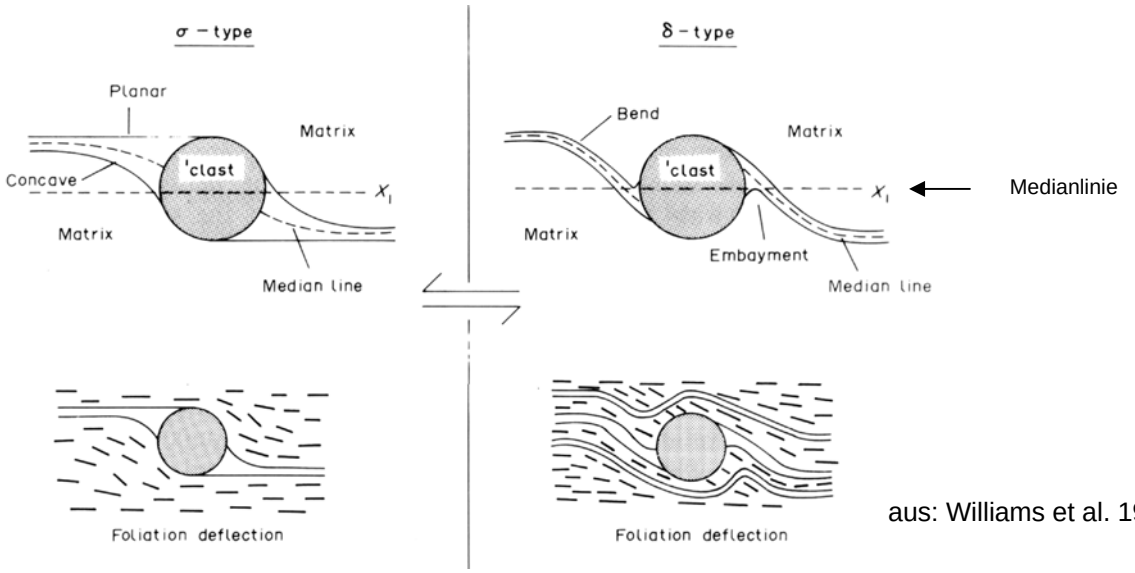

aus: Williams et al. 1994

Scherverformungsgefüge / Schersinn-Indikatoren 2

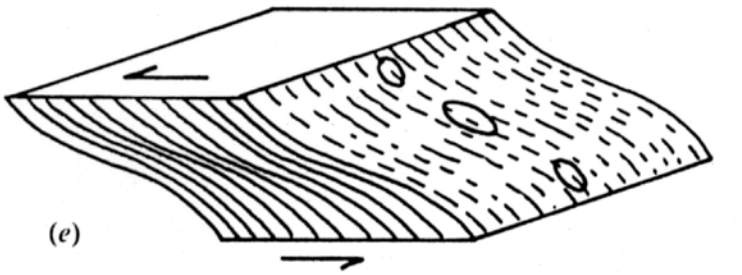

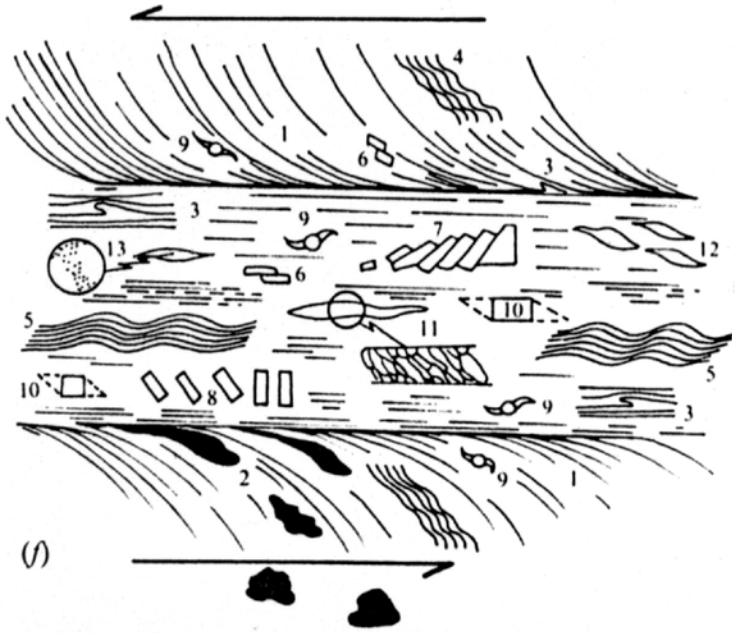

(1) rotation of a pre-existing or generated foliation:
(2) rotation of deformed markers:
(3) asymmetry of intrafolial folds;
(4) normal kink-bands (microshears) in the margin or
(5) central fabric of the shear zone:
(6) sheared porphyroclasts;
(7) rotation of fragments owing to shear fractures;
(8) rotation of fragments owing to tensile fractures;
(9) asymmetry of trails growing around rotating clasts;
(10) asymmetry of trails growing around non-rotating clasts;
(11) asymmetry of elongate recrystallised quartz grains;
(12) asymmetry of dragged-out mica porphyroclasts;
(13) asymmetry of quartz c-axia fabrics.

Quelle unbekannt

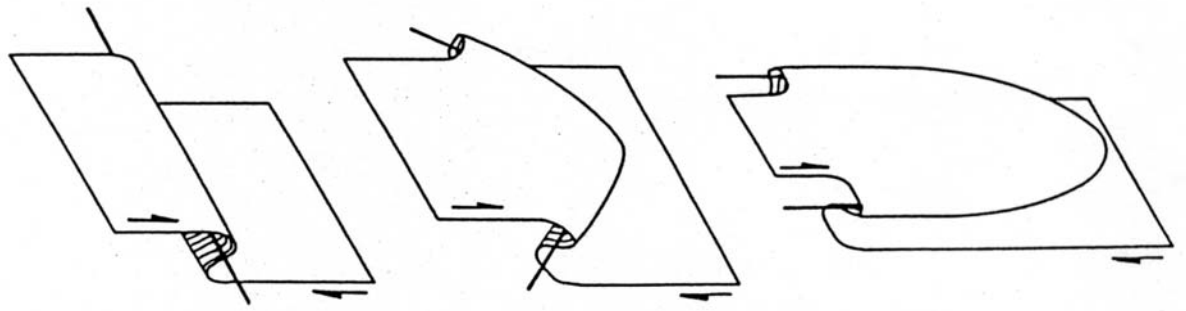

Entwicklung einer Zungenfalte (sheath fold), Quelle ungekannt

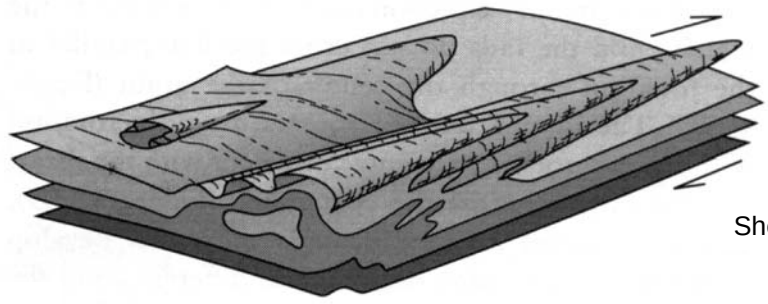

Sheath fold, aus: Twiss & Moores 1992

Scherzonen und Gänge 1 (aus: Passchier et al. 1990)

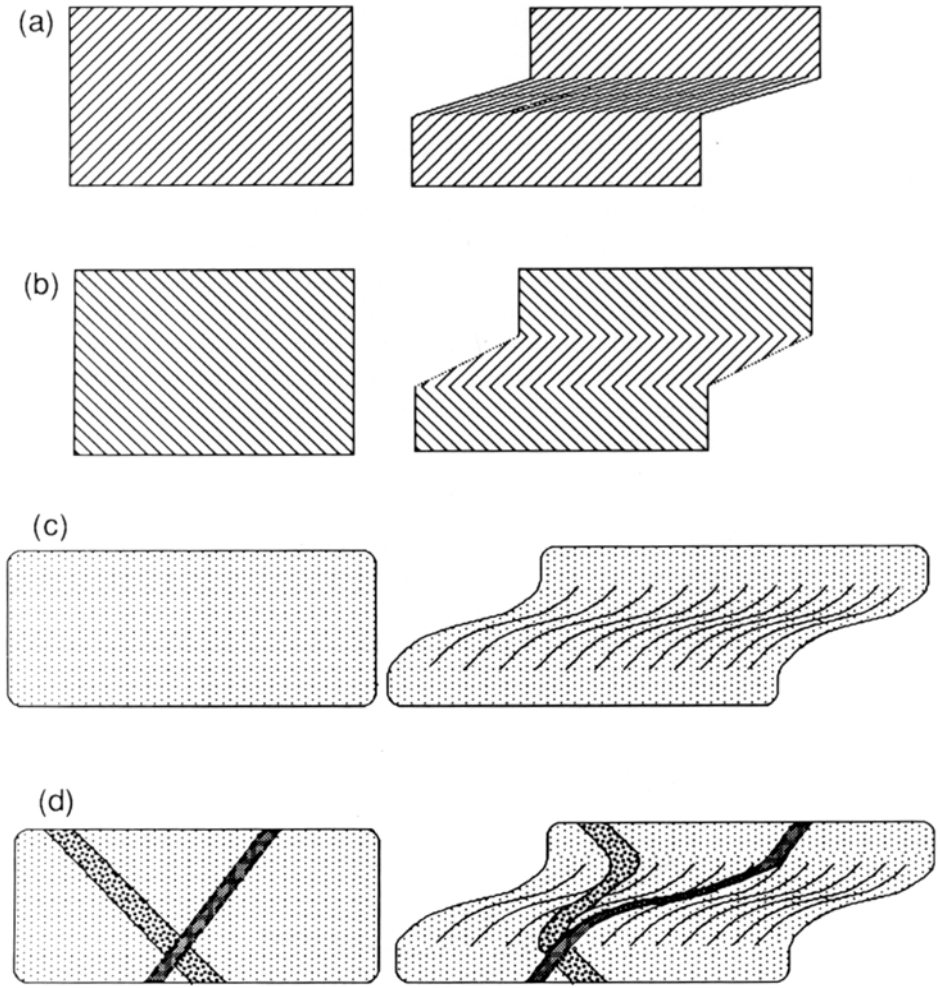

Fig. 4.9. Diagrammatic sections showing the deformation of older fabric elements by a shear zone. Pre-existing foliations will become reoriented in the shear zone, and their new orientation may be steeper (b), or shallower (a), than that of a newly developed foliation in structureless rock at the same finite strain (c); the same applies to dykes which are cut by shear zones (d).

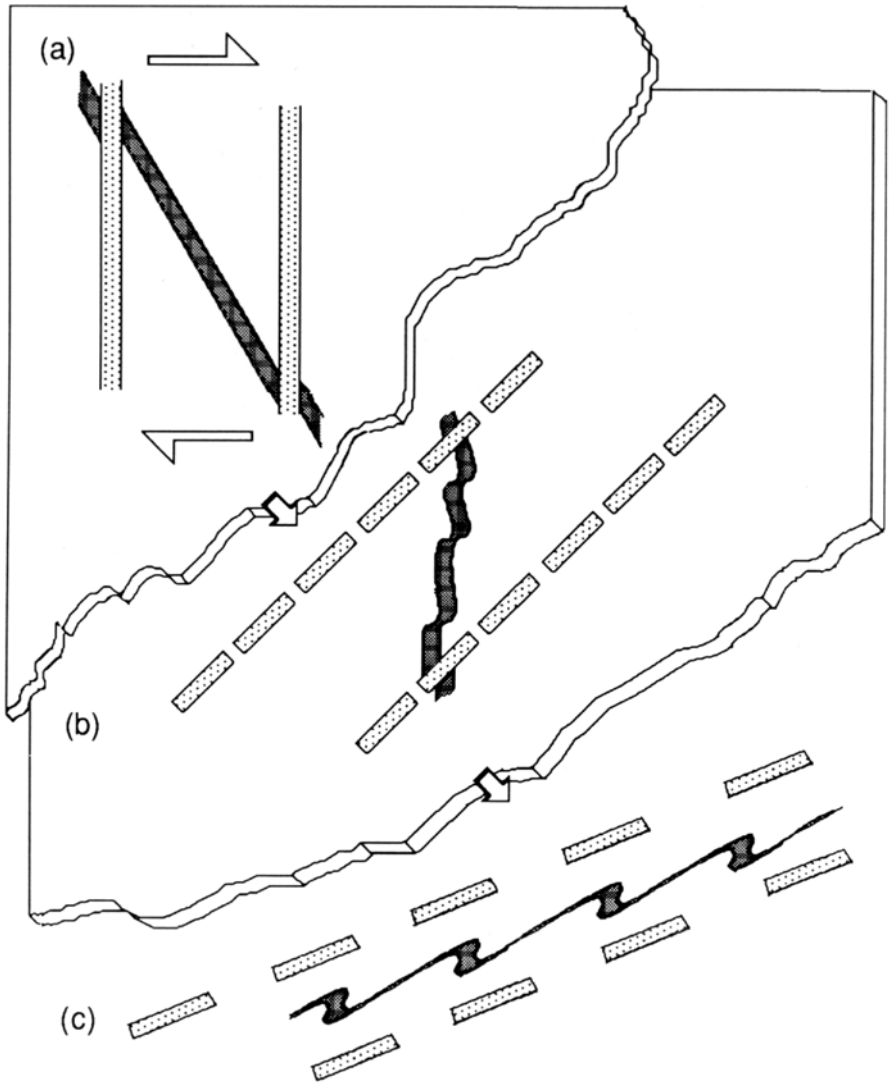

Fig. 4.17. At high strain, extension by non-coaxial flow of originally parallel layers or veins with different rheologic properties (a) may lead to parallel layers with rootless folds, boudins, and even thinned but intact and apparently undeformed layers (b and c). A fabric as shown in (c) can therefore develop by one phase of (strong) deformation and is not necessarily the result of polyphase deformation or intrusion.

Scherzonen und Gänge 2 (aus: Passchier et al. 1990)

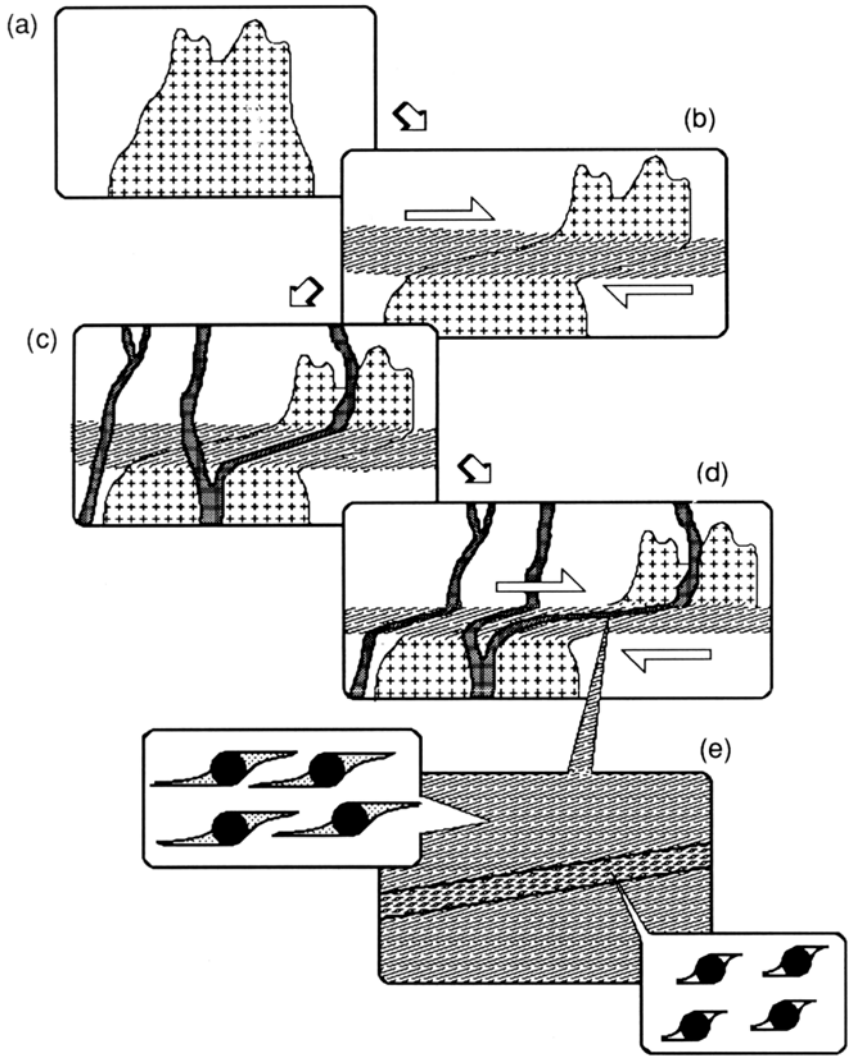

Fig. 4.36. Sketch maps showing some of the complexities of synkinematic intrusions. A granite (a) is cut by a ductile shear zone (b). During this deformation, granite dykes (black) are intruded across the shear zone (c). The dykes are deformed within the shear zone, but less so than the host rock (d). It may be difficult to recognise the different deformation states of these two rocks within the shear zone. The kind of evidence that might be seen is shown enlarged in (e); the tails on porphyroclasts in the dyke are less well developed than those seen in the more deformed host rock.

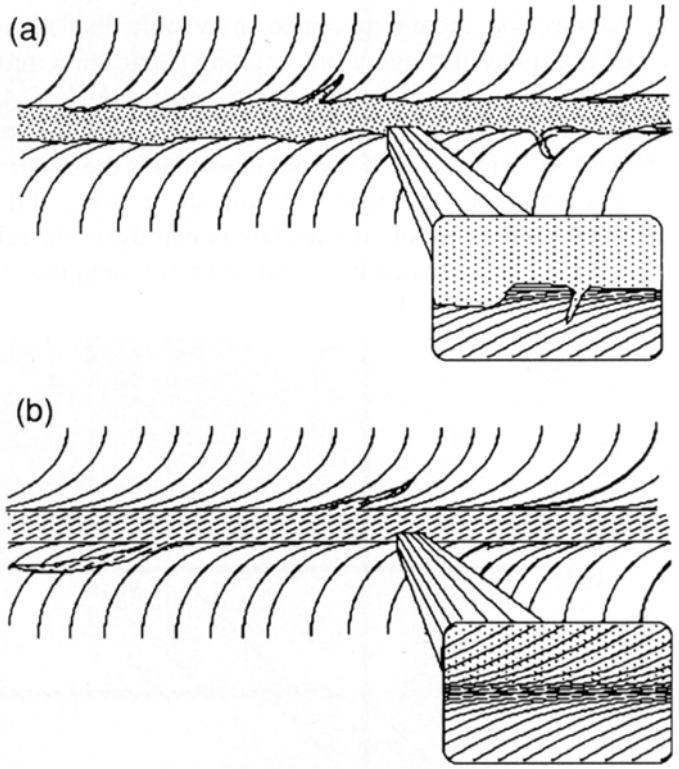

Fig. 4.38. Two superficially similar situations representing opposite sequences of events: (a) A vein was intruded along an older shear zone; it cuts the foliation of the shear zone, and displays angular jogs and branching veinlets in the margin of the zone. (b) An intrusive vein that was the nucleus of a younger shear zone may have an internal foliation and flattened jogs and branching veinlets.

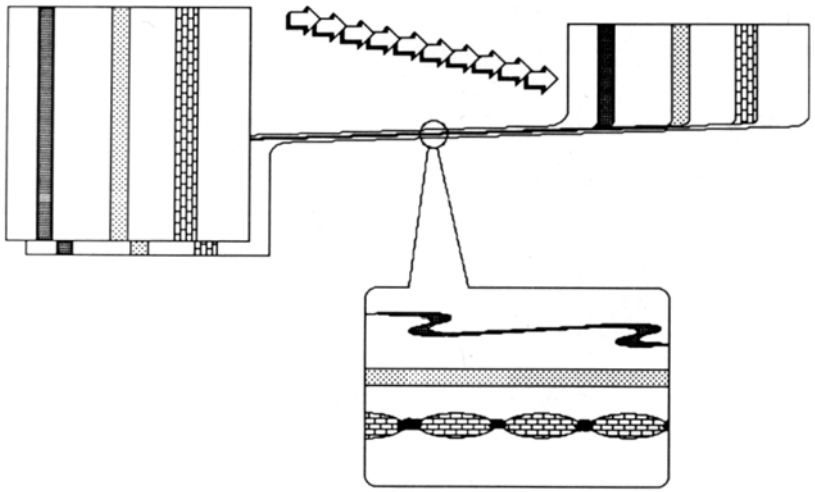

Fig. 4.18. Depending on their original orientation, veins may become folded and/or boudinaged and may rotate into parallelism at high strain; coexisting boudinaged and folded veins (bottom) may therefore belong to the same phase of deformation.

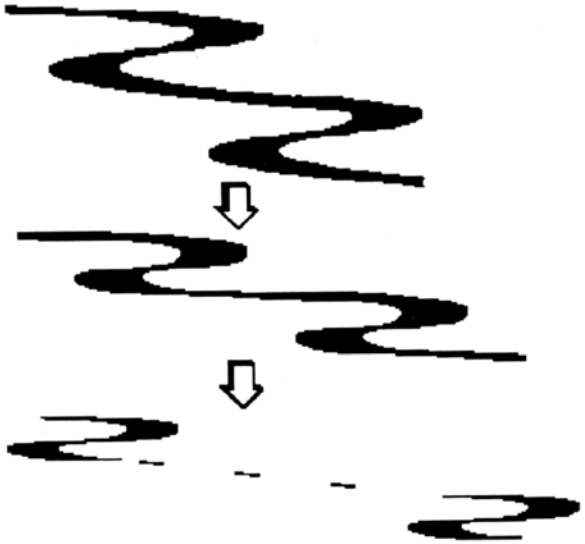

Fig. 4.19. Development of rootless folds; flattening of an isoclinally folded layer (black) which is more competent than its host rock will preferentially cause boudinage in the thin and relatively weak limbs.

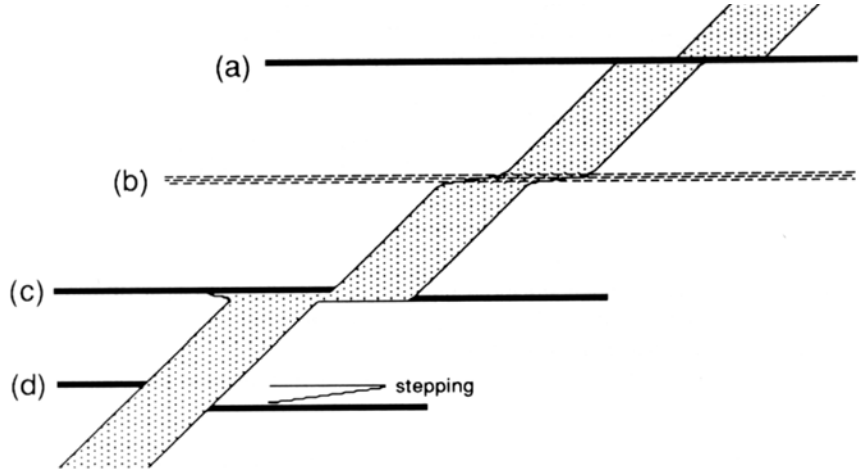

Fig. 4.39. Intersection relation between a planar intrusion and faults or narrow ductile shear zones: (a) a fault cuts an older dyke; (b) a ductile shear zone cuts an older dyke, and deflects the dyke margin; (c) a dyke cuts an older fault and forms a jog; (d) a dyke cuts an older fault without jogs, and causes 'stepping' of the fault. Situations a, b and c could be confused if the intersections are not carefully examined.

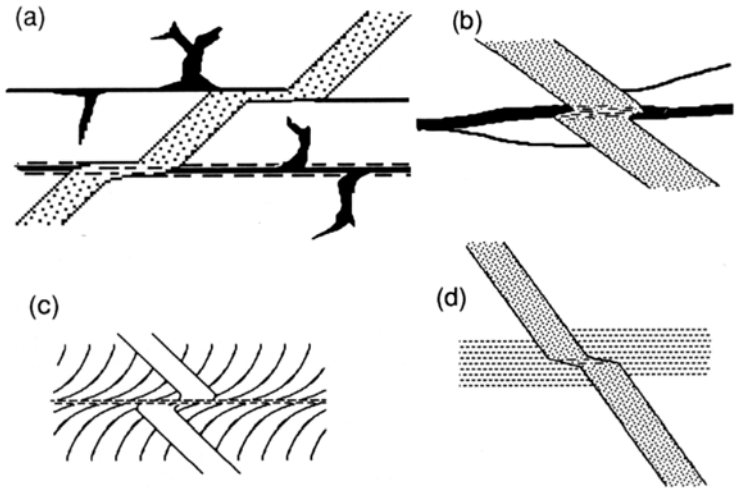

Fig. 4.43. Intersection relations of planar intrusions and polyphase shear zones. In (a) two pseudotachylyte veins (black) were cut by an intrusion (stippled), and the lower pseudotachylyte vein was reactivated as a ductile shear zone. Reactivation is indicated by the presence of a foliation in the zone and of deflected injection veins. The situation might be confused with those in Fig 4.39a and b. In (b) a branching brittle fault (black) was cut by an intrusion (stippled); one branch on each side was reactivated as a ductile shear zone, the others were not used because they were not in the same orientation suitable for reactivation. In (c) a major high-grade ductile shear zone was cut by an intrusion which was later cut by a low-grade shear zone that developed along the centre of the pre-existing zone. In (d) a wide shear zone (open stipple) was cut by an intrusion (dense stipple) that was subsequently deformed by reactivation of the centre of the shear zone.

Scherbänder (aus: Passchier & Trouw 1996)

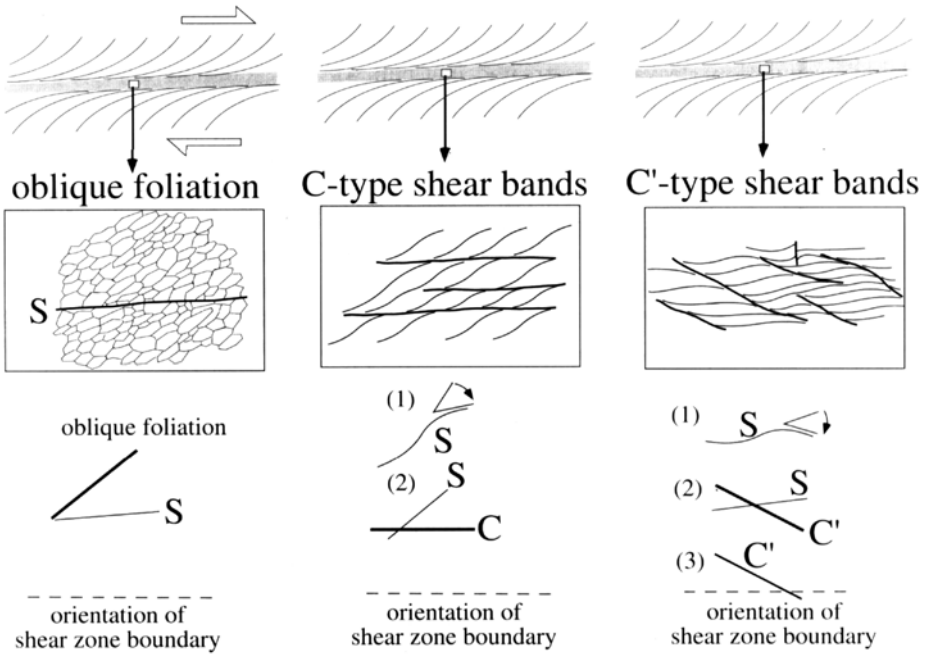

Fig. 5.13. Three types of foliation pairs that are common in ductile shear zones. The shear zone is shown with typical foliation curvature. The main differences in geometry between the foliation pairs are shown in the ***centre.*** Elements used to determine sense of shear are shown ***below.*** Further explanation in text

Mehrfachfaltung/Schieferung/Crenulation (aus: Passchier & Trouw 1996)

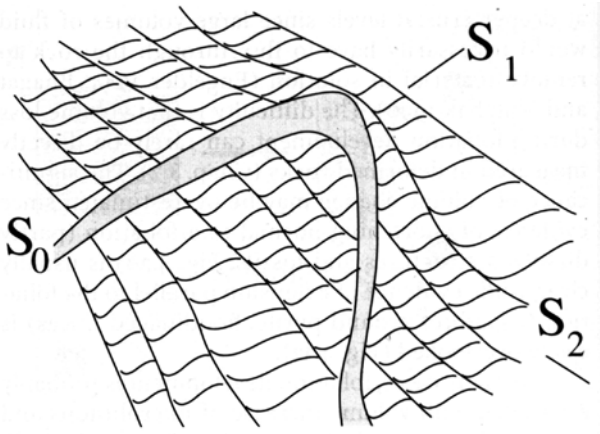

Fig. 4.33. D_1 fold, folding bedding (S_0) with development of S_1 foliation along the axial surface of the fold. Later D_2 deformation folded S_1 to produce an S_2 crenulation cleavage in pelitic layers that cut the D_1 fold through both limbs. Note the deviation of S_2 around the more resistant fold hinge

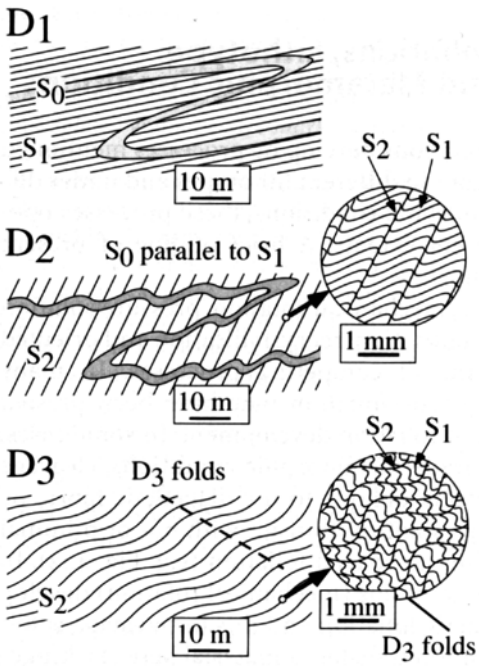

Fig. 4.34. Schematic presentation of a common sequence of foliation development in slate and schist belts. Enlargements of typical microstructures are shown at ***right.*** Further explanation in text

Spröde - duktile Scherzonen

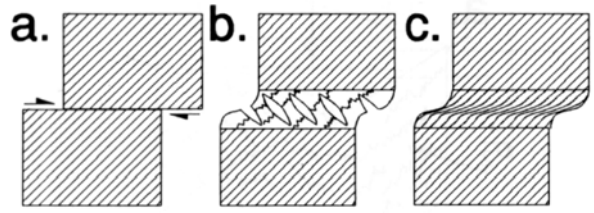

Fig. 5.9. (a) Brittle shear zone (fault). (b) Brittle – ductile shear zone with en échelon veins and stylolitic cleavage. (c) Ductile shear zone modifying foliation of country rock. Modified from Ramsay (1980b).

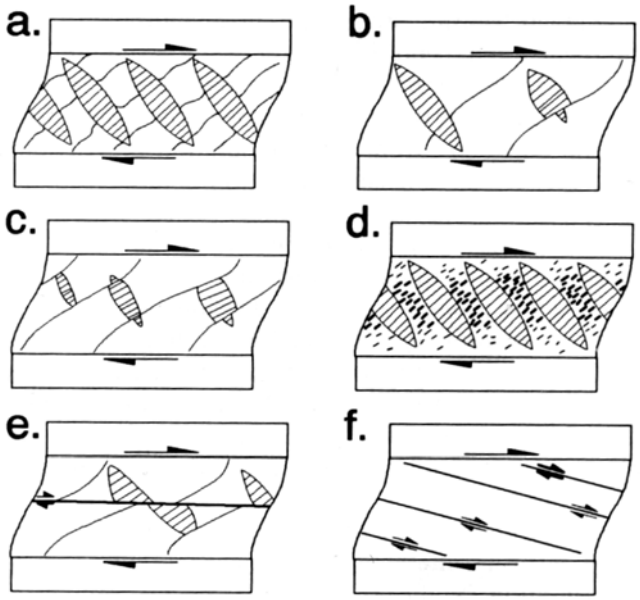

Fig. 5.10. Internal geometries of secondary structures in brittle – ductile shear zones (all right-lateral as shown by shear couples on boundaries of zones). (a) Veins (elliptical shapes with internal lines showing geometry of vein fibres) younger than cleavage (curvilinear lines within zone). (b) Veins and cleavage same age. (c) Veins older than cleavage. (d) Veins with elongate grains (tick marks between veins). (e) Late-stage fault (solid line with shear couple) offsetting cleavage and veins. (f) Riedel fractures (parallel lines with shear couples).

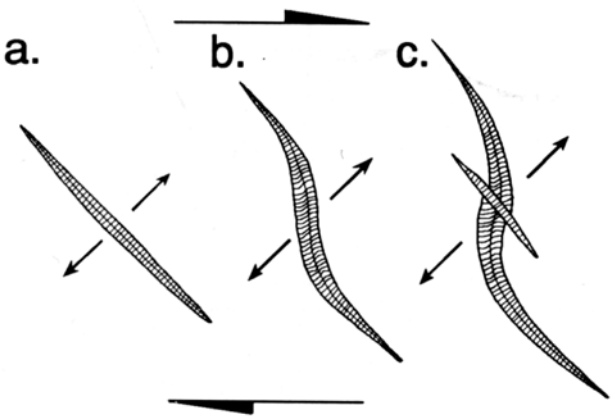

Fig. 5.13. Progressive vein development in a brittle – ductile shear zone with syntaxial fibres. (a) Planar vein with straight fibres. (b) Vein rotation producing sigmoidal veins with curved fibres. (c) Initiation of younger cross-cutting planar vein to accommodate additional strain. After Durney & Ramsay (1973).

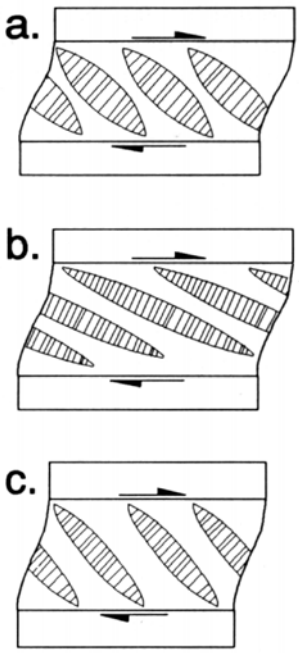

Fig. 5.11. Geometry of en échelon veins (elliptical shapes with internal straight lines to show fibre geometry) within brittle – ductile shear zone related to different deformation regimes. (a) Simple shear. (b) Simple shear with volume increase (analogous to transpression on a large scale). (c) Simple shear with zone-parallel pure shear that elongates normal to zone boundaries (analogous to transtension on a large scale).

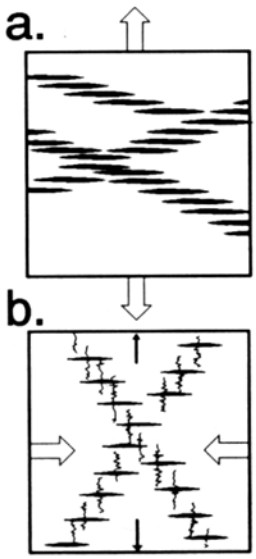

Fig. 5.12. Change in abundance, overlap and attitude of en échelon veins (black elliptical shapes) in shear zones between (a) bulk volume increase (white arrows show direction of increase), and (b) bulk volume decrease with pure shear (white arrows show direction of decrease, small black arrows show direction of elongation for pure shear, and curvilinear lines are stylolites). Modified from Ramsay & Huber (1983).

aus: Dunne & Hancock 1994

Faserwachstum

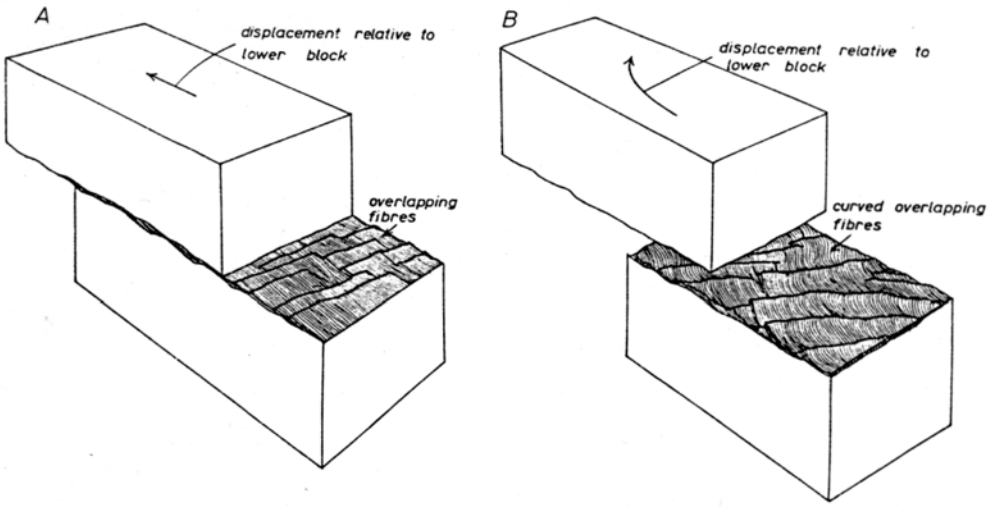

Figure 13.37. *The geometry of fibre sheets developed on shear surfaces* (A) *where the relative shear displacement vector is constant and* (B) *where this displacement vector changes direction with progressive evolution of the shear.*

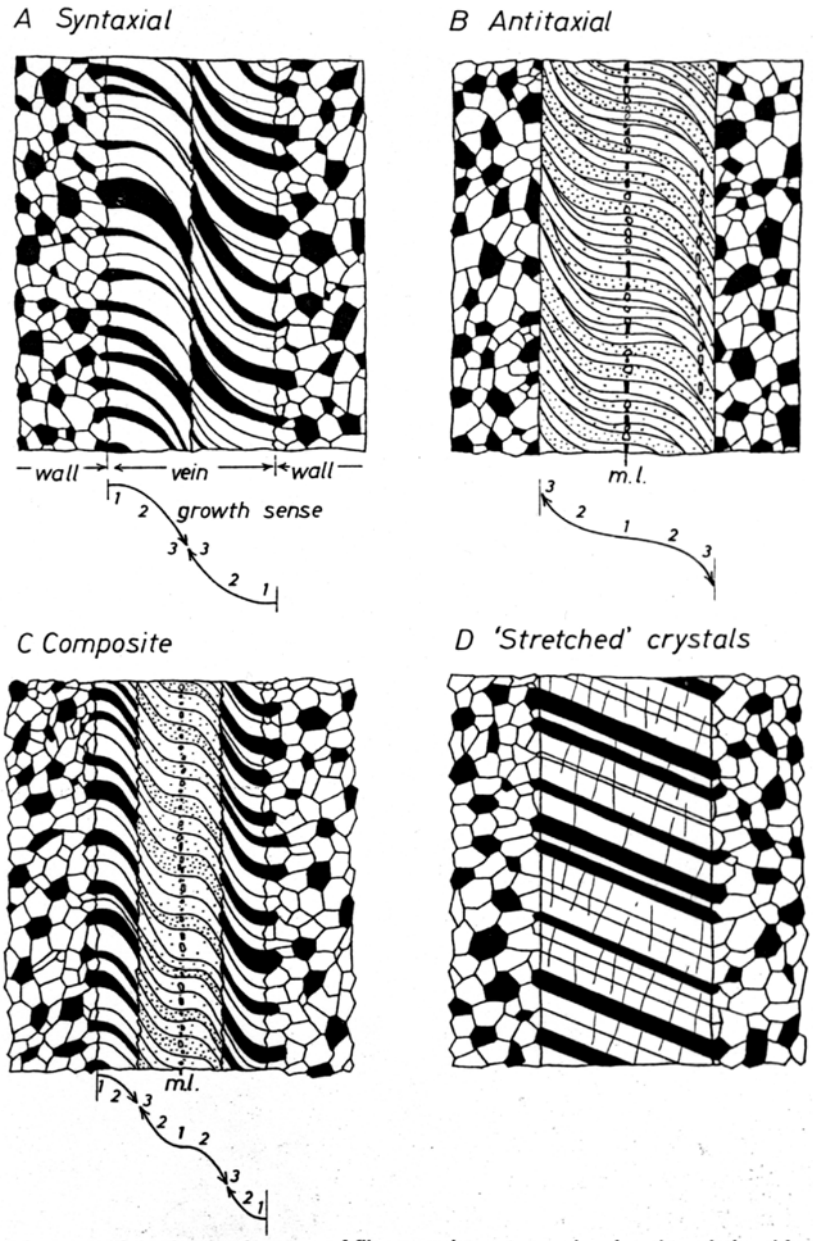

Figure 13.9. *Principal features of the four main types of fibrous vein systems showing the relationship of the composition and crystallographic orientations of vein and wall rock crystals. The black and white unstippled areas are crystals of the same species but with differing crystallographic orientations. The stippled areas are crystals of another species, and their crystallographic orientations are indicated by differing intensities of stippling.*

Sekundäre Bruchflächen in Scherzonen

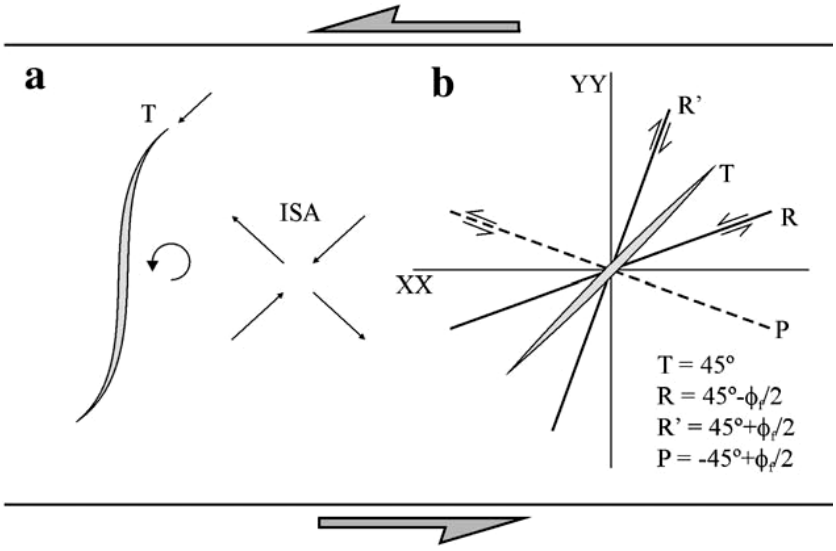

(a) Geometry of an idealised tension gash in sinistral simple shear. ISA, instantaneous stretching axes; (b) theoretical distribution of tensional fractures (T) and shear fractures (R, R0 and P) in the same kinematical framework.
ff, internal friction angle.

aus Coelho et al. 2006

Klassifizierung von Kluftscharen

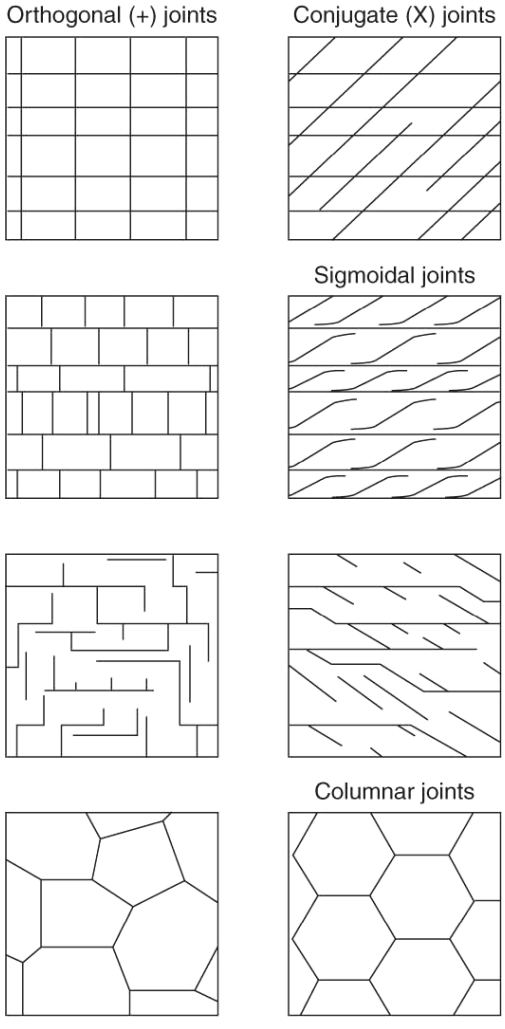

(a)

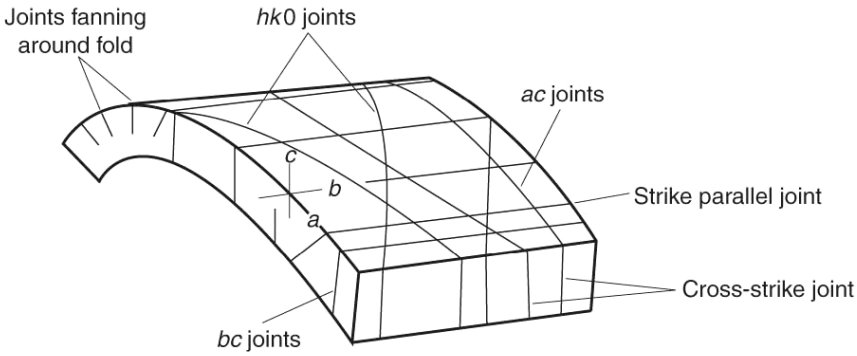

(b)

Schersinn-Indikatoren im Bereich von Störungsflächen/Bewegungsflächen

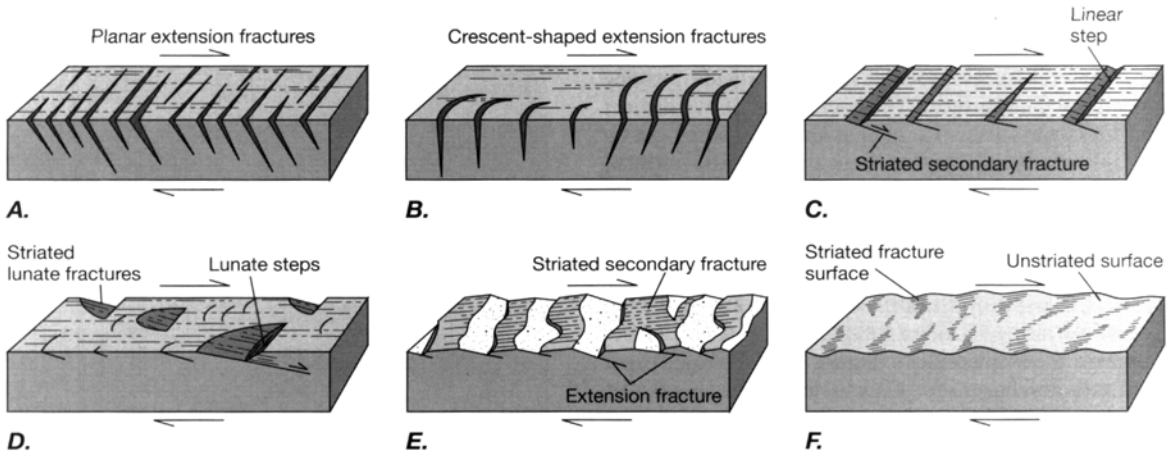

Figure 4.16 Shear sense criteria on brittle faults. Block diagrams show the relationship between secondary fractures and the sense of shear on a brittle fault. The top plane is the shear plane; relative motion is indicated by arrows. Extension fractures are unstriated and may be filled with secondary minerals. Striated fracture surfaces are shear fractures.

aus: Twiss & Moores 1992

Ergänzung:

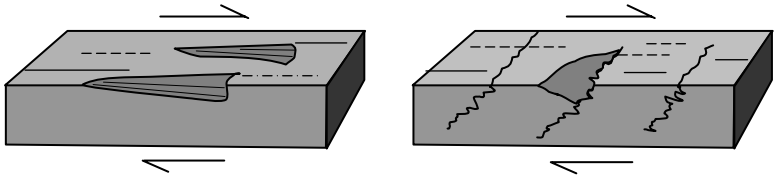

Frässpuren durch resistente „Schleifpartikel“

Stylolithen

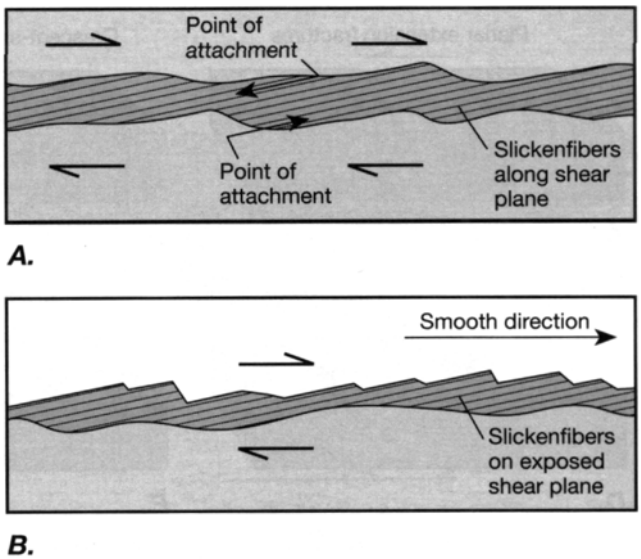

Figure 4.15 Slickenfibers as indicators of shear sense and minimum displacement. *A*. An arrow along a slickenfiber with its base at the point of attachment to one wall of the fault points in the direction of relative slip of the opposite wall of the fracture. The length of the fiber from one wall to the other is a measure of the minimum displacement on that fault. *B*. The smooth, or "downstairs," direction on the stepped surface of an exposed set of slickenfibers defines the direction of relative slip of the missing block.

aus: Twiss & Moores 1992

Störungsflächenanalyse

Jede Harnischfläche, auf der eine Lineation (u.a. Faser- oder Reibungsharnisch) zu erkennen ist und deren Bewegungssinn bekannt ist, kann auf die Einwirkung eines bestimmten Spannungsfeldes zurückgeführt werden. Zwischen diesem Spannungsfeld und der Harnischfläche besteht ein geometrischer Zusammenhang, der für die Bestimmung des Paläospannungstensors genutzt werden kann.

Zur Darstellung solcher Datensätze mit Angabe von Aufschiebung (+) oder Abschiebung (-) gibt es zwei Arten der graphischen Datenprojektion:

a) Großkreisdarstellung

- Spur der Verschiebungsfläche eintragen
- Linear eintragen (liegt auf der Flächenspur)
- Linearpunkt mit Pfeil versehen: bei Aufschiebung zeigt der Pfeil zum Zentrum, bei Abschiebung zum Rand des Schmidtschen Netzes
- Blattverschiebungen als Doppelpfeil eintragen: verlaufen parallel zur Flächenspur

b) Polpunktdarstellung (nach **Hoeppener**, s. Abb. unten)

- Polpunkt der Verschiebungsfläche darstellen
- Linear eintragen
- beide auf gemeinsamen Großkreis drehen
- Kreissegment am Polpunkt einzeichnen
- Pfeil einzeichnen: bei Abschiebung in Richtung Schnittflächenspur, bei Aufschiebung von der Schnittflächenspur weg

  Bei Blattverschiebungen wird ein Doppelpfeil parallel zum Außenkreis eingetragen (sinistral oder dextral).

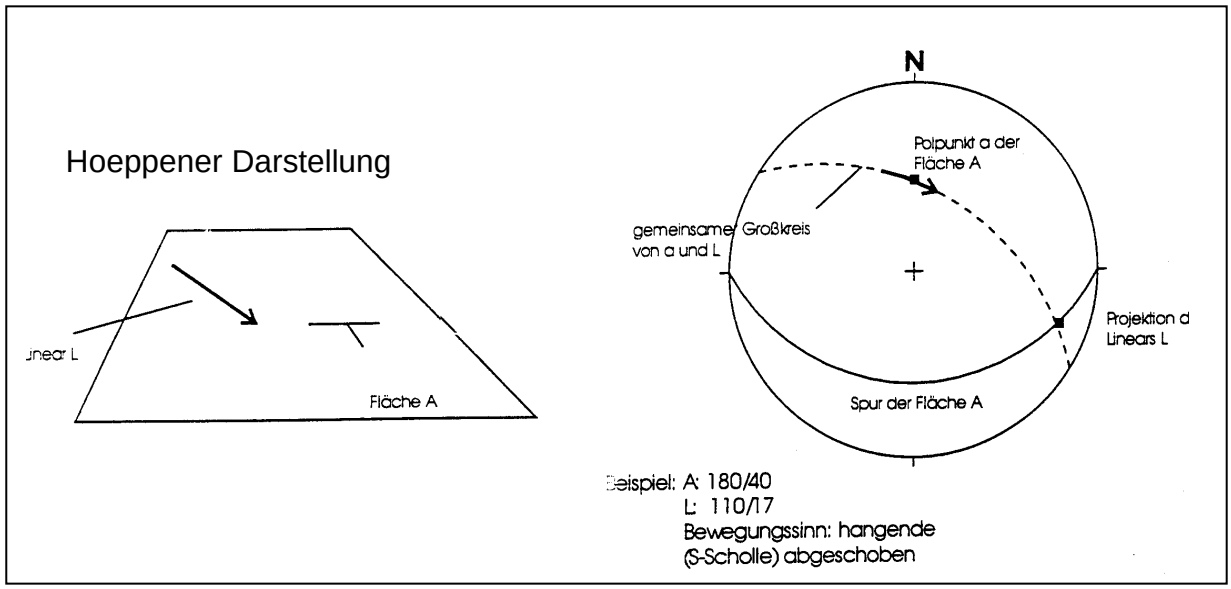

Wichtig für die Datenerfassung:
Immer für ein Linear auch die Fläche einmessen, auf der das Linear beobachtet wird.

Boudinage 1 (aus: Price & Cosgrove 1990)

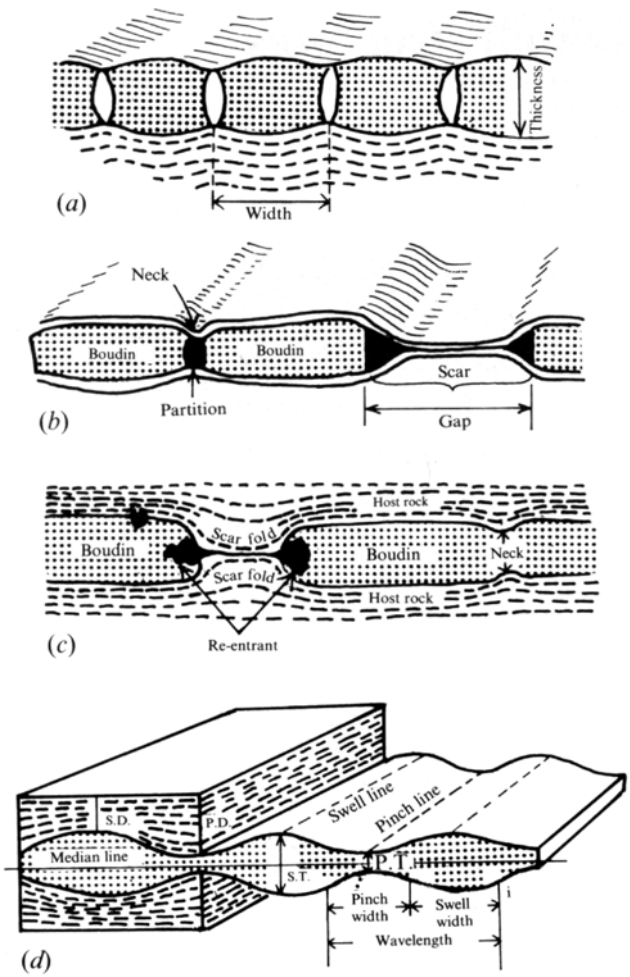

Fig. 16.2. (*a*)–(*c*) Terminology used to describe boudins. (After Wegmann, 1932; Jones, 1959; and Wilson, 1961.) (*d*) Terminology used to describe pinch-and-swell structures. S.T. and S.D. are swell thickness and swell disturbance and P.T. and P.D. pinch thickness and pinch disturbance. i denotes an inflection point. (After Penge, 1976.)

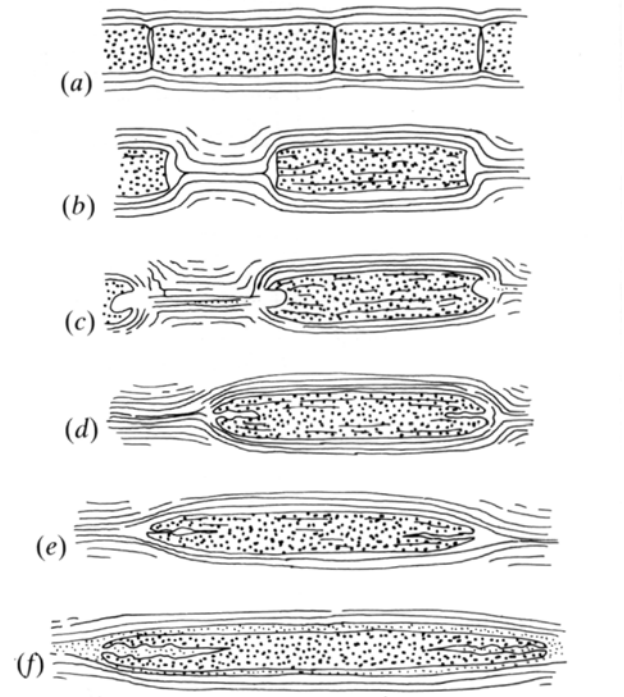

Fig. 16.25. Various stages in the development of lens-shaped boudins from originally rectangular boudins formed by tensile failure of a relatively competent layer in a less competent matrix. (Compiled from field observations by Wegmann, 1932.)

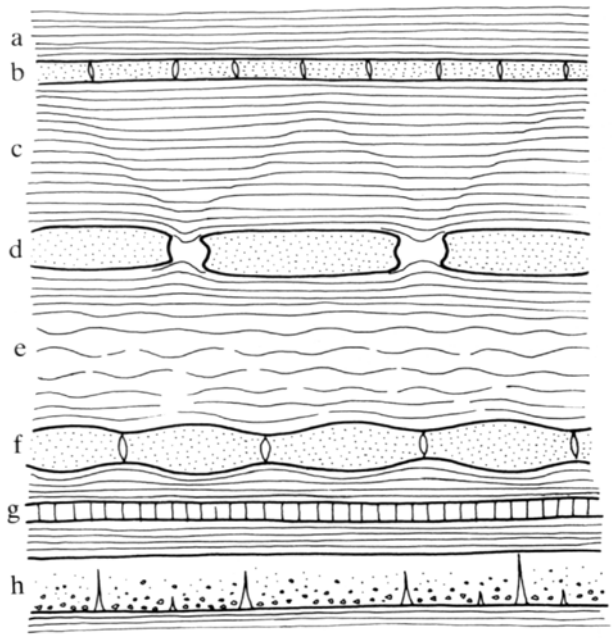

Fig. 16.58. A sketch showing a variety of structures all of which may form when the maximum principal compression is normal, or at a high angle, to the rock layering or fabric. (*a*) Homogeneous flattening (*b*) extension veins (*c*) normal kink-bands (*d*) boudins (*e*) internal pinch-and-swell structures (*f*) pinch-and-swell structures (*g*) extension fractures (*h*) tapered veins in graded bed.

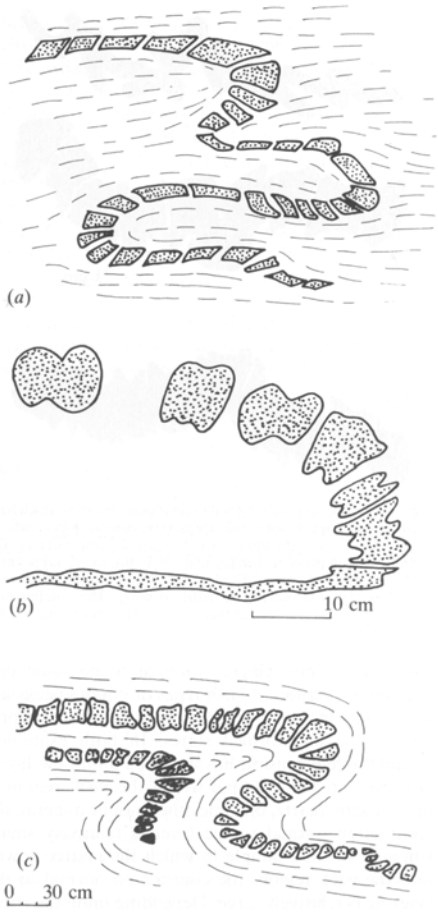

Fig. 16.54. Natural examples of folded boudinaged layers. (*a*) amphibolite bands in a quartzo-feldsparthic gneiss. (After Ramberg, 1952.) (*b*) Amphibolite layer in quartz-gneiss from the Pre-Cambrian rocks of Jashidih, E. India. (After Sengupta, 1983.) (*c*) Quartzite band in a semi-pelite. (After Gindy, 1952.)

Boudinage 2

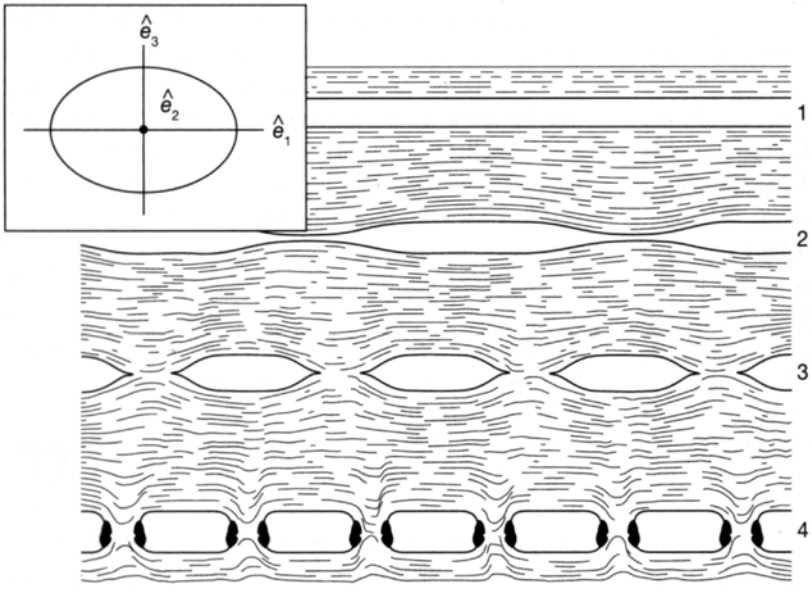

Figure 14.3 Formation of boudins. *A.* Competent layers imbedded in an incompetent matrix and oriented parallel to the axis of maximum stretch accommodates the lengthening by segmenting into boudins. The contrast in competence between the layer and the matrix increases from zero (top) to high (bottom), resulting in a progression from (1) uniform stretching and thinning through (2) pinch and swell and (3) necked boudins to (4) fractured boudins. *B.* The length of each boudin is determined by the yield or tensile strength of the layer and the balance of forces created by the shear stresses σ_s on the layer surface and the deviatoric tensile stress within and parallel to the layer ${}_{\Delta}\sigma_n$.

aus: Twiss & Moores 1992

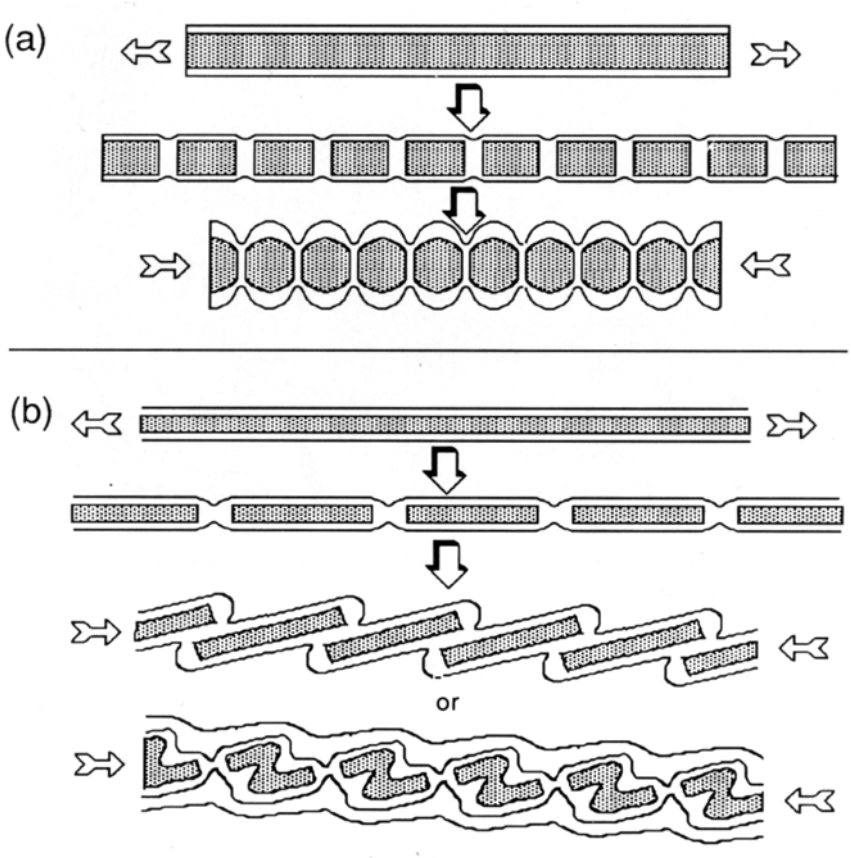

Fig. 4.30. Two types of shortened boudins; (a) semi-spherical shortened boudins are formed if original boudins were relatively equidimensional ; (b) 'rooftile' structures or folded boudins may form if original boudins were elongate.

aus Passchier et al. 1990

Boudinage 3 (aus Swanson 1992)

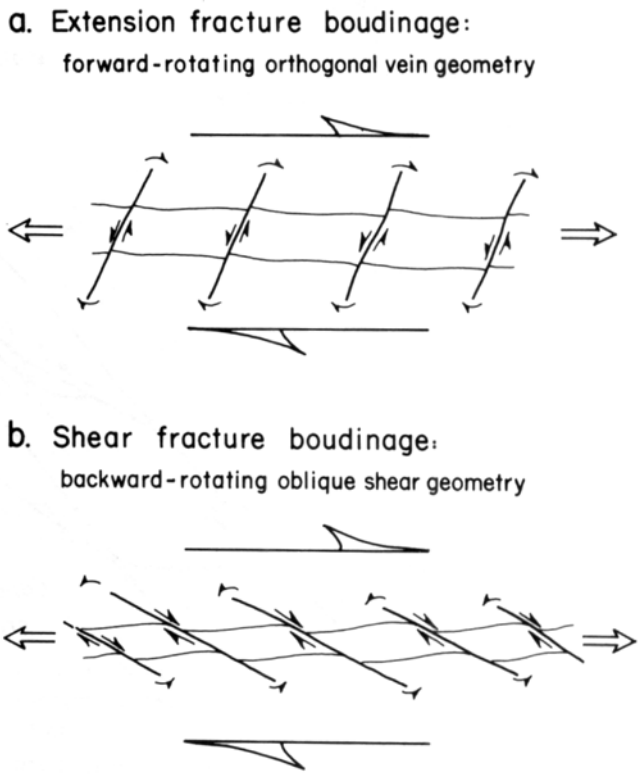

Fig. 1. Types of asymmetric boudinage discussed in the text formed under intermittent extension and layer-parallel dextral shearing. (a) Extension fracture boudinage with forward-rotating, orthogonal vein geometry (Type I). (b) Shear fracture boudinage with backward-rotating, oblique shear-band geometry (Type II).

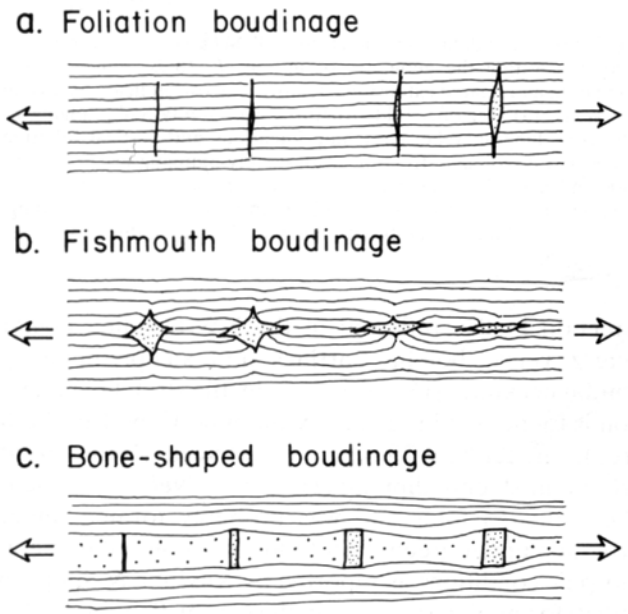

Fig. 4. Symmetric boudinage features with increasing elongation from left to right (arrows indicate extension direction). (a) Initiation and dilation of orthogonal vein partings for symmetric foliation boudinage. (b) Collapse of initial partings to form quartz stars and fishmouth boudins. (c) Continued layer-parallel elongation about initially rectangular boudins and quartz partition mineralization to form bone-shaped boudins.

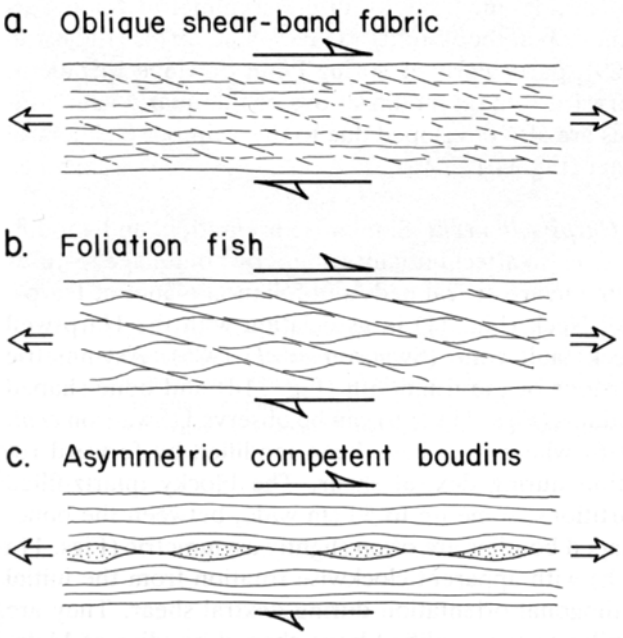

Fig. 6. Asymmetric shear fracture boudinage as (a) distributed dextral oblique shear band fabric, (b) oblique dextral shear zones and intervening foliation fish and (c) remnant asymmetric competent boudins.

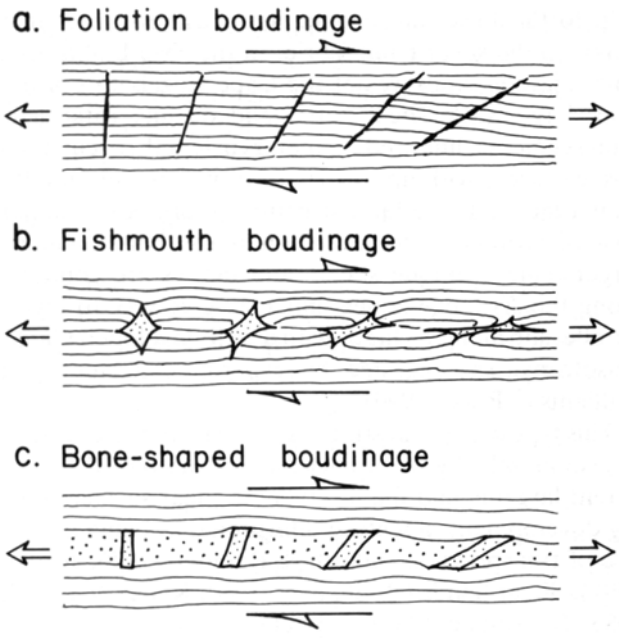

Fig. 7. Modified asymmetric boudinage features with increasing dextral shear strain from left to right. (a) Clockwise rotation and sinistral slip on initial orthogonal vein partings. (b) Modification and distortion of fishmouth boudinage during dextral shear. (c) Reorientation of rectangular mineral partitions in bone-shaped boudinage.

Boudinage 4

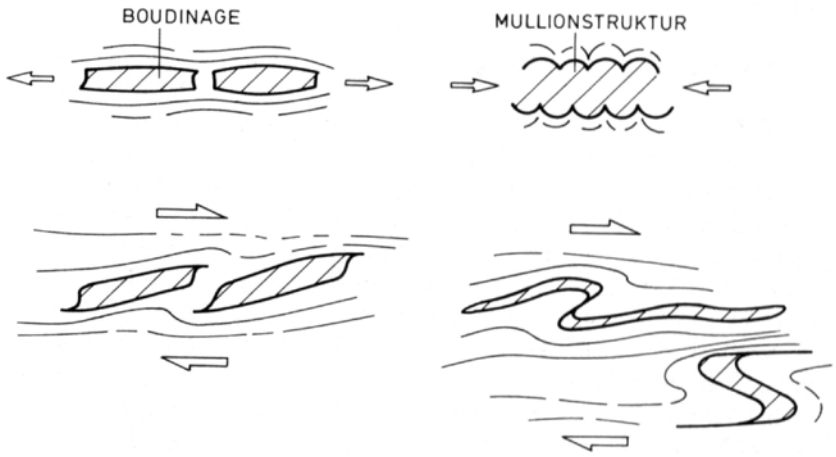

Abb. 15.4 Oben: Schema für das Verhalten kompetenter Lagen in einer weniger kompetenten Matrix bei Extension (Boudinage) bzw. Kontraktion (Mullions) der Lage. Unten: Fließverhalten von kompetenten Gesteinslagen und -linsen bei penetrativer Scherung einer weniger kompetenten Matrix.

aus: Eisbacher 1991

Strukturen durch schiefe Transpression

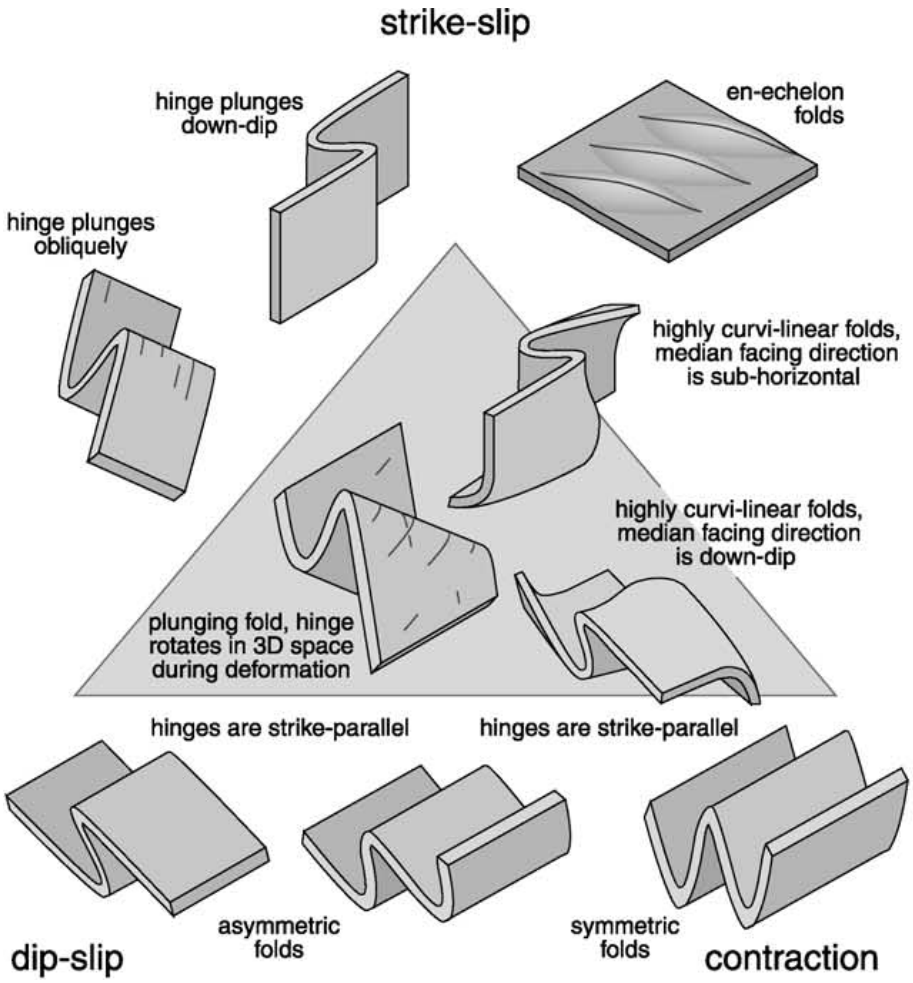

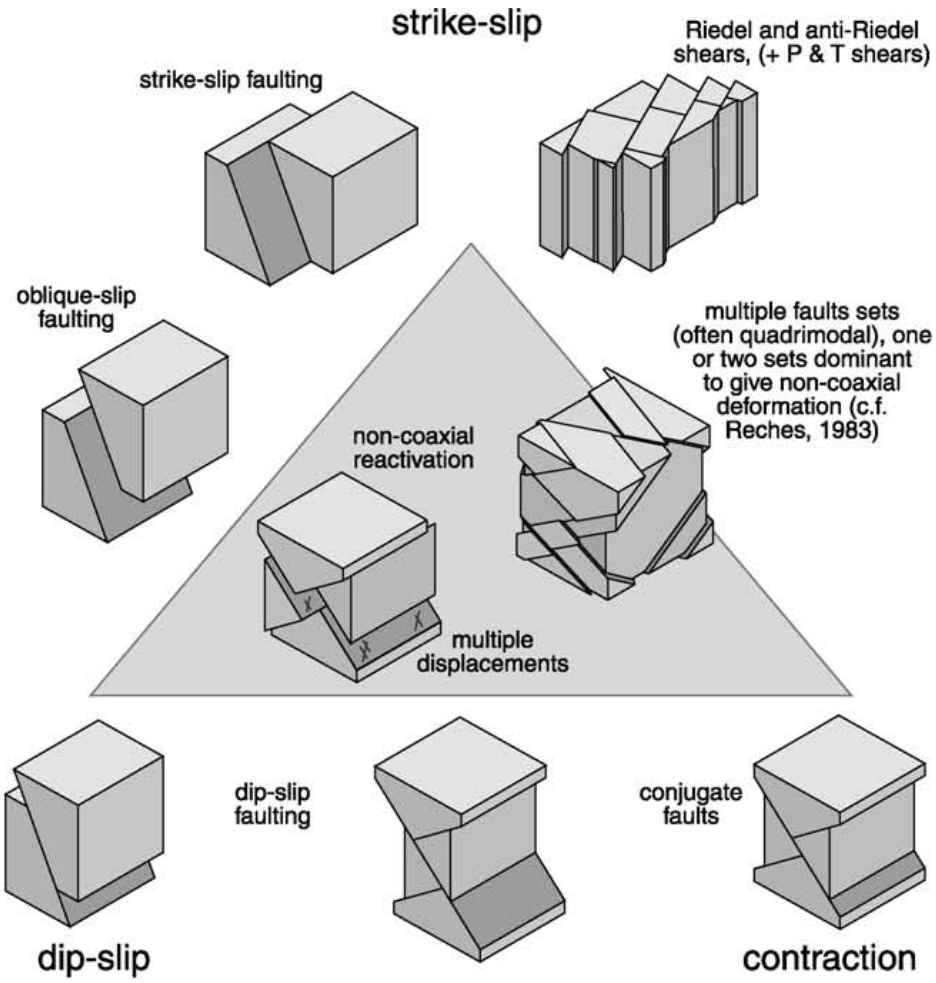

aus Jones et al. 2004

Schätztafeln 1

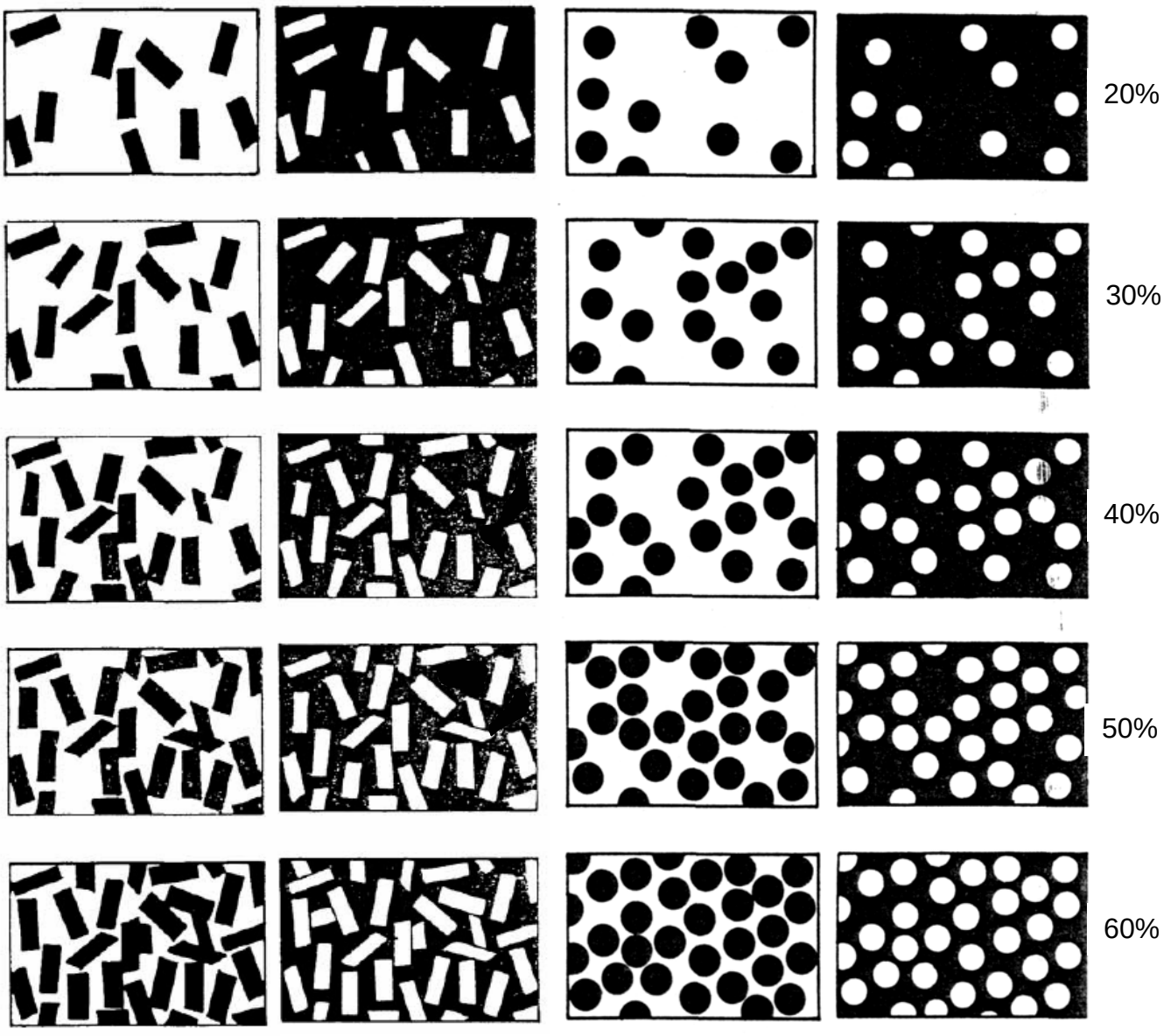

1 %

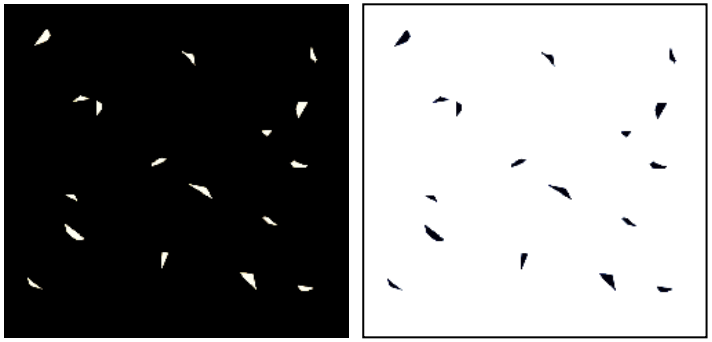

2 %

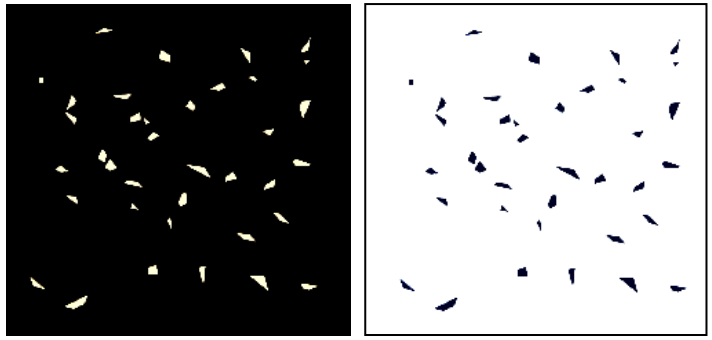

3 %

5 %

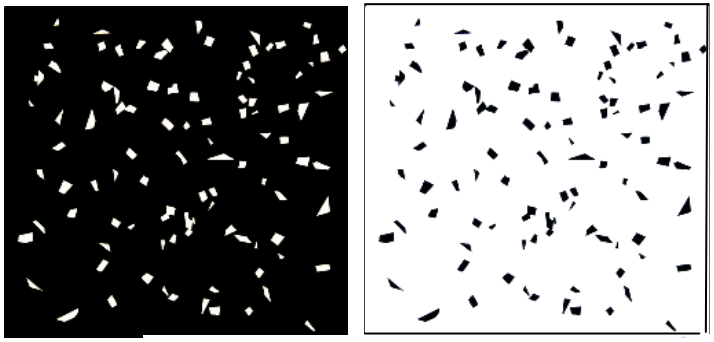

10 %

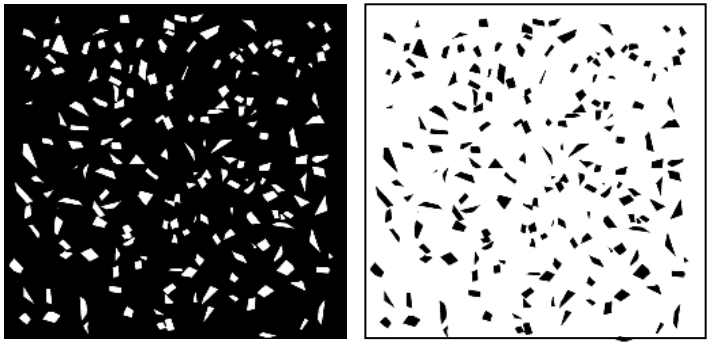

15 %

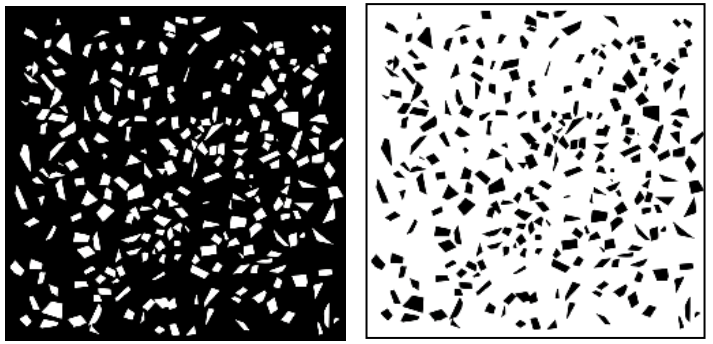

25 %

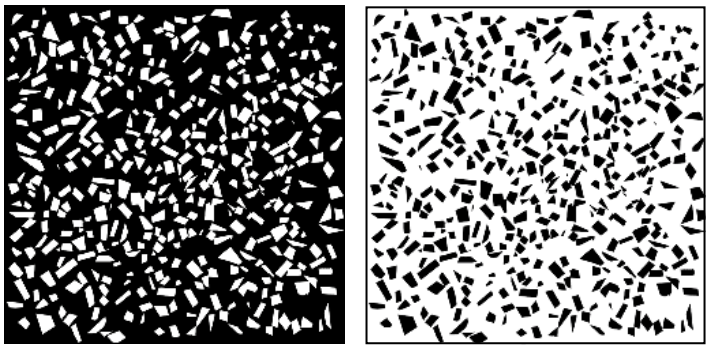

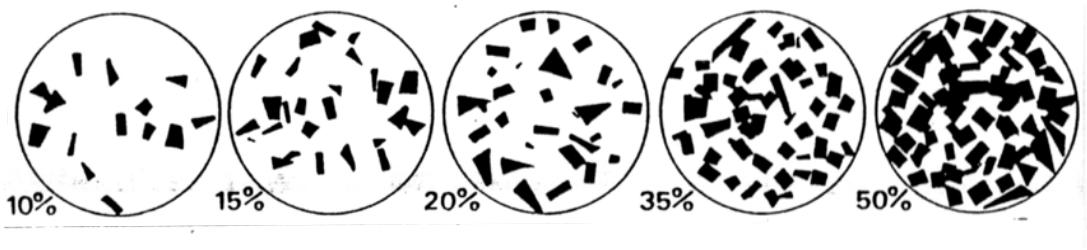

aus: www.kristallin.de/index.htm

Anleitung Ganganalyse

- Rahmengestein
  - Petrographie
    - Gesteinsart
    - Mineralbestand
    - Korngröße
    - Farbe
  - Gefüge
    - Foliation(en)
    - Lineation(en)
    - Kontaktzone (Alterationen)
    - Raumlagebeziehung Foliation/Gang

- Ganggefüge

  - Gang 1
    - Grundtyp (Dike, Sill, nicht charakterisierbar)
    - Art
      - Magmatit: Gesteinart
      - Mineral(e)
      - Sediment
    - Raumlage
      - Einfallrichtung/Einfallwinkel; ggf. Raumlage anhand von Schnittlinearen konstruieren (Schmidt-Netz); notfalls nur Streichrichtung (für Rosendiagramm)
    - Dimensionen
      - Ausdehnung (Längserstreckung soweit aufgeschlossen; vertikal, horizontal)
      - Mächtigkeit (wahre, scheinbare)
    - Form
      - Grenzflächenverlauf
      - Gangterminierung
      - Schärfe der Grenzfläche
      - Anordnung Gangschar (parallel, unregelmäßig vernetzt)
      - Kinematische Indikatoren (Gangöffnungsart und -richtung)
    - Interngefüge
      - Kontakt zum Rahmengestein
      - Zonierung
        - Korngrößen
        - Stofflich
        - graduell, gleiches Gestein
        - abrupt
          - gleiches Gestein
          - unterschiedliche Gesteine („composite“)
      - Formregelungen
        - Foliation
        - Lineation
          - intern
          - auf Grenzfläche
        - Kristallform (Mineralgänge)

    - Gang 2 bis X dito

    - Altersbeziehungen zwischen Gang 1 bis X

- Kluftgefüge
  - Kluftschar 1
    - Raumlage (mehrere Messungen)
    - Abstände
    - Richtungsbeziehung zu Gängen
    - Oberflächenstruktur
    - Belag
    - plumose Strukturen, Linear→Öffnungsrichtung einmessen

  - Kluftschar 2 bis X dito

  - Abstufung der Kluftscharen 1 - X gemäß ihrer Dimension (Haupt- und Nebenklüfte)

- Störungen (falls Bezug zu Gängen besteht)
  - Raumlage
  - Bewegungssinn
  - Altersbeziehung zu Gängen

Erfassung strukturgeologischer Daten 1 (aus: McClay 1987)

Table 3.4 Data to be collected from observations when mapping folds from a single phase of deformation.

Structure	*What to Measure*	*What Observations to Record*	*Results of Analysis*
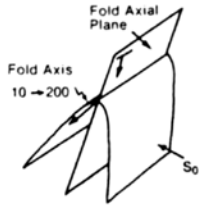	Orientation of fold axial surface (dip direction) (Figs. 2.5–2.8).	Nature of axial surface. Relationships of axial planes in a group of folds.	Orientation of fold structure. (Table 3.2)
	Orientation of fold axis (plunge) (Figs. 2.11–2.13).	Nature of hinge line — straight or curved, Relationships of hinge lines in a group of folds.	
	Vergence (azimuth) (Figs. 3.9 & 3.10).	Vergence and sense of asymmetry. S, Z, M (parasitic folds) facing. (Figs.3.8, 3.5, 3.10)	Vergence boundaries. (Fig. 3.11) Axes of major fold structures. (Fig. 3.8) Tectonic transport direction. (Fig. 3.4)
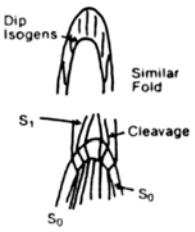	Profile section of fold (Figs. 3.2–3.4).	Thickness changes in profile section. Cylindricity. Fold type. (Figs. 3.3, 3.4, 3.5)	Fold classification: 2D or 3D, dip isogons. (Fig. 3.4) Projection of fold down plunge. (Fig. 9.6)
	Cleavage orientations around the fold (Fig. 4.3).	Nature of cleavage. (Fig. 4.1)	Mean cleavage approximates to fold axial plane. (Fig. 4.3b) Deformation mechanisms.
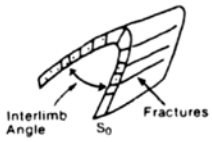	Fracture patterns around fold (Figs. 7.4 & 7.5).	Nature of fractures – veining. (Figs 7.1 and 7.6)	Deformation mechanisms.
	Interlimb angle. (Table 3.1)	Nature of limbs planar curved. (Fig. 3.3)	Shortening across fold, (chevron folds).
	Limb lengths. Strain of deformed objects around the folded layer(s) (Fig. 3.12).	Asymmetry. (Fig. 3.8) Nature of strain in deformed objects. (Appendix III)	Quantification of asymmetry. Strain distribution, mechanisms of folding. (Fig. 3.12)

Table 3.3 Data to be collected from observations on kink bands.

Structure	*What to Measure*	*What Observations to Record*	*Results of Analysis*
Kink bands (KB) 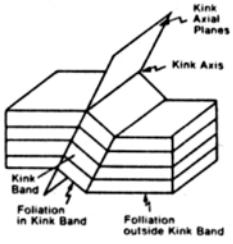	Orientation of foliation outside kink band (Figs. 2.5–2.8).	Nature of foliation that is kinked. Nature of foliation in kink band: Veining (reverse kinks) pressure solution (normal kinks).	Deformation processes during kinking.
	Orientation of kink band axial plane (Figs. 2.5–2.8).	Normal or reverse kink angle between kink band and mean foliation. (Fig. 3.14)	Stress analysis giving σ_1, σ_2, σ_3.
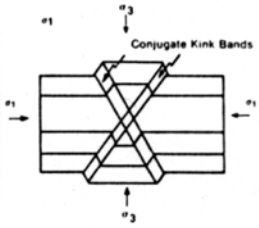	Orientation of conjugate kink band axial plane (Figs. 2.5–2.8).	Angles between conjugate kink bands.	σ_1 bisects obtuse angle between conjugate kink bands.
	Line of intersection of conjugate kink bands (Figs. 2.11–2.13). Fold axes of kink bands (Figs. 2.11–2.13).	Crenulation/kink lineation associated with kink bands.	σ_2 orientation.

Erfassung strukturgeologischer Daten 2

Table 4.1 Data to be collected from observations on the first cleavage (or schistocity), S_1 (commonly a slaty cleavage).

Structure	*What to Measure*	*What Observations to Record*	*Results of Analysis*
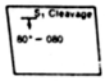	S_1 dip direction (or strike and dip) (Figs. 2.5–2.7). Of cleavage or schistosity	Orientation of cleavage relative to bedding. (Figs 2.15 and 4.5) Sense of vergence. (Figs 3.9, 3.10) Facing. Cleavage refraction. (Fig. 4.4) Nature of cleavage. (Fig. 4.1)	Position relative to fold axis. (Fig. 4.5) Vergence of structure. (Fig. 3.9, 3.10) Facing of structure. Mean cleavage approximates to fold axial plane.
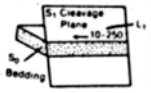	L_1 bedding lineation on cleavage plane (plunge) (Figs. 2.11–2.13).	Nature of lineation. (Figs 5.1 to 5.4)	Orientation of fold axis (b_1 axis). (Fig. 4.3b)
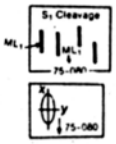	Mineral stretching ML_1 lineation on cleavage plane (plunge) (Figs. 2.11–2.13).		Orientation of stretching axis $\approx$ X axis of bulk strain ellipsoid (a_1 axis). (Fig. 3.2 and Appendix III)
	Orientation and magnitude of strain of deformed objects in the cleavage plane (Appendix A.III).	Nature of strain relative to cleavage. (Appendix III)	XY plane of strain ellipsoid. (Appendix III)
In polyphase terranes. 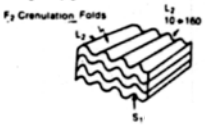	L_2, on S_1. The intersection of subsequent cleavages on the first cleavage plane, i.e. crenulation lineations (plunges) (Figs. 2.11–2.13).	Nature of intersection of second-phase cleavage with first cleavage.	Orientation of second-phase fold axes (for folded first-phase cleavage planes). (Fig. 8.3)

Table 5.1 Data to be collected from observations on intersection lineations L_1, L_2, etc.

Structure	*What to Measure*	*What Observations to Record*	*Results of Analysis*
L_1 Bedding S_0/ cleavage S_1 intersection on either S_0 or S_1 surfaces. 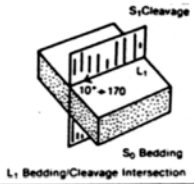	Plunge of lineation L_1 (note: orientation data for S_0 and S_1 also required) (Figs. 2.11–2.13).	Nature of lineation. (Figs. 5.1 to 5.4) Orientation and nature of bedding and cleavage. (Fig. 4.1)	Lineation generally parallels F_1 fold axis (b_1). (Fig. 5.1b)
	Strain of deformed objects parallel to lineation (Appendix III).	Nature of strain. Fibre growth parallel to lineation. Fractures parallel to lineation.	Y axis of F_1 strain ellipsoid. (Appendix III)
L_2 First cleavage S_1/ second cleavage S_2, intersection on either S_1 or S_2 surfaces (S_2 is generally a crenulation cleavage). 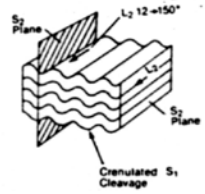	Plunge of lineation L_2 (note data for S_0, S_1 and S_2 are also required) (Figs. 2.11–2.13).	Nature of lineation. (Figs. 5.1 to 5.4) Orientation and nature of S_0, S_1, and S_2. (Fig. 4.1)	Lineation generally parallels F_2 fold axis b_2 (for S_1 surfaces). (Fig. 5.1b)
	Strain of deformed objects parallel to lineation (Appendix III).	Nature of strain. Fibre growth parallel to lineation. Fractures parallel to lineation.	Y axis of F_2 strain ellipsoid. (Appendix III)

Erfassung strukturgeologischer Daten 3

Table 4.2 Data to be collected from observations on the second cleavage S_2(commonly a crenulation cleavage or schistosity).

Structure	*What to Measure*	*What Observations to Record*	*Results of Analysis*
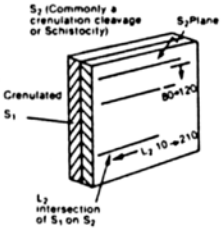	Dip direction (or strike and dip) (Figs. 2.5–2.7) of S_2.	Nature of S_2 cleavage: orientation of S_2 cleavage relative to S_1 cleavage and relative to bedding S_0. (Fig. 4.7) Sense of vergence. (Fig. 3.9, 3.10) Facing on cleavage.	Position relative to F_2 fold axis. (Fig. 4.5) Mean cleavage approximates to F_2 axial plane. Vergence and facing of F_2 structure.
	L_2 Intersection of first cleavage on second cleavage plane S_2 (Figs. 2.11–2.13).		Orientation of F_2 fold axis (b_2 axis) of folded S_1 surface. (Figs. 4.7, 5.1d)
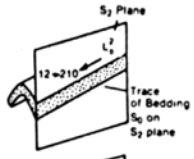	L_0^2 Intersection of bedding on second cleavage plane (Figs. 2.11–2.13).		Orientation of F_2 fold axis for folded bedding S_0 surface (note that this depends upon bedding S_0 and F_1 limbs). (Fig. 8.3)
	Mineral stretching ML_2 lineation on cleavage plane (Figs. 2.11–2.13).	Nature of lineation. (Fig. 5.1 to 5.4)	Orientation of stretching axis ≈ X axis of bulk strain ellipsoid for F_2 deformation (a_2 axis). Fig. 3.2 and Appendix III)
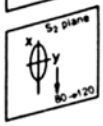	Orientation and magnitude of strain in deformed objects in the cleavage plane (Appendix III).	Nature of strain relative to cleavage. (Appendix III)	XY plane of F_2 strain ellipsoid. (Appendix III)

Table 5.2 Data to be collected from observations on mineral stretching lineations ML_1, ML_2.

Structure	*What to Measure*	*What Observations to Record*	*Results of Analysis*
ML_1 Mineral stretching lineation in S_1. 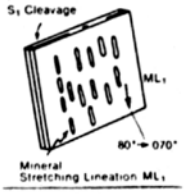	Plunge of ML_1 lineation (orientation data for S_0 and S_1 also required) (Figs. 2.11–2.13).	Nature of lineation (nature of bedding and cleavage also required). Overgrowths parallel to lineation, fibre directions.	Lineation generally parallels the X axis of the F_1 finite strain ellipsoid, ('a_1' tectonic axis). (Fig. 3.2; Appendix III)
	Strain of deformed objects parallel to lineation (Appendix III).	Nature of strain. Fibre overgrowths.	X axis of F_1 finite strain ellipsoid.(Appendix III)
ML_2 Mineral stretching lineation in S_2. 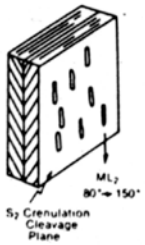	Plunge of lineation (orientation data for S_0, S_1, and S_2 are also required) (Figs. 2.11–2.13).	Nature of lineation (nature of S_0, S_1 and S_2 also required). Overgrowths parallel to lineation, fibre directions.	Lineation generally parallels X axis of the F_2 finite strain ellipsoid (a_2 tectonic axis). (fig. 3.2; Appendix III)
	Strain of deformed objects parallel to lineation (Appendix III).	Nature of strain. Fibre overgrowths.	X-axis of F_2 finite strain ellipsoid. (Appendix III)

Erfassung strukturgeologischer Daten 3A

Table 5.3 Data to be collected from observations on lineations associated with faults.

Structure	*What to Measure*	*What Observations to Record*	*Results of Analysis*
Grooving (no crystal fibre growth). 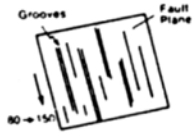	Plunge of lineation. Orientation of fault surface. Orientation of displaced units (Figs. 2.11–2.13).	Nature of grooving. Fault rocks. Sense of movement from steps in fault plane. Width of fault zone. Displacement. Stratigraphic separation.	Sense and direction of movement of fault (solutions for exact displacements are not common).
Slickensides (crystal fibre growth). 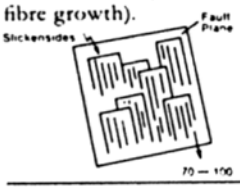	Plunge of lineation. Orientation of fault surface. Orientation of displaced units (Figs. 2.11 2.13).	Nature of fibre growth. Sense of movement from fibres and steps in fault plane. Fault rocks. Width of fault zone. Displacement. Stratigraphic separation.	Sense and direction of movement of fault (solutions for exact displacements are not common).
Slickolites (Fig. 5.6c) 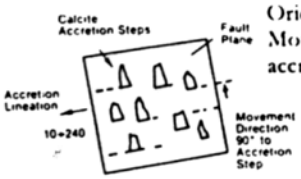	Plunge of lineation. Orientation of fault surface. Orientation of displaced units Movement direction 90° to accretion steps.	Nature of fibre growth. Sense of movement from fibres and steps in fault plane. Fault rocks. Width of fault zone. Displacement. Stratigraphic separation.	Sense and direction of movement of fault (solutions for exact displacements are not common).

Table 6.1 Data to be collected from extensional faults.

Structure	*What to Measure*	*What Observations to Record*	*Results of Analysis*
	Orientation of fault plane (dip direction) (Figs. 2.5–2.8).	Nature of fault plane: fault rocks. Curvature of fault plane? Width of fault.	Deformation processes. Listric/planar faulting. (Fig. 6.8)
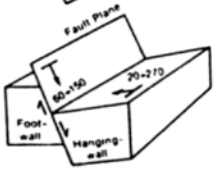	Orientation of displaced units on both sides of fault (Figs. 2.5–2.8).	Stratigraphic separation. (Fig. 6.2) Sense of movement. Sense of shear.	Displacement direction. (Fig. 6.6) Minimum slip. Amount of extension.
	Lineations on fault plane: grooving, slickensides, slickolites (Figs. 2.10–2.13; Figs. 5.6 & 6.4).	Nature of lineations on fault plane (fibrous slickensides?). (Table 5.3) Movement sense. (Fig. 5.6)	Movement direction. (Fig. 5.6)
		Relationship to other faults. Cross-cutting relationships. Associated folding. (Fig. 3.13)	Fault sequences. (Fig. 6.8) Kinematic development.
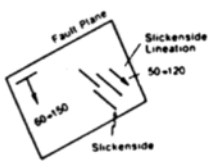	Orientation data on synthetic structures (Fig. 6.8c): faults and fractures (Figs. 2.5–2.8; 2.11–2.13).	Nature of synthetic structures. Movement directions. (Fig. 5.6)	Fault systems. (Fig. 6.6) Movement patterns. Stress systems. (Fig. 6.1)
	Orientation data on antithetic structures (Fig. 6.8c): faults and fractures (Figs. 2.5–2.8, 2.11–2.13).	Nature of antithetic structures. Movement directions. (Fig.5.6)	Fault systems. (Fig. 6.6) Movement patterns. Stress systems. (Fig. 6.1)

Erfassung strukturgeologischer Daten 4

Table 6.3 Data to be collected from wrench faults.

Structure	*What to Measure*	*What Observations to Record*	*Results of Analysis*
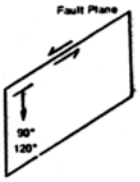	Orientation of fault plane (dip direction) (Figs. 2.5–2.8 and 6.1).	Nature of fault plane fault rocks. (Fig. 6.18 and Table 6.4) Width of fault zone.	Deformation processes.
	Orientation of displaced units on both sides of fault (Figs. 2.5–2.8).	Movement direction. (Fig. 5.6) Sense of shear.	Displacement direction. (Fig. 5.6) Amount of slip/offset.
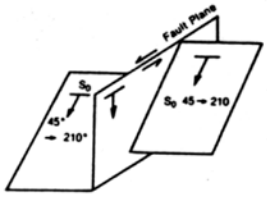	Lineations on fault plane: grooving, slickensides, slickolites (Figs. 5.6, 6.4; 2.11–2.13).	Nature of lineations on fault plane (fibrous slickensides?). (Table 5.3) Movement sense. (Fig. 5.6)	Movement direction. (Fig. 5.6)
		Relationships to other faults. Cross-cutting relationships. Associated folding.	Fault sequences. (Figs. 6.16 and 6.19) Kinematic development. (Fig. 6.16a)
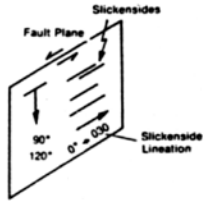	Orientation data on synthetic structures Riedel shears R_1, R_2, P shear (Fig. 6.16a). Second and third order faults Associated folds (Fig. 6.16a).	Nature of synthetic structures. (Fig. 6.16a) Movement directions. (Fig. 5.6)	Fault systems. (Fig. 6.16a) Movement patterns. (Fig. 6.16a) Stress systems. (Fig. 6.16a)

Table 6.2 Data to be collected from contractional faults.

Structure	*What to Measure*	*What Observations to Record*	*Results of Analysis*
	Orientation of fault plane (dip direction) (Figs. 2.5–2.8).	Nature of fault plane: fault rocks. (Fig. 6.18, Table 6.4) Curvature/stepped nature of fault plane? Width of fault zone. (Fig. 6.11)	Deformation processes. Listric/planar/stepped fault. (Fig. 6.11a)
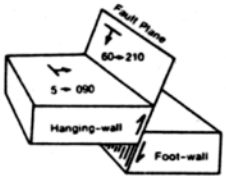	Orientation of displaced units on both sides of fault (Figs. 2.5–2.8).	Stratigraphic separation/overlap. Sense of movement. Sense of shear.	Displacement direction. (Fig. 5.6) Minimum slip. Amount of contraction.
	Lineations on fault plane: grooving, slickensides, slickolites (Figs. 2.4–2.13, 5.6 and 6.4).	Nature of lineations on fault plane (fibrous slickensides?). (Table 5.3) Movement sense. (Fig. 5.6)	Movement direction. (Fig. 5.6)
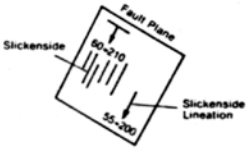		Relationships to other faults. Cross-cutting relationships: Imbricate fan? duplex? out of sequence? Ramps? Associated folding. (Figs. 6.11a and 3.13)	Fault sequences. Kinematic development.
	Orientation data on synthetic structures: faults and fractures (Figs. 2.5–2.8, 2.11–2.13),	Nature of synthetic structures. Movement directions. (Fig. 5.6)	Fault systems. Movement patterns. Stress systems. (Fig. 6.1)
	Orientation data on antithetic structures: faults and fractures (Figs. 2.5–2.8, 2.11–2.13).	Nature of antithetic structures. Movement directions. (Fig. 5.6)	Fault systems. Movement patterns. Stress systems. (Fig. 6.1)

Erfassung strukturgeologischer Daten 5

Table 6.6 Data to be collected from observations on shear zones.

Structure	*What to Measure*	*What Observations to Record*	*Results of Analysis*
Brittle shear zone 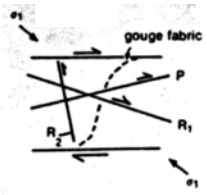 	Orientation of shear zone boundaries (Figs. 2.5–2.8). Orientation of Riedel fractures R_1 and R_2 (Fig. 6.19. & Figs. 2.5–2.8). Orientation of fabric in fault gouge. (Fig. 6.8) Orientation of P fracture (if developed). (Fig. 6.19) (Additional data—orientation of structures outside shear zone). (Fig. 6.23)	Nature of shear zone. (Fig. 6.19) Width of shear zone. Fault rocks developed. (Fig. 6.18, Table 6.4) Veining and/or pressure-solution. (Fig. 6.23 and 7.6b) Fracture orientations relative to shear zone. (Fig. 6.19a) Sense of shear, (Fig. 6.19a) Displacement. Structures outside shear zone.	Stress systems. (Fig. 6.19a) Sense of shear. (Fig. 6.19a) Displacement. Deformation processes.
	Orientation data on conjugate array. (Fig. 6.22)	Observations on conjugate array. (Table 6.5)	Stress systems. (Fig. 6.19a) Sense of shear. (Fig. 6.19a) Displacement. Deformation processes.
Semi-brittle shear zone (en-echelon tension gashes) 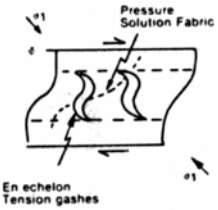 	Orientation of shear zone boundaries (Figs. 6.20 & 2.5–2.8). Orientation of crack tips. (Fig. 6.20a) Orientation of intersection of crack tips with shear zone boundary. (Fig. 6.20a) Orientation of pressure-solution fabric at shear zone margins. (Fig. 6.20a)	Nature of shear zone. (Figs. 6.20, 6.22) Width of shear zone. Nature of veins—fibrous or massive. (Figs. 6.20a, 7.6) Nature of foliation in shear zone. (Figs. 4.1, 4.2) Sense of shear. (Fig. 6.20a) Displacement. Photograph/sketch of shear zone. Structures outside of shear zone.	Stress systems. (Fig. 6.20a) Sense of shear. (Fig. 6.20a) Displacement. Strain in shear zone. Deformation processes.
	(Additional data on orientation of structures outside shear zone). Orientation data on conjugate array. (Fig. 6.22)	Observations on conjugate array.	Stress systems. (Fig. 6.20a) Sense of shear. (Fig. 6.20a) Displacement. Strain in shear zone. Deformation processes.
Ductile shear zone 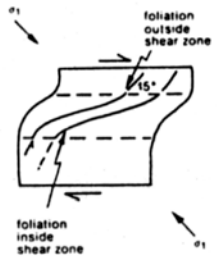 	Orientation of shear zone boundaries (Figs. 6.21 & 2.5–2.8). Orientation of foliations at shear zone boundaries. (Fig. 6.21) Orientation of lineations in shear zone (ML). (Figs. 2.11 to 2.14) Orientation/vergence of folds in shear zone. (Fig. 3.9) Strain of deformed objects across shear zone. (Appendix III) (Additional data on orientation of structures outside shear zone).	Nature of shear zone. (Fig. 6.21a) Width of shear zone. Nature of foliation. (Figs. 4.1, 4.2) Sense of shear.(Figs. 6.21, 6.26, 6.27) Displacement. Nature of folds/vergence. (Fig. 3.9) Strain in deformed objects. (Appendix III) Photograph/sketch of shear zone. Structure outside shear zone.	Stress systems. (Fig. 6.21a) Strain distribution. Sense of shear. (Fig. 6.21a, 6.26, 6.27) Displacement. Deformation processes.
	Orientation data on conjugate array. (Fig. 6.22)	Observations on conjugate array. (Table 6.5)	Stress systems. (Fig. 6.21a) Strain distribution. Sense of shear. (Fig. 6.21a, 6.26, 6.27) Displacement. Deformation processes.

Erfassung strukturgeologischer Daten 6

Table 7.1 Data to be collected from observations on joints, veins and stylolites.

Structure	*What to measure*	*What observations to record*	*Results of analysis*
Joints J_1 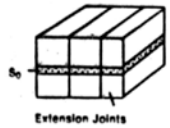 	Dip direction (or strike and dip) (Figs. 2.6 & 2.5). Dip direction of conjugate fracture array (if developed). Line of intersection of conjugate arrays (Figs. 2.11–2.13).	Fracture type (dilational, shear, or hybrid). (Fig. 7.1) Conjugate fracture system. (Fig. 7.2) Bedding and uniformity of bedding dip. Fracture spacing. Bed thicknesses. Length of fractures relative to bed thicknesses. Nature of fracture surface. (Fig. 7.3) Nature of fracture infilling (quartz; carbonate; fibrous or massive).	For conjugate shear-fractures — stress systems. Bed competencies. History of fracture movement.
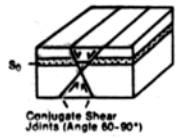 			
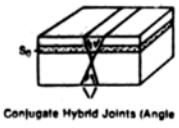 	Line of bedding intersection on fracture plane (Figs. 2.11–2.13).		Gives apparent dip of bedding. Used to calculate true bedding attitude.
Additional information required for analysis.	Dip direction of bedding (fractures are best analysed in areas of uniform bedding). Orientation of fold axis. Orientation of fold axial plane.	Relationship of fracture to bedding. (Figs. 7.4, 7.5) Relationships of fractures to fold. Cylindrical (Fig. 7.4) Non-cylindrical (Fig. 7.5)	Analysis of fracture systems with respect to bedding and fold limbs. (Figs. 7.4, 7.5) Gives fracture systems: a–c, b–c, etc.

Nomogramm wahres/scheinbares Einfallen

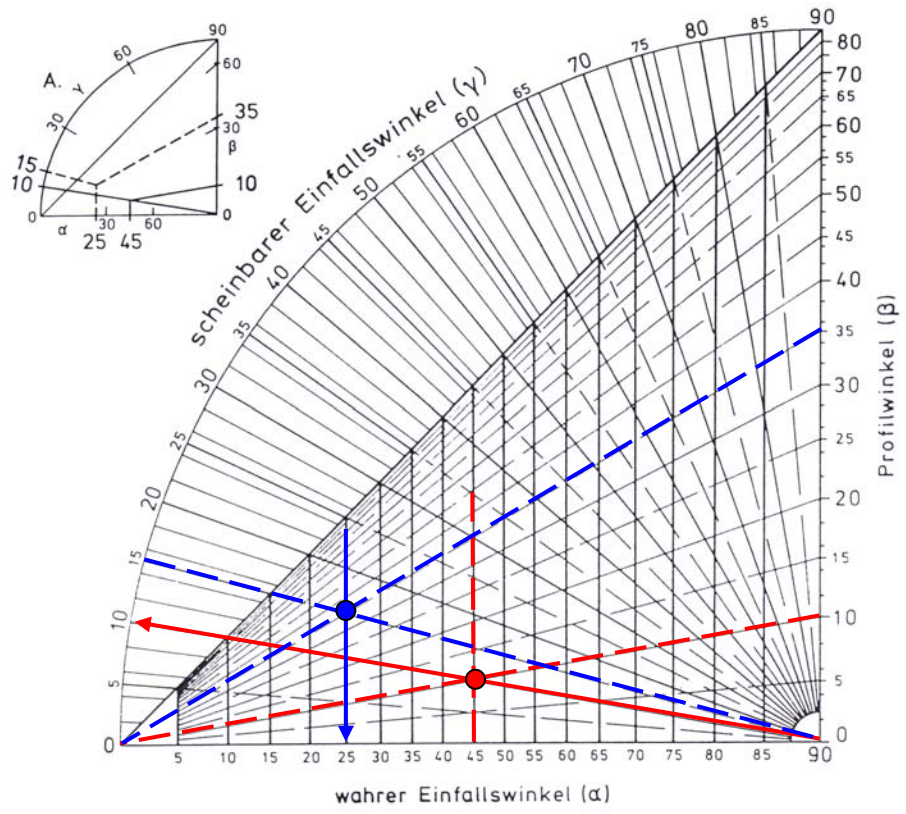

Beispiele:

Wahres Einfallen α=45°,
Profilwinkel β= 10°

Scheinbares Einfallen γ =10°

Scheinbares Einfallen γ = 15°
Profilwinkel β= 35°

Wahres Einfallen α=25°

Tabelle 1.8 Beispiele für Signaturen von Magmatiten und Metamorphiten

Magmatite

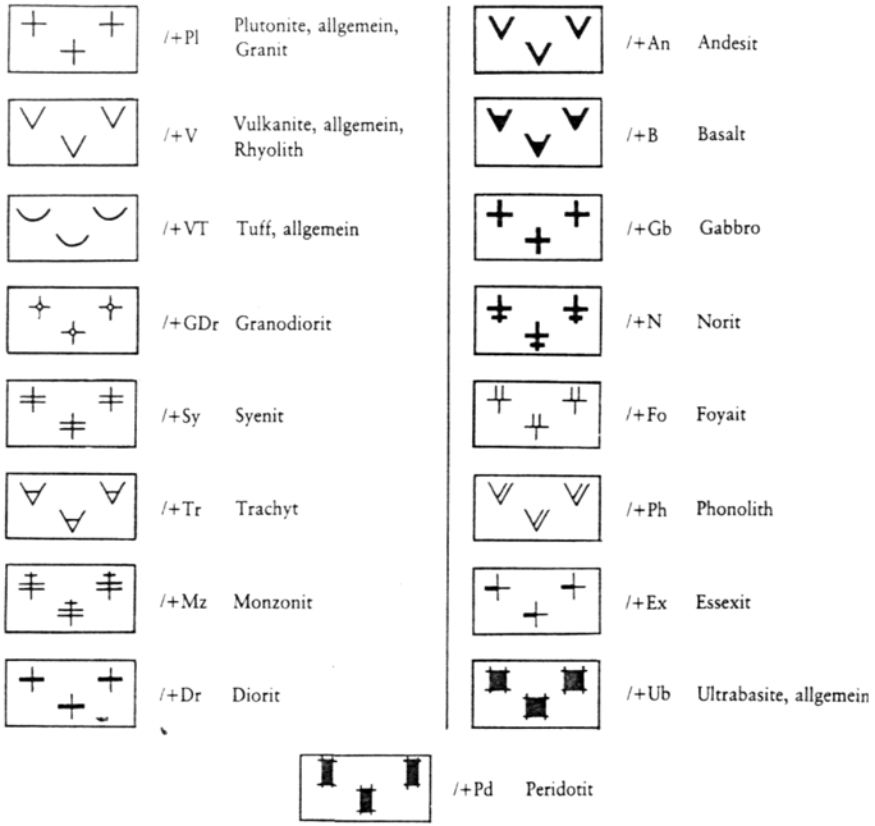

Paläovulkanite

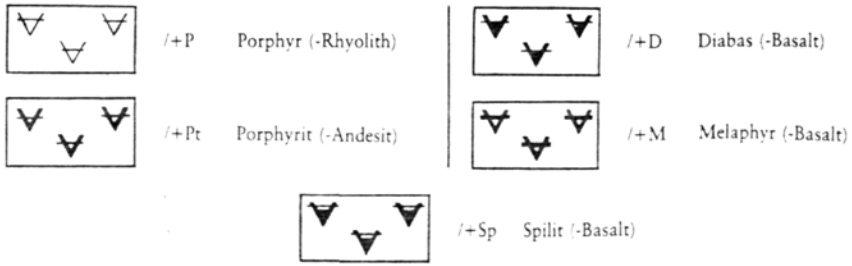

Tabelle 1.8 (Fortsetzung)

Metamorphite
Orthogesteine

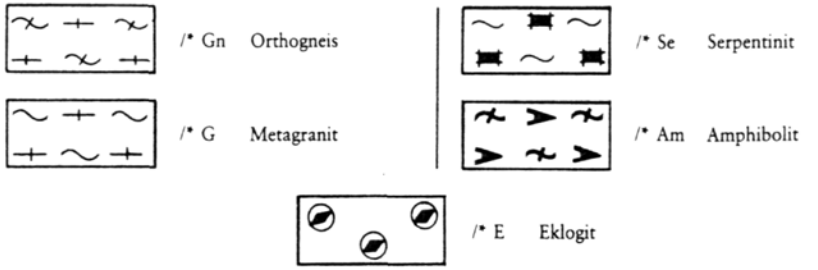

Parageseteine
Regionalmetamorphose

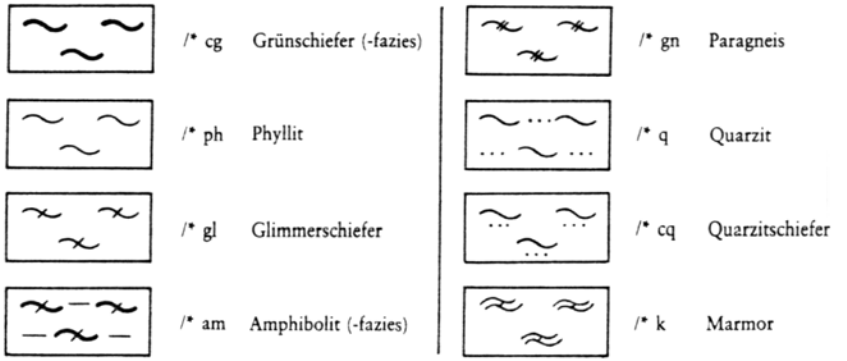

Ultrametamorphose (auch Anatexis)

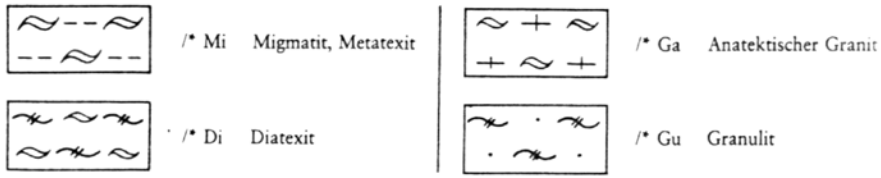

Kontaktmetamorphose

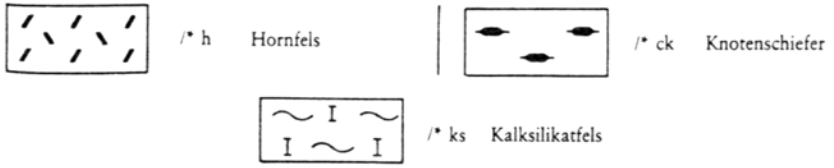

Kartierberichte

Vorschlag für eine Gliederung von Kartierberichten mit dem Ziel der Straffung und Erleichterung der Arbeit. Die Gliederung ist nur als Grundgerüst zu verstehen und soll keinesfalls zwingend vorgeschrieben sein. Anpassungen an spezielle Gegebenheiten sind erwünscht.

Erster Entwurf als Diskussionsgrundlage

Vorwort

Im wesentlichen Danksagung (nicht zu blumig, im Kern ehrlich aber nicht zu direkt). Außerdem: Zeitraum der Anfertigung, Kooperationen etc., - ggf. Einbindung in bestimmte Forschungsprojekte, Förderungen

1. Einleitung

- Lage des Arbeitsgebietes (geographisch und geologisch) im größeren Rahmen mit entsprechenden Übersichtskarten
- Literaturhinweise zur Erforschungsgeschichte und zu neueren geologischen Modellen - generelle, kurze Beurteilung der Aufschlußverhältnisse - Aufgabenstellung nur, wenn diese über die der Standardkartierung hinausgeht, z.B. falls Kartierung in Verbindung mit einer weiterführenden Diplomarbeit angefertigt wird. - Hinweis auf ältere Kartiervorlagen

2, Lithologie/Stratigraphie der kartierten Einheiten

- Makroskopische Beschreibung mit Handstückfoto
- Mikroskopische Beschreibung mit Dünnschlifffoto (Petrographie)
- Unterscheidungsmerkmale bzw Abgrenzungskriterien gegenüber anderen Einheiten - Dokumentation aussagekräftiger Aufschlüsse (Fotos, Skizzen) - Literaturhinweise zu neuen, detaillierteren Bearbeitungen.

3 Strukturgeologie

- Lagerungsverhältnisse (grobe Übersicht, Großstrukturen)
- Möglichst vollständige Beschreibung der Gefügeelemente (Falten, Schieferungen, Scherzonen, Klüfte etc.)
- Dokumentation der Gefüge/Strukturen anhand von Gefügediagrammen sowie einer Auswahl von Aufschlüssen (Makro) und Dünnschliffen (Mikro) mit entsprechenden Fotos und Skizzen.

4. Zusammenfassende Interpretation

- Kurze Beschreibung der anhand der Kartierung und ergänzenden Beobachtungen (z.B. Dünnschliffe) rekonstruierbaren Entwicklungsgeschichte (z.B. Sedimentation, Diagenese/Metamorphose, Deformationsereignisse, Erosionsformen); - Neue Ergebnisse kurz dem bisherigen Kenntnisstand gegenüberstellen.

5. Literatur

nur Arbeiten, die auch im Text vorkommen unter Beachtung der vorgeschriebenen Zitierweise (s.u.)

6. Anhang

- Komplettes Aufschlußverzeichnis: allgemeine Ortsangabe, R- und H-Werte, aufgeschlossene Phänomene in Stichworten
- Komplettes Probenverzeichnis für Handstücke und Dünnschliffe: Probennummer, Fundpunkt (Ortsangabe einschl. R- und H-Werte), Material, ggf. spez. Präparate für anderweitige Verwendung (z.B. Diplom-Arbeit), ggf. Orientierungsdaten angeben. - Datentabellen (z.B. Kompassmeßwerte, getrennt nach o.g. Aufschlüssen).

Anlagen

- Geologische Karte mit strukturgeologischen Signaturen, mit Legende Geologische Querprofile
- ggf. Spezialkarten und -profil

Was sollte nicht im Kartierbericht enthalten sein? (eine Auswahl auf der Basis bisheriger Erfahrungen)

1) Ausführliche Darstellungen des großregionalen geologischen Rahmens
2) Breite Erläuterung der Erforschungsgeschichte
3) Beschreibung der Lebensgewohnheiten der Eingeborenen (Landwirtschaft, Entwicklung der Besiedlungsdichte etc.)
4) Lehrbuchhafte Kapitel (z.B. Nomenklaturen von Faltengeometrien), stattdessen nur Methode mit Zitat nennen
5) Beschreibung von Standardmethoden
6) Zusätzliche Untersuchungen/Ergebnisse, die mit der eigentlichen Kartierung nichts zu tun haben und auch nicht in der Aufgabenstellung gefordert wurden.

7) Wissenschaftliche Diskussionen, die keinen unmittelbaren Bezug zur Kartierung haben
8) Angewandte bzw. lagerstättenkundliche Aspekte nur in Ausnahmefällen (z.B. Kartierung steckt i. W. den Rahmen eines Abbaugeländes ab).
9) Zu weit führende Interpretationen bzw. Spekulationen (z.B. aus zwei beobachteten Verschiebungsflächen komplexe Duplexstrukturen konstruieren). Interpretationen sollten sich auf das Kartiergebiet bzw. engeres Umfeld beziehen und nicht in das Großreginale ausschweifen.

Technische Hinweise (in ungeordneter Reihenfolge)

Karte: Name des Kartierers und Jahreszahl (Abgabe) nicht vergessen, Rahmen mit Koordinatensystem versehen, Lage der Querprofile eintragen, in lithostratigraphischen Säulenprofilen soll Unten = alt und Oben = jung sein. Übliche Farben (?DIN) für bestimmte Lithologien bzw. stratigraphische Einheiten verwenden (bitte nicht grün für Granite), Lage des Kartiergebietes in einer Übersichtskarte ist sehr hilfreich, ggf. mit Lage benachbarter Kartiergebiete;

Geologische Ouerprofile: Nicht überhöhen. Profile sollten einen gewissen Tiefgang haben, was gleichzeitig ein bestimmtes Maß an Interpretation erfordert. Gleiche Farben und Symbole wie in der Karte verwenden. An den Rändern Hohe über NN, Himmelsrichtungen und Profilbezeichnungen (z.B. A-B) angeben. Bei (falls deutlich von Fallrichtung abweichend) in scheinbare umrechnen.

Abbildungen (Fotos): Alle Dunnschliffbilder mit Größenangabe versehen (Angabe der Bildkantentlänge oder Maßstab einfügen). Bei „texturierten" Gesteinen Schliffe aus definierten Schnittlagen abbilden (z.B. senkrecht Foliation, parallel Lineation und senkrecht Foliation/senkrecht Lineation). Aufschlußfotos mit Himmelsrichtungen und Maßstab versehen. Wenn nötig, bestimmte Objekte in Fotos durch Markierungen (z.B. Pfeile, Zahlen, Buchstaben) hervorheben, u.U., auch Foto durch Strichzeichnung ergänzen. Abbildungstexte möglichst ausführlich Abbildungen nach Möglichkeit nach erstem Zitieren im Text positionieren. Der Text muss auf jede Abbildung Bezug nehmen.
Abbildungen (Zeichnungen) Großenangabe am besten in Form eines Maßstabes, der dann bei anschließenden Vergrößerungen oder Verkleinerungen gültig bleibt. Strichstärken und Zahler/Buchstabengrößen so wählen, dass sie auch bei Verkleinerungen noch gut zu erkennen sind Zu enge Punkraster und Schraffuren verlaufen oft bei zu starken Verkleinerungen. Geländeskizzen nicht zu naturalistisch gestalten, nur das Wesentliche hervorheben.

Manuskripte: Vor Beginn der Berichtabfassung Gliederungsentwurf mit dem Betreuer durchsprechen. Manuskripte, die zur ersten Beurteilung dem Betreuer vorgelegt werden, sollten genügend Platz für schriftliche Anmerkungen bieten (breiter Rand, nicht zu enger Zeilenabstand). Es sollten nur vollständige Manuskripte zur ersten Durchsicht eingereicht werden (einschl. Abbildungen, Literatur etc.). Die Vorlage beim Betreuer sollte nicht zu kurzfristig vor dem offiziellen Abgabetermin erfolgen (Absprache wegen möglicher terminlicher Engpässe anzuraten)

Text: Immer den gleichen Fachausdruck für bestimmtes Phänomen verwenden, auch wenn dies zu vielfachen Wiederholungen führt. Oft ist es günstig, Beobachtung und Interpretation deutlich zu trennen. Nach Möglichkeit im deutschen Text auch immer den deutschen Fachausdruck verwenden (z.B. Stress=Spannung). Darauf achten, dass der Text Verweise auf alle Abbildungen und Tabellen enthält.

Literatur zur geologischen Kartierung einschl. Bericht bzw. Geländearbeit:

Barnes, J.W. (1981) Basic geological mapping - Open University Press, Milton Keynes 112 PP

Levshon, P.R. & Lisle, R L(1996) Stereographic projection techniques in Structural Geology
Butterworth-Heinemann, Oxford, 104 pp

McClay, K.R (1992) The mapping of geological structures. - Geological Society of London Handbock, Butterworth-Heinemann, Oxford, 161 pp.

Passchier, C.W., Myers, J.S & Kroner, A: Field Geology of high-grade gneiss terrains. - Springer, Berlin Heidelberg New York, 150 pp

Ramsay, J.G. & Huber, M.I. (1987): Modern Structural Geology - VoL 2: Folds and Fractures, Appendix F: Geological Mapping: 673-684

Rowland, S.M. & Duebendorfer, E.M. (1994): Strucrural analysis and sythesis (2nd ed.). - Blackwell Scientific Publications, Boston 279 pp.

Thorpe, R.S. & Brown, G.C. (1995): The field description of igneous rocks - Geological Society of London Handbock, John Wiley & Sons, London, 154 pp.

Tucker, M. (1990): Field description of dsedimentary rocks. - Geological Society of London Handbock, John Wiley & Sons, London Toronto, 112 pp

Wimmenauer, W. (1985): Petrographie der magmatischen und metamorphen Gesteine. - Ferdinand EnkeVerlag, Stuttgart, 382 pp.

Regeln zum Zitieren von Literatur in einem deutschsprachigem Text (z.B. Diplomarbeit)

Generell: im Text gibt es kein Komma zwischen Autor und Jahreszahl (wie es bei englisch sprachigen Texten üblich ist).
Für den Biotitstandard HD-B1 wurde ein K_2O-Gehalt von 9,621 Gew.% angenommen (FUHRMANN, LIPPOLT & HESS 1987).

Mehrere Publikationen werden nach ihrem Erscheinungsjahr geordnet.
Grundlagen, Arbeitstechniken, Möglichkeiten und Grenzen der K/Ar-Altersdatierung werden ausführlich diskutiert in DALRYMPLE & LANPHERE (1969), BONHOMME et al. (1975), HUNZIKER (1979) und FAURE (1986).

Bei gleichem Erscheinungsjahr wird alphabetisch sortiert.
Korrektur für den Lorentz-Polarisationsfaktors (KLUG & ALEXANDER 1974, KRISCHNER 1974).

Ausgewählte Publikationen, die stellvertretend für eine Vielzahl von Untersuchungen stehen werden mit „z. B." gekennzeichnet:
K/Ar-Datierungen an Mineralen, die unterhalb ihrer Schließungstemperatur gebildet wurden und somit als Bildungs- oder Rekristallisationsalter interpretiert werden können, beschränkten sich bisher ebenfalls auf die aufsteigende Metamorphose (z.B. AHRENDT et al. 1977, 1978, 1983).

Zitat einer regelmäßig erscheinenden Zeitschrift:
AHRENDT, H., HUNZIKER, J.C. & WEBER, K. (1977): Age and Degree of Metamorphism and Time of Nappe Emplacement along the Southern Margin of the Damara Orogen/Namibia (SW-Africa). - Geol. Rdsch., **67:** 719-742.

Regelmäßig erscheinende Zeitschriften können ohne Erscheinungsort zitiert werden. Falls doch mit Ort, dann alle: Geol. Rdsch., **67:** 719-742; Stuttgart
Die Nummer des Bandes in Fettdruck oder unterstrichen (heute weniger gebräuchlich).
Die Abkürzungen für die Zeitschriften sind festgelegt (s. Zitatleiste der Zeitschrift. Diese steht oft auf der ersten Seite jeder Publikation oder auf der ersten Seite der des Zeitschriftenbandes). Bitte nichts selbst ausdenken. Im Zweifelsfall ausschreiben. In älteren Zitaten findet man oft die Angaben: Anzahl der Tabellen und Anzahl der Abbildungen. Dies ist heute nicht mehr üblich.

Zitat einer nicht regelmäßig erscheinenden Zeitschrift:
AHRENDT, H. (1972): Zur Stratigraphie, Petrographie und zum tektonischen Aufbau der Canavese-Zone und ihrer Lage zur Insubrischen Linie zwischen Biella und Cuorgne (Norditalien). – Göttinger Arb. Geol. Paläont., **11:** 1-89 ; Göttingen.

Hierbei ist es üblich den Erscheinungsort anzugeben.

Zitat einer Monographie (Buch):
DALRYMPLE, G. B. & LANPHERE, M. A. (1969): Potassium-Argon Dating - Principles, Techniques and Applications to Geochronology. - 1-258; San Francisco (Freeman).

Anzahl der Seiten, entweder 258 S., oder 1-258, Erscheinungsort, der Name des Verlags in Klammern.

Zitat eines einzelnen Artikels aus einer Monographie (Buch):
AHRENDT, H., CLAUER, N., HUNZIKER, J.C. & WEBER, K. (1983): Migration of Folding and Metamorphism in the Rheinische Schiefergebirge deduced from K-Ar and Rb-Sr Age Determinations. - In: MARTIN, H. & EDER, F.W. (Hrsg.): Case studies in the Variscan Belt of Europe and the Damara Belt in Namibia: 323-338; Berlin (Springer).

Zitat einer unveröffentlichten Arbeit (z.B. Dipl. Arb.):
WEMMER, K. (1988): Vergleichende, systematische Untersuchungen der korngrößenabhängigen Illit-Kristallinität an Peliten und Psammiten des Frankenwaldes. - Dipl. Arb. Univ. Göttingen, Teil B: 40-90. - [Unveröff.].

Zitat von Posterbeiträgen zu Konferenzen:
WEMMER, K. & AHRENDT, H. (1994): Age determinations on retrograde processes and investigations on the blocking conditions of isotope systems of KTB rocks. - KTB-Report **94-2**: S.32, Posterbeitrag zum 7. KTB-Schwerpunktkolloquium in Gießen (1.-2.6.1994); Hannover.

Zitat von Kurzfassungen (Abtract) zu Konferenzen:
AHRENDT, H., HANSEN, B., LUMJUAN, A., MICKEIN, A. & WEMMER, K. (1997): Tectonometamorphic evolution of NW-Thailand deduced from U/Pb-, Rb-Sr-, Sm/Nd- and K/Ar-isotope investigations. - Abstract, International Conference on Stratigraphy and Tectonic Evolution of Southeast Asia and the South Pacific, Bangkok, Thailand, 19.-24. August 1997: 314-319; Bangkok.

Aufnahmeschema Petrographie/Gefüge: Durchlichtmikroskopie (Blatt 1) Bearbeiter:

Probenbezeichnung:	Fundort:			Gesteinsart:	
Makroskopische Gefügemerkmale:					
Orientierung:		Präparat/Nr.:		Schnittlage:	
Hauptgemengteile:		Nebengemengteile:		Akzessorien:	

Mineral, Anteil /%									Skizze/Foto Nr.
Aggregatform/Anordnung:									
Kornform:									
Korngröße/Sortierung:									
Korngrenzen:									
Formregelung:									
Internverformung:									
Einschlüsse:									
Zonarbau:									
Alteration:									
Schersinn-Indikator:									
Textur (Schnelltest):									

Weitere Analysen:

Aufnahmeschema Petrographie/Gefüge (Blatt 2): **Probe:** Bearbeiter:

Skizzen/Fotos Nr. (lt. Blatt1)

Zusammenfassende Interpretation:

Literatur / Quellen

Barker, A.J. (1990): Introduction to Metamorphic textures and microstructures. - Blackie Academic & Professional Glasgow, 162 pp.

Barbarin, B. (1989) : Schweizerische Mineralogische und Petrographische Mitteilungen, 69, 303-315.

Burg, J.-P. (1991): Syn-migmatization way-up criteria. - J. Struct. Geol. 13/6: 617-623.

Coelho, S., Passchier, C. & Marques, F. (2006) : Riedel-shear control on the development of pennant veins: Field example and analogue modelling. - J. Struct. Geol. 28: 1658-1669.

Dunne, W.M. & Hancock, P.L. (1994): Paleostress analysis of small scale brittle structures. - In: P.L. Hancock,(ed.): Continental Deformation. Pergamon Press Oxford New York Seoul Tokyo, 421 pp.

Eimer, M. (2008): Lithologische und strukturgeologische Kartierung im Bereich der Loftahammar-Linköping DeformationszoneE' Loftahammar, W-Gebiet zwischen Äskedal und Aleglo, SE-Schweden, unveröff. Diplomkartierung, Univ. Göttingen

Eisbacher, G.H. (1991): Einführung in die Tektonik. - Ferdinand Enke Verlag Stuttgart, 310 S.

Hatcher, R. D. jr. (1995): Structural Geology. - Prentice Hall Englewood Cliffs, New Jersey, 525 pp.

Hoek, J.D. (1991): A classification of dyke-fracture geometry with examples from Precambrian dyke swarms in the Vestfold Hills, Antarctica. - Geologische Rundschau 80/2, 233-248.

Jones, R.R., Holdsworth, R.E., Clegg, P., McCaffrey, K. & Tavarnelli, E. (2004): Inclined transpression. - J. Struct. Geol., 26 (2004): 1531-1548.

Koopmann, A. (2004): Mangma mingling: Die hydrodynamische Genese magmatischer Dispersionen. - Diss. Universität Würzburg, 148 S.

McClay, K. (1987): The mapping of geological structures. - Geological Society of London Handbook, John Wiley & Sons Chichester, 161 pp.

Mehnert, K.H. (1968): Migmatites and the origin of granitic rocks. - Amsterdam, 391 pp.

Passchier, C.W., Myers, J.S. & Kröner, A. (1990): Field geology of high-grade gneiss terrains. - Springer Berlin Heidelberg New York, 150 pp.

Passchier, C.W. & Trouw, R.A.J. (1996): Microtectonics. - Springer Heidelberg, 289 pp.

Pitcher, W.S. (1993): The nature and origin of granite. - Blackie Academic & Professional, London Glasgow New York Tokyo Melbourne Madras, 321 pp.

Price, N.J. & Cogrove, J.W. (1990): Analysis of geological structures. - Cambridge University Press, 502 pp.

Sawyer, E.W. (2008): Atlas of Migmatites. - The Canadian Mineralogist, Spec. Publ. 9, 371 pp.

Schofield, D.I. & D´Lemos, R.S. (1998): Relationships between syn-tectonic granite fabrics and regional PTt paths: an example from the Gander-Avalon boundary of NE Newfoundland. - J. Struct. Geol. 20/4: 459-471.

Shelley, D. (1993): Igneous and metamorphic rocks under the microscope. - Chapman & Hall Glasgow, New York Tokyo Melbourne Madras, 445 pp.

Swanson, M.T. (1992): Late Acadian-Alleghian transpressional deformation: evidence from asymmetric boudinage in the Casco Bay area, coastal Maine. - J. Struct. Geol. 14/3: 323-341.

Tanaka, H. (1992): Cataclastic lineations. - J. Struct. Geol. 14/10: 1239-1252.

Thorpe, R. & Brown, G. (1985): The field description of igneous rocks. - Geological Society of London Handbook, John Wiley & Sons Chichester, 154 pp.

Tucker, M.E. (1985) Einführung in die Sedimentpetrologie, Ferdinand Enke Verlag, Stuttgart, 265 S

Twiss, R.J. & Moores, E.M. (1992): Structural Geology. - W.H. Freeman and Company New York, 532 pp.

Vaughan, A.P.M. & Thistlewood, L. (1995): Small-scale convection at the interface between stratified layers of mafic and silicic magma, Campbell Ridges, NW Palmer Land, Antartic Peninsula: syn-magmatic way-up criteria. - J. Struct. Geol. 17/7: 1071-1075.

Williams, P.F., Goodwin, L.B. & Ralser, S. (1994): Ductile deformation processes.- In: P.L. Hancock,(ed.): Continental Deformation. Pergamon Press Oxford New York Seoul Tokyo, 421 pp.

Wise, D.U., Dunn, D.E., Engelder, J.T., Geiser, P.A., Hatcher, R.D. Jr., Kish, S.A., Odom, A.L. & Schamel, S. (1984): Fault-related rocks: Suggestions for terminology, Geology 12: 391-394.

Wimmenauer, (1985): Petrographie der magmatischen und metamorphen Gesteine. - Ferdinand Enke Verlag Stuttgart, 382 S.